Georgian E. Kharadze Abastumani National Astrophysical Observatory

with the rights of manuscript

George Mamatsashvili

VELOCITY SHEAR INDUCED PERTURBATION DYNAMICS IN ATMOSPHERIC, OCEANIC AND ASTROPHYSICAL FLOWS

Candidate Dissertation

in Physical and Mathematical Sciences

01.03.02-Astrophysics

Tbilisi 2006

Contents

Chapter 1

Introduction

We frequently deal with shear flows of various kinds in astrophysics or in meteorology, that is, flows where processes are driven and sometimes energetically maintained by inhomogeneous background velocity profile. They are equally important together with systems where energetic processes and instabilities are associated with thermodynamic sources, for example, temperature and entropy inhomogeneities. Gas flow in accretion and circumstellar discs around normal stars and compact objects, galactic rotation, planetary rings, protoplanetary discs, astrophysical jets are only few examples from a wide variety of flows met in astrophysical objects. On the other hand, zonal or azimuthal geostrophic flows in the atmosphere and ocean, jet streams related to atmospheric fronts, various kinds of winds are all examples of shear flows in meteorology. Due to a large occurrence of shear flows in nature and a wide variety of energetic processes therein, they have attracted basic interest and their investigation has been initiated for more than a century. Traditionally, the main subject of study and interest in shear flows is their stability to various types of perturbations to which they are unavoidably subject (Drazin & Reid 1981). These perturbations may be of stochastic nature intrinsic to flows or may be caused by some other extrinsic factors. The stability study is very important. It is concerned with when and how laminar state breaks down, its subsequent evolution and eventual emergence of coherent structures or onset of

turbulence. Turbulence itself is a very common phenomenon in nature and has serious consequences in both meteorology and astrophysics (for example, in accretion discs turbulent stresses can remove angular momentum outwards allowing matter to accrete (Balbus & Hawley 1998, Balbus 2002, 2003). Interstellar medium in galaxies is often turbulent and this fact has important observational consequences (Elmegreen et al. 2003a)). It is much less amenable to analytical treatment and investigators often have to resort to numerical simulations or experiments to extract necessary information on the process.

Generally, the characteristic properties, first of all, the stability and other behaviour of shear flows present in astrophysics or in meteorology are best revealed in various laboratory experiments where small-scale analogs of real flows are reproduced. Perhaps the best first study of shear flows was made by Osborne Reynolds (1883) in his classic series of experiments on the instability of flow in a pipe. He showed that laminar flow breaks down and becomes turbulent when a characteristic number of a flow, which was afterwards named after him (*Re*), exceeds a certain critical value. Theoretical investigation of the stability of shear flows was pioneered in the nineteenth century, notably by Helmholtz, Kelvin and Rayleigh. At this time the method of *normal modes* for studying the oscillations and stability of dynamical systems of particles and rigid bodies was already highly developed. A known solution of Newton's equations for the system was perturbed and the equations were linearized by neglecting second order terms. Then by assuming the perturbed quantities to be proportional to $e^{-i\omega t}$ (normal modes), where ω is some complex constant, values of ω were calculated from the linearized equations. If at least one mode happened to have ω with positive imaginary part then the system was deemed unstable because a general initial small perturbation would grow exponentially in time. Stokes, Kelvin and Rayleigh applied this method of normal modes to hydrodynamic problems. This proceeds in two stages: the linearization of fluid dynamical equations about a mean (laminar) background flow and then seeking for unstable solutions of the linearized problem depending on time in the same exponential manner. However, Lord Kelvin developed another so-called *non-modal*

method in 1887, which we describe below and stress its advantages over the modal approach. The fluid dynamical equations are partial differential equations in contrast to Newtonian equations that are ordinary differential equations. This fact leads to many technical difficulties in hydrodynamic stability, which, to this day, have been overcome analytically for only a few classes of flows with very simple configurations.

A basic procedure of linearization of hydrodynamic equations and finding normal modes is described in a great detail in an excellent monograph by Drazin and Reid (1981). Here we would like to note only that a normal mode depends on time exponentially and eigenfrequencies are found from the linearized hydrodynamic equations supplemented with appropriate boundary conditions. If at least one eigenfrequency has positive imaginary part then the flow is said to be unstable. Experiments show that there exists some critical maximum value of Reynolds number below which a flow is stable for all wavenumbers and above which unstable modes begin to emerge. Despite a huge success of modal approach in the stability study of shear flows they are still far from being completely understood. There are an increasing number of cases where results predicted by this modal analysis lead to controversy. These cases involve smooth (without inflection point) shear flows the stability study of which was revisited in the 1990s by means of different approach (cf. Reddy et al. 1993, Reddy & Henningson 1993, Craik & Criminale 1986, Butler & Farrel 1992, Trefethen et al. 1993, Trefethen 1997, Gustavsson 1991, Gustavsson & Hultgren 1980, Criminale & Drazin 1990, Farrell & Ioannou 1993a,b, 1996, 2000, Chagelishvili et al. 1994, 1997a,b). Smooth shear flows were commonly deemed stable according to the classical stability criterion, which states that the existence of an inflection point in the equilibrium velocity profile is a necessary condition for the spectral instability (Fjørtøft 1950) and, accordingly, it was believed that the energy extraction from the mean flow is possible only in the presence of the inflection point in the mean velocity profile. However, it was found in the 1990s that flows without inflection point are rich in energetic processes – processes of mean flow energy extraction, energy exchange between perturbations, etc. owing to non-orthogonal eigenfunctions of governing operators (see below). As we will

see throughout the thesis, transiently amplified perturbations can efficiently extract energy from mean flow and cause instability.

The problem has a long history. As was mentioned above, the traditional and generally acknowledged paradigm in the stability study is the modal analysis. The necessary condition for the flow to behave unstably (in the sense of the standard linear theory) is the existence of exponentially groining eigenmodes. For some processes (e.g. thermally driven instabilities in Rayleigh-Benard convection flow, or centrifugally driven instabilities in rotating Couette flow) results based on the modal approach well match laboratory experiments. At the same time, for other kinds of smooth shear flows, especially those driven predominantly by shear forces, the predictions of the normal mode approach fail to match most experiments. For plane Couette flow, for instance, turbulence is observed in experiments for Reynolds numbers $Re \approx 1300$ (see e.g. Dauchot & Daviaud 1995, Bottin et al. 1998), whereas the common eigenvalue analysis predicts stability for all Reynolds numbers. The same is true for Couette flow between two counter rotating and co-rotating cylinders (Coles 1965), where turbulence is observed despite the absence of exponentially growing linear perturbations. Plane Poiseuille flow becomes linearly unstable at Re=5772 (Orszag 1971), while experiments exhibit well-developed turbulence already at Re=1000. This fact indicates that the onset of turbulence must be different from the eigenvalue instability. Attempts to resolve the problem questioned the validity of the linearization process and appealed to nonlinear effects (nonlinear instability in hydrodynamics) (cf. Bayly 1986, Bayly et al. 1988, Orszag & Kells 1980, Orszag & Patera 1980, Herbert 1988). However, it turned out that the basic cause of the discrepancy was the eigenmode analysis itself (Reddy et al. 1993, Trefethen et al. 1993, Butler & Farrell 1992, Reddy & Henningson 1993).

In was shown mathematically by Reddy et al. (1993) (see also Trefethen 1993) that the application of modal approach to some smooth shear flows leads to incorrect results regarding the stability of flows. The thing with it is that the operators that figure in the modal study of shear flows; in particular, in plane Couette or Poiseuille flows are not self-adjoint and, correspondingly, their eigenfunctions are not mutually orthogonal and

strongly interfere with each other. Due to interference a non-normal system can exhibit large amplification of small perturbations (by factors of thousands and more (Reddy & Henningson 1993)) in a limited time interval even when all the eigensolutions (and, correspondingly, a perturbation itself) die out at large times, i.e. when the system is stable according to modal analysis. This transient amplification of perturbations is overlooked in the modal treatment because it focuses on the asymptotic (at large times) stability of the system (Case 1960, Dykii 1960, Van Kampen 1957) and, therefore, is unable to fully account for phenomena arising from the interference of non-orthogonal eigensolutions and taking place during finite time intervals. Hence, the use of the full spectral expansion for this category of shear flows may be quite misleading: the study of an individual normal mode evolution does not give adequate description of the system behavior. Even if we, in spite of all, stay in the modal approach and wish to analyze a finite time dynamics correctly we must sum over all interfering eigenfunctions which is, without doubt, a formidable task. In practice it can only be done numerically. However, in this process we may easily lose salient features of the dynamics of non-normal systems.

These difficulties provoked a change in the paradigm. A new notion of pseudospectrum was developed (Trefethen et al. 1993, Trefethen 1997, see also Reddy & Henningson 1993) that generalizes the spectral approach and easily captures features characteristic of non-orthogonal systems (shear flows). One of the main applications of pseudospectrum is to the analysis of energy growth for initial value problems (Pazy 1983, see also Reddy & Henningson 1993). Roughly speaking energy growth in non-normal systems depends on how far pseudospectrum extends into the upper half-plane of complex numbers. There was formulated theorem (Hille-Yosida theorem) that defines necessary and sufficient conditions for no energy growth in non-normal systems. Numerical calculations of pseudospectra were performed for various smooth shear flows to specify more accurately its stability characteristics. Reddy and Henningson (1993), Gustavsson (1991), Farrell (1988), Butler & Farrell (1992) extensively investigated numerically transient growth of perturbations in bounded Poiseuille and Couette flows.

Their results show that growth by a factor O (1000) may occur at subcritical Reynolds numbers. For Couette flow it was found that the maximum energy growth is proportional to Re^2 and that growth by a factor ≈19000 may occur for Re=4000. For both flows it was shown that the initial perturbation that achieves the large growth is essentially a streamwise vortex. The existence of transient amplification was vividly demonstrated by Landahl (1980), who by integrating the equations of motion showed that perturbations can be amplified despite the spectral stability of a flow and introduced the notation of algebraic instability. All these show that instability mechanism is different from that predicted by modal treatment.

As mentioned above, Lord Kelvin introduced another method in 1887 that is able to easily capture transiently growing solutions in inviscid incompressible parallel shear flows. The method was developed well before the realization of non-normality of shear flows. This method is now known as *non-modal* approach and consists in transforming coordinates from laboratory to co-moving frame and studying the evolution of individual spatial Fourier harmonics (SFH) without any spectral expansion in time. The wavenumber of each SFH becomes variable in time: there exists "drift" of SFH in wavenumber **k**-space (Marcus & Press 1997, Chagelishvili 1993). The non-modal formalism is also well described in the case of bounded compressible plane shear flows (Criminale & Drazin 1990). This method can be considered as a certain modification of an initial value problem in contrast to boundary value problem in modal analysis. Together with applications in hydrodynamical problems (cf. Farrell & Ioannou 2000, Criminale & Drazin 1990, Craik & Criminale 1986, Chagelishvili et al. 1994, 1996a, 1997a,b) this method has been extensively exploited both in astrophysical (cf. Goldreich & Lynden-Bell 1965, Goldreich & Tremaine 1978, Nakagawa & Sekiya 1992, Julian & Toomre 1966, Jog 1992, Balbus 1988, Ryu & Goodman 1992, Goodman & Balbus 2001, Chagelishvili et al. 2003, Tevzadze et al. 2003) and meteorological (cf. Barcilon and Bishop 1998; Hakim 2000, Hodyss and Grotjahn 2003, Kalashnik et al. 2004, 2006) contexts. The non-modal approach greatly simplifies the mathematical description and helps to grasp phenomena that were overlooked in the framework of the modal approach.

It is more productive when combined with numerical calculations. The non-modal approach allowed revealing two novel channels of energy exchange in shear flows: transient extraction of energy from mean flow by perturbations (especially by vortical perturbations), which plays a central role in the *bypass* scenario of transition to turbulence (Broberg & Brosa 1988, Bagget et al. 1995, Gebhardt & Grossman 1994, Grossman 2000, Reshotko 2001, Chapman 2002, Chagelishvili et al. 2003, Rempfer 2003, Waleffe 1997), and mutual transformation of different modes (exchange of mode energies) into each other at the linear stage of evolution which results from flow shear (cf. Bodo et al. 2001, Chagelishvili et al. 1996b, 1997a,c, 1999, Chagelishvili & Chkhetiani 1995, Rogava & Mahajan 1997, Rogava et al. 1999, Poedts et al. 1998, Poedts & Rogava 2002, Tevzadze 1998).

1.1 Aim of the thesis

The main purpose of the presented thesis is to examine non-orthogonality induced perturbation dynamics in some atmospheric, oceanic and astrophysical smooth shear flows. Our main tools of investigation are non-modal approach and numerical analysis. These allow us to disclose many interesting phenomena and properties that were not seen/observed in the framework of the modal approach both in astrophysical and meteorological flows. In particular, non-modal approach enables us to find mixed explosive/exponential-linear-type of instability in meteorological flows and a new phenomenon, which has not been discussed in the meteorological literature before, of transformation of vortices into waves. This phenomenon is important in view of the fact that traditionally in quasigeostrophic models of geophysical hydrodynamics the role of fast wave motions is underestimated and the main subject of study is the dynamics of slow vortical geostrophic perturbations, while the former type of motion can potentially render flow unstable. We also show that vortices can effectively extract energy from the mean flow and possibly cause turbulence via bypass scenario, which has recently been advocated by many researchers in hydrodynamics. We also derive a useful and elegant

criterion for the stability of flows with boundaries that does not require spectral expansion in time. We also discuss the viscosity effects on the perturbation dynamics.

The second part of the thesis is devoted to analyzing the properties of spiral density waves and vortices in gaseous galactic, protoplanetary or accretion discs, which can be considered as special cases of shear flows since all these objects are in differential rotation. Compared with flows present in meteorology here we have additional factor self-gravity of the medium, which considerably changes the dynamics.

Traditionally density waves are analyzed in the framework of Lin-Shu theory (Lin & Shu 1964, 1966, see also Bertin et al. 1989), which itself is a modal theory and well suited for studying grand-design spiral structures, while flocculent and open spiral structures can be interpreted as transiently amplified density waves, which are best studied in the shearing sheet model/approximation (Goldreich & Lynden-Bell 1965) using non-modal approach (by this method combined with numerical simulations it was possible to numerically get observationally obtained threshold for star formation in the interstellar medium of galaxies (Kim & Ostriker 2001)). Transient instabilities are also invoked in explaining bar modes as a superposition of leading and swing amplified trailing spiral density wave packets (Toomre 1981, see also Binney & Tremaine 1987). In this thesis we more closely analyze the properties of density wave packets in the shearing sheet approximation based on the dynamics of individual SFH. This approximation enable us to simply interpret many properties seen in global disk simulations (see e.g. Sellwood & Carlberg 1984, where the properties of recurrent spirals in N-body simulations of disc galaxies are well described by swing amplification in the shearing sheet). We show that the energy of individual sheared waves grow asymptotically linearly in addition to swing amplification during finite time intervals.

Another noteworthy phenomenon considered here is an essentially linear mechanism of the generation of spiral density waves by vortices in astrophysical discs. This was investigated by Bodo et al. (2005) and Tevzadze (2006) in the non-self-gravity limit. We analyze this phenomena taking into account self-gravity, which changes vortex mode dynamics and enhances wave generation. Vortical perturbations are important in their

own right because they can represent aggregation regions of solid particles for the eventual formation of planets in protoplanetary discs (Barge & Sommeria 1995). Potential role of vortical perturbations as drivers of turbulence in accretion discs by transient amplification (*bypass* scenario) has been recently explored by several authors (Yecko 2004, Umurhan 2004, Afshordi et al. 2005, Chagelishvili et al. 2003). Vortical motions were also observed in several spiral galaxies (Fridman & Khoruzhii 1999a,b) and the present study can be applied to this case as well.

1.2 **Plan of the thesis**

In chapter 2 we study the linear dynamics of wave and vortex perturbations in geostrophic zonal nonuniform flow of an incompressible, inviscid and stratified (along the z-axis) fluid. In section 2.1 we introduce the basic equations describing the motion of a rotating stratified fluid written in the Boussinesq approximation on an f plane. Then after linearizing about the mean qeostrophic zonal shear flow and expansion in normal vertical modes we reduce the equations to the form most convenient for non-modal analysis. Then depending on the value of the Rossby number we consider two regimes. In subsection 2.2.1 we study small $Ro << 1$ case and in subsection 2.2.2 we consider moderate values $Ro \sim 1$, when most of the interesting phenomena take place and explain non-axisymmetric instability in terms of symmetric instability. In section 2.3 we briefly discuss viscosity effects. In section 2.4 we derive a theorem for stability using variational method. In chapter 3 we study dynamics of density waves, vortical perturbations and localized packets in the shearing sheet approximation using non-modal approach combined with numerical calculations. In section 3.1 we introduce the basic equations of the shearing sheet and make Fourier transformation in spatial coordinates. We also make identification of perturbation modes. In section 3.2 we analyze the properties of individual SFH; their time-evolution, reflection and transmission phenomenon and generation of spiral density waves by vortices. In section 3.3 we examine the peculiarities of the propagation of packets of spiral density waves. In chapter 4 we give a summary of the thesis.

Chapter 2

Linear dynamics of non-symmetric perturbations in geostrophic horizontal shear flows

The theory of hydrodynamic stability of zonal geostrophic shear flows plays a central role in dynamic meteorology. It comprises a broad range of problems regarding the generation and propagation of vortical and wave motions in the atmosphere and ocean. Due to a large variety of spatial and temporal scales of the dynamic phenomena various approximations and approaches are used in their study. The investigation of the stability of zonal geostrophic flows with respect to perturbations that are independent of the streamwise coordinate forms the basis for the theory of symmetric instability (Hoskins 1974; Weber 1980; Emanuel 1983; Xu Qin 1986). Linear and nonlinear symmetric instabilities are intensively studied in connection with the formation of frontal cloud bands, circulations of Hadley in planets' atmosphere and etc. (Bennets & Hoskins 1979; Mu, Vladimirov and Wu 1999, Kalashnik 2000, 2001). The problem of general (non-symmetric) instability is much more complicated. This type of instability is commonly studied in the framework of simplified models based on the equation governing the transport of potential vorticity in the quasigeostrophic approximation (Pedlosky 1987). In quasigeostrophic models fast inertial gravitational waves (as we will show below, so essential to instabilities) are filtered and the main subject of study is the dynamics of slow vortical geostrophic perturbations. The number of papers on the quasigeostrophic stability theory rapidly rises because of the problems of cyclogenesis in the atmosphere

(numerous references on this topic can be found in the monographs Gill (1982), Pedlosky (1987), Shakina (1990) and in the review Pierrehumbert & Swanson (1995)). However, many of them, considering quite complex background geostrophic flows, overlook basic phenomena (existing even in the simplest shear flows) due to the described in the Introduction imperfection of classical hydrodynamic methods in regard to non-normal smooth shear flows of a general kind, because in geophysical hydrodynamics as well as in classical hydrodynamics the main tool of investigation of linear stability is the selfsame canonical/spectral method. It should be noted that the non-normality of the linear dynamics of perturbations in shear flows was recognized by the meteorological community in the 1990s (cf. Farrell & Ioannou 1993a, 1996, 2002; Nolan & Farrell 1999a, 1999b; Nolan & Montgomery 2000). As a result, elements of non-modal approach have been exploited more extensively since then (Barcilon & Bishop 1998; Hakim 2000; Hodyss & Grotjahn 2003). The non-modal approach to such problems leads to important novelties to which the present chapter is devoted. Among these novelties we should stress the discovery of a new linear mechanism of transformation of vortices into acoustic waves at moderate ($O(1)$) Rossby numbers in atmospheric and oceanic zonal geostrophic shear flows.

In this chapter we investigate the linear dynamics of vortex and wave type perturbations in geostrophic zonal nonuniform flow of an incompressible, inviscid and stratified (along the z-axis) fluid. A somewhat similar problem, linear dynamics of three-dimensional perturbations in a two-dimensional basic flow, is studied by Straub (2003). However, in that study interest lies with the stability of time-dependent (chaotic) flows, while we study the basic stationary flow with a constant horizontal shear ($V_0 = (Ay,0,0)$; $A = const$). Consequently, in these studies perturbation dynamics and the physics of energy exchange between perturbations and basic flow are different. Our study is carried out on the basis of the full linearized system of dynamic equations without invoking the filtering approximation. It is well known that symmetric perturbations (that do not depend on the zonal/streamwise coordinate) are stable if the Rossby number Ro < 1 (Ro = A/f, where f is the Coriolis parameter) and unstable if Ro > 1 (Bennets & Hoskins

1979; Kalashnik 2000, 2001; Xu Qin 1986). We analyze the dynamics of non-symmetric perturbations using the non-modal approach. Depending on the value of potential vorticity perturbation (PV) non-symmetric perturbations can be divided up into two types: wave/oscillatory with zero PV and slow vortex/aperiodic with nonzero PV. At Ro<<1 perturbations of these two types represent, correspondingly, fast inertial gravity waves and slow vortical geostrophic perturbations. Such a classification of perturbations is analogous to that accepted in the adjustment theory (Obukhov 1949; Blumen 1972; Gill 1982; Zeitlin, Reznik and Ben Jelloul 2003, Bartello 1995). We show that the energy of non-symmetric wave perturbations increases linearly for large times at Ro < 1. In other words, there takes place an algebraic amplification of non-symmetric shear internal waves. At Ro > 1 a time interval of the linear growth is preceded by an interval of exponential (explosive) growth. Such a behaviour represents mixed explosive-linear type of instability specific to shear flows. We also show that vortex and wave modes are coupled; pure vortical perturbations gain the basic flow energy and then are transformed into non-symmetric shear internal waves at Ro > 0.8. This kind of wave generation by vortices is also typical of smooth shear flows in hydrodynamics (Chagelishvili et al. 1997a) and casts doubt on the use of filtration of fast wave perturbations in the traditional quasigeostrophic models of geophysical hydrodynamics (Pedlosky 1987; Dimnikov & Filatov 1990; Doljanski et al. 1990; Shakina 1990). Coupling among modes of different timescales occurs also in stratified, rigidly (without shear) rotating flows (Bartello 1995), but in that case the coupling is of nonlinear origin, while in our problem the mode coupling due to flow shear is already present in the linear regime. The content of the present chapter includes the description of the following three basic effects:

(i) Algebraic growth of wave perturbations for Ro < 1,

(ii) Transient exponential/explosive growth of wave perturbations for Ro > 1,

(iii) Transformation of vortical perturbations into wave ones at Ro ~ 1.

None of these effects can be described/analyzed in the framework of the traditional spectral hydrodynamic stability theory.

2.1 **Mathematical formalism**

It is well known that (Pedlosky 1987) in the Boussinesq approximation the motion of a rotating stratified fluid on an *f* plane is governed by the system of equations:

$$\frac{d\mathbf{v}}{dt} + f[\hat{\mathbf{z}}, \mathbf{v}] = -\nabla\Phi + \sigma\hat{\mathbf{z}}, \qquad (1)$$

$$\frac{d\sigma}{dt} = 0, \qquad \mathrm{div}\mathbf{v} = 0,$$

where ***v*** is the velocity vector with the components *u, v, w* along the axes *x* (zonal coordinate)*; y* (azimuthal coordinate) and *z* (height from the earth's surface) respectively, $\sigma = -g\rho/\rho_*$, ρ is the deviation of density from the background value $\rho_* = const$, $\Phi = p/\rho_*$, p is the deviation of pressure from the hydrostatic value that corresponds to ρ_*, g – gravitational acceleration, f – Coriolis parameter (Gill 1982, Pedlosky 1987, LeBlond & Mysak 1978), **z** –the unit vector along the z-axis; $d/dt = \partial/\partial t + (\vec{v}, \nabla)$ -the total derivative operator. Consider Eq.(1) in the region of limited vertical extent $-\infty < x, y < +\infty$, $0 \le z \le H$ given $w = 0$ at the horizontal boundaries $z = 0$ and $z = H$ (there is no flow through the boundaries). From Eqs. (1) follows the conservation of potential vorticity (see Gill (1982) and Pedlosky (1987)):

$$\frac{dq}{dt} = 0, \qquad q = (\boldsymbol{\Omega}, \nabla\sigma), \qquad (2)$$

where **Ω**=*rot***v**+*f***z** – is the absolute curl of the velocity. In geophysical hydrodynamics instead of Eqs.(1) one often considers a simplified system replacing the equation of motion along the *z*-axis with the hydrostatic equation $\partial\Phi/\partial z = \sigma$. The hydrostatic approximation is valid if the horizontal scale of perturbations is much larger than the vertical one. For hydrostatic systems the conservation of potential vorticity has the form (2) where **Ω**=$(-\partial v/\partial z, \partial u/\partial z, \partial v/\partial x - \partial u/\partial y + f)$.

Investigate the linear stability of the following exact solution

$$\mathbf{V}_0 = (Ay, 0, 0), \qquad \sigma_0 = N^2 z, \qquad \Phi_0 = \Phi_*(z) - \frac{Af}{2}y^2, \qquad (3)$$

where $\partial\Phi_* / \partial z = N^2 z$, here the Brunt-Väisälä frequency is defined as $N^2 = -(g/\rho_*) d\rho_0 / dz \equiv d\sigma_0 / dz > 0$. It is simply a frequency with which fluid particles make vertical small oscillations around equilibrium height. Solution (3) represents a zonal horizontal flow with a constant horizontal shear *A,* vertical stratification and potential vorticity $q_0 = (f - A)N^2$. Such a representation of real meteorological flows corresponds to the second linear term of the power expansion of background velocity field in the small parameter $(l / V_0)\partial V_0 / \partial y$, where l – is the azimuthal length scale of the perturbation and V_0 - is the background flow. For simplicity we suppose that the mean flow has a constant Brunt-Väisälä frequency. Assuming $\mathbf{v}=\mathbf{V_0}+\mathbf{v`}, \sigma = \sigma_0 + \sigma', \Phi = \Phi_0 + \Phi'$ in Eqs.(1) and considering hydrostatic approximation for the small deviations from (3) we get (primes are ommited):

$$\frac{Du}{Dt} + (A - f)v = -\frac{\partial \Phi}{\partial x}, \qquad \frac{Dv}{Dt} + fu = -\frac{\partial \Phi}{\partial y}, \tag{4}$$
$$\frac{\partial \Phi}{\partial z} = \sigma, \qquad \frac{D\sigma}{Dt} + N^2 w = 0, \qquad \frac{\partial u}{\partial x} + \frac{\partial v}{\partial y} + \frac{\partial w}{\partial z} = 0,$$

where $D / Dt = \partial / \partial t + 2Ax\partial / \partial y$. From Eqs. (4) we can derive the conservation law:

$$\frac{Dq}{Dt} = 0, \qquad q = N^2 \left(\frac{\partial v}{\partial x} - \frac{\partial u}{\partial y} \right) - (A - f)\frac{\partial \sigma}{\partial z}, \tag{5}$$

representing the linearized form of Eq.(2) and playing a central role in the further study.

Equations (4) admit separation of variables – seek solutions in the form of a series of eigenfunctions of the operator d^2 / dz^2:

$$(u, v, \Phi) = \sum_{n=1}^{\infty} (u_n, v_n, \Phi_n) \cos \frac{n\pi z}{H}, \tag{6a}$$

$$(w, \sigma) = \sum_{n=1}^{\infty} (w_n, \sigma_n) \sin \frac{n\pi z}{H}. \tag{6b}$$

Such a procedure is well known in dynamic meteorology (cf. Gill 1982, Straub 2003). Substituting (6) into Eqs.(4) and excluding w_n, σ_n we arrive at the following equations of a rotating shallow water type

$$\frac{Du_n}{Dt} + (A - f)v_n = -\frac{\partial \Phi_n}{\partial x}, \qquad \frac{Dv_n}{Dt} + fu_n = -\frac{\partial \Phi_n}{\partial y}, \tag{7}$$

$$\frac{D\Phi_n}{Dt} + c_n^2 \left(\frac{\partial u_n}{\partial x} + \frac{\partial v_n}{\partial y} \right) = 0,$$

where $c_n = HN/\pi n$ is the velocity of *n*-th vertical mode of internal waves.

2.2 Dynamics of non-symmetric perturbations

Consider non-symmetric perturbations (when all perturbed quantities depend on the *x* coordinate) and, following the non-modal approach, introduce new co-moving coordinates:

$$t_1 = t, \qquad x_1 = x - Ayt, \qquad y_1 = y. \tag{8}$$

It is easy to verify that under this transformation Eqs.(7) become homogeneous with respect to the new coordinates x_1, y_1. So we can seek its solution in the following form:

$$(u_n, v_n) = (\tilde{u}, \tilde{v}) \cos(kx_1 + ly_1), \qquad \Phi_n = \tilde{\Phi} \sin(kx_1 + ly_1), \tag{9}$$

where *k, l* are the zonal and azimuthal wavenumbers respectively, $\tilde{u}, \tilde{v}, \tilde{\Phi}$ are the amplitudes depending only on time. It is convenient to rewrite the main equations in the nondimensional variables $tA \to t, (\tilde{u}/v_0, \tilde{v}/v_0) \to (\tilde{u}, \tilde{v}),$, $\Phi k/fv_0 \to \tilde{\Phi}$ where v_0 is the characteristic scale of the velocity and $A > 0$ (as we will show later, $A > 0$ is the range of main peculiarities/novelties). These amplitudes then evolve according to:

$$\mathrm{Ro}\frac{d\tilde{u}}{dt} = (1 - \mathrm{Ro})\tilde{v} - \tilde{\Phi}, \tag{10a}$$

$$\mathrm{Ro}\frac{d\tilde{v}}{dt} = -\tilde{u} - p(t)\tilde{\Phi}, \tag{10b}$$

$$\mathrm{FRo}\frac{d\tilde{\Phi}}{dt} = \tilde{u} + p(t)\tilde{v}, \tag{10c}$$

where $Ro = A/f$ is the Rossby number and $F \equiv f^2/c_n^2 k^2$ is the nondimensional parameter equal to the square of the ratio of the perturbation scale to the radius of the Rossby deformation. $p(t) \equiv l(t)/k = t_* - t, l(t) = l - kt, t_* \equiv l/k$. Note that in the physical variables (*x, y*) the solution (9) describes a harmonic plane wave with a time-dependent amplitude and phase $\Theta = kx + l(t)y$. As the azimuthal wavenumber $l(t)$ is time-dependent, the lines of constant phase rotate around the *z*-axis and become parallel to the streamwise in the limit $t \to \infty$. The parameter t_* defines the initial orientation of the phase lines: at $t_* > 0$ the angle between the phase lines and the direction of the mean flow is obtuse, at $t_* < 0$ -- sharp.

A remarkable feature of (10) is that it possesses the first integral

$$\mathrm{F}(1 - \mathrm{Ro})\tilde{\Phi} + \tilde{v} - p(t)\tilde{u} = \tilde{q} = const, \tag{11}$$

that corresponds to the conservation of potential vorticity (5). Using Eq. (11), system (10) is reduced to the second order inhomogeneous differential equation

$$\mathrm{FRo}^2 \frac{d^2\tilde{u}}{dt^2} + \omega^2(t)\tilde{u} = -p(t)\tilde{q}, \tag{12}$$

$$\omega^2(t) = 1 + \mathrm{F}(1 - \mathrm{Ro}) + p^2(t). \tag{13}$$

The other physical quantities $\tilde{v}, \tilde{\Phi}$ are expressed through $\tilde{q}, \tilde{u}$ and $d\tilde{u}/dt$

$$\tilde{v} = \frac{1}{1 + \mathrm{F}(\mathrm{Ro} - 1)^2}\left[p(t)\tilde{u} + \tilde{q} - \mathrm{FRo}(\mathrm{Ro} - 1)\frac{d\tilde{u}}{dt}\right], \tag{14a}$$

$$\tilde{\Phi} = \frac{1}{1 + \mathrm{F}(\mathrm{Ro} - 1)^2}\left[(1 - \mathrm{Ro})(p(t)\tilde{u} + \tilde{q}) - \mathrm{Ro}\frac{d\tilde{u}}{dt}\right]. \tag{14b}$$

The perturbation energy density has the form

$$\tilde{E} = \frac{1}{2}(\tilde{u}^2 + \tilde{v}^2 + \mathrm{F}\tilde{\Phi}^2) \tag{15}$$

and its time derivative equals the Reynolds stress term $\tilde{u}\tilde{v}$ with the minus sign $d\tilde{E}/dt = -\tilde{u}\tilde{v}$.

It is possible to classify modes involved in Eq. (12) from the mathematical and physical standpoints separately. Mathematically the general solution of Eq. (12) may be

written as the sum of two parts: a *general* solution of the corresponding homogeneous equation (oscillatory, wave mode) and a *particular* solution of this inhomogeneous equation. It should be emphasized that the particular solution of the inhomogeneous equation is not uniquely determined: the sum of a particular solution of the inhomogeneous equation and any particular solution of the corresponding homogeneous equation (i.e. wave mode solution) is also a particular solution of the inhomogeneous equation, i.e. the particular solution may comprise any dose of the wave mode.

Physically Eq. (12) describes two different modes/types of perturbations:

(1) wave mode $\tilde{u}^{(w)}$*;* that is oscillatory and is determined by a general solution of the corresponding homogeneous equation and has zero potential vorticity,

(2) vortex mode $\tilde{u}^{(v)}$*;* that is aperiodic, originated from the equation inhomogeneity ($-p(t)\tilde{q}$), and represents a nonoscillatory particular solution of the inhomogeneous equation. In the shearless limit this mode is independent of time and has zero divergence, but nonzero potential vorticity. Therefore, vortex/aperiodic mode is uniquely determined. From the above argument it follows that the correspondence between the aperiodic vortex mode and the particular solution of the inhomogeneous equation is quite unambiguous; the vortex mode is associated only with such a particular solution that does not contain any oscillatory part. The amplitude of the vortex mode is proportional to $\tilde{q}$ and goes to zero when $\tilde{q} = 0$. We will see below that such a separation of modes is possible only far from the point t_*. In the following we will keep to the physical standpoint of separation of perturbation modes.

Thus, the general solution of Eqs.(12-14) can be expressed as a superposition of oscillatory/wave and aperiodic/vortex components and we write:

$$\tilde{u} = \tilde{u}^{(\mathrm{w})} + \tilde{u}^{(\mathrm{v})}, \quad \tilde{v} = \tilde{v}^{(\mathrm{w})} + \tilde{v}^{(\mathrm{v})}, \quad \tilde{\Phi} = \tilde{\Phi}^{(\mathrm{w})} + \tilde{\Phi}^{(\mathrm{v})}. \qquad (16)$$

In fact, the (modified) initial value problem is solved by Eqs. (12-14) (or equivalently by Eqs. (10)). The character of the dynamics depends on a mode of perturbation inserted

initially in Eqs. (10, 12-14): a pure wave mode (without admixes of aperiodic vortices) or a pure aperiodic vortex mode (without admixes of waves).

The performed classification of perturbations (into vortex and wave ones) depending on the value of the potential vorticity corresponds to an analogous classification of perturbations into stationary (geostrophic) and non-stationary (wave), accepted in the classical linear theory of geostrophic adaptation (Obukhov 1949; Blumen 1972; Gill 1982).

From Eq. (13) it follows that one has to distinguish between two cases in the analysis of Eq. (12): at Ro < 1 $\omega^2(t)$ is always positive, while at Ro > 1 it may change sign. This change results in the qualitative changes of the structure of the solution.

For purposes of further analysis let us evaluate the characteristic values of the parameters. For the Earth's atmosphere in the middle latitudes ($f = 10^{-4} s^{-1}, N = 10^{-2} s^{-1}, H = 10 km$) the deformation radius of the first baroclinic mode is $L_{R.atm} = 1000/\pi = 318.5 km$ and for oceans ($N = 10^{-3} s^{-1}, H = 5 km$) is $L_{R.ocean} = 50/\pi = 15.9 km$. Values of Ro depend on the structure of the flow and may vary substantially. For smooth atmospheric flows of synoptic scale L = 1000 *km*~ $L_{R\ atm}$ and characteristic velocity U = 10 $m\ s^{-1}$, horizontal shear equals $a = U/L = 10^{-5}\ s^{-1}$; consequently, Ro = 0.1. The Rossby number Ro is considerably higher in the areas of jet streams related to atmospheric fronts, where the characteristic velocity variation U = 30 $m\ s^{-1}$ is achieved on a scale L = 100 *km* (see Gill (1982) and Pedlosky (1987)). In this case $A = 3 \square 10^{-4}$ s^{-1} and Ro = 3. Similarly, for oceanic synoptic vortices with L = 50 *km* and U = 5 $cm\ s^{-1}$, the horizontal shear equals $A = 10^{-6}\ s^{-1}$ and consequently Ro = 10^{-2}. Again, this value is considerably higher for intensive oceanic jet streams. Thus, the Rossby number of realistic meteorological flows may be either Ro<<1 or Ro ~1. In the following we focus on such values.

2.2.1. **Ro<<1 regime. WKB analysis**

Here we study (Kalashnik et al. 2004) the dynamics of perturbations for the values of parameters (Ro<<1, $F = O(1)$) typical for the synoptic scale atmospheric and oceanic flows (Gill 1982; Pedlosky 1987). In this limit one can use WKB analysis and find an asymptotic solution of Eq. (12). In the first approximation the general solution of homogeneous equation (at $\tilde{q} = 0$) has the form

$$\tilde{u}^{(\mathrm{w})} = \sqrt{\frac{C}{\omega(t)}}\cos\phi(t), \qquad \phi(t) = (\sqrt{\mathrm{F}}\mathrm{Ro})^{-1}\int_0^t dt'\omega(t') + \phi_0,$$

where ϕ_0 is the initial phase. It is clear that the value of the constant C defines the amplitude of the wave and the sign defines the direction of wave propagation. Below will be considered for simplicity the positive values of C and $\omega(t)$. In the first approximation the aperiodic particular solution of Eq. (12) has the form (Nayfeh 1982; Moiseev 1987):

$$\tilde{u}^{(\mathrm{v})} = -\frac{p(t)\tilde{q}}{\omega^2(t)}.$$

Note that adding to this particular solution any solution of the homogeneous equation one gets also particular solution. However, it is the only slow solution free from oscillations. Thus, accurate to $O(\mathrm{Ro})$ for $\tilde{u}, \tilde{v}, \tilde{\Phi}$ one can write:

$$\begin{aligned}
\tilde{u} &= \tilde{u}^{(\mathrm{w})} + \tilde{u}^{(\mathrm{v})} = \sqrt{\frac{C}{\omega(t)}}\cos\phi(t) - \frac{p(t)\tilde{q}}{\omega^2(t)}, \\
\tilde{v} &= \tilde{v}^{(\mathrm{w})} + \tilde{v}^{(\mathrm{v})} = \frac{\sqrt{C}}{1+\mathrm{F}}\left(\frac{p(t)}{\sqrt{\omega(t)}}\cos\phi(t) - \sqrt{\mathrm{F}\omega(t)}\sin\phi(t)\right) + \frac{\tilde{q}}{\omega^2(t)}, \\
\tilde{\Phi} &= \tilde{\Phi}^{(\mathrm{w})} + \tilde{\Phi}^{(\mathrm{v})} = \frac{\sqrt{C}}{1+\mathrm{F}}\left(\frac{p(t)}{\sqrt{\omega(t)}}\cos\phi(t) + \sqrt{\frac{\omega(t)}{\mathrm{F}}}\sin\phi(t)\right) + \frac{\tilde{q}}{\omega^2(t)}.
\end{aligned} \tag{17}$$

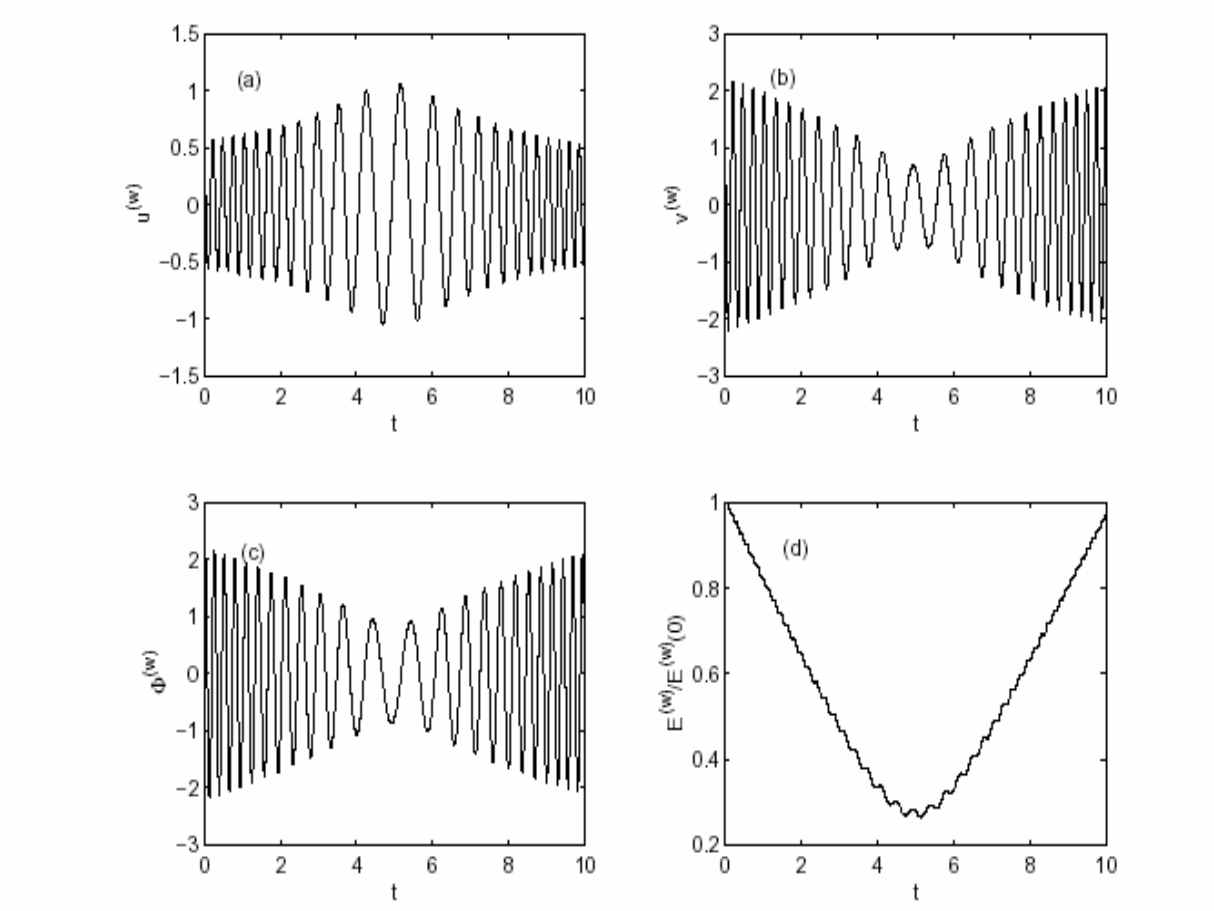

Figure 1. Evolution of the perturbed quantities $\tilde{u}^{(w)}$, $\tilde{v}^{(w)}$, $\tilde{\Phi}^{(w)}$ and the normalized energy $\tilde{E}^{(w)}/\tilde{E}^{(w)}(0)$ for a wave mode perturbation $(\tilde{q}=0)$ with the initial values $\tilde{u}^{(w)}(0)=0.5$, $\tilde{v}^{(w)}(0)=0.9$, $\tilde{\Phi}^{(w)}(0)=2$ at $\mathrm{Ro}=0.2$, $\mathrm{F}=1$ and $t_*=5$ are presented in panels (a)–(d), respectively. The perturbed quantities oscillate with a variable frequency due to the velocity shear and exchange energy with the mean flow. This exchange results in the linear amplification of the wave mode energy at $t \gg t_*$ (algebraic instability).

Outline peculiarities of the wave and vortex components separately. The wave parts of the solutions (17) describe oscillations with an amplitude $a(t)$ and phase $\Theta(t)$, for instance, $\tilde{v}^{(w)} = a_{\tilde{v}}(t)\cos\theta_{\tilde{v}}(t)$ where $\theta_{\tilde{v}}(t) = \phi(t) + \alpha_{\tilde{v}}(t)$, $tg\,\alpha_{\tilde{v}}(t) = \sqrt{F}\,\omega(t)/p(t)$ and $a_{\tilde{v}}(t) = \sqrt{F\omega(t) + p^2(t)\omega^{-1}(t)}\sqrt{C}/(1+F)$. Simple analysis shows that $a_{\tilde{u}}(t)$ reaches a maximum at $t = t_*$ and then decreases. Contrary to this, amplitudes $a_{\tilde{v}}(t), a_{\tilde{\Phi}}(t)$ reach a minimum at $t = t_*$ and then increase according to the square root law. The growth of the amplitudes results in the unlimited growth of the wave energy at asymptotically large times. The same is true for the time-dependent frequency $\omega(t)$ that grows linearly with time at $t \to \infty$*:* This peculiarity is due to the flow shear; in the shearless limit the wave

perturbations represent ordinary internal gravitational waves. Examples of the numerically calculated time development of $\tilde{u}^{(w)}, \tilde{v}^{(w)}, \tilde{\Phi}^{(w)}$ at $\tilde{q} = 0, Ro = 0.2, F = 1, t_* = 5$ are shown in Fig. 1. The numerical solutions are in perfect accord with the analytical ones. Draw attention that the vortical solutions (see vortex parts of (17) in the coordinate representation are reduced to the geostrophic relations $fv_n = \partial\Phi_n / \partial x, fu_n = -\partial\Phi_n / \partial y$, i.e., the vortex components of the solutions (17) describe slowly varying geostrophic perturbations. It is not difficult to understand that the traditional quasigeostrophic approach involving filtration of fast wave motions (Pedlosky 1987, Dimnikov & Filatov 1990, Doljanski et al. 1990, Shakina 1990) is not able to describe the flow instability associated with the linear growth of the wave perturbations.

Analyze the energy equation. As the solution contains rapidly oscillating components, main interest represents not energy itself, but its averaged value $\tilde{e} = \langle \tilde{E} \rangle$ over the fast oscillation period $T = 2\pi / \phi(t)$

$$\tilde{e}(t) = \frac{1}{2}\left\langle \left[\sqrt{\frac{C}{\omega(t)}} \cos\phi(t) - \frac{p(t)\tilde{q}}{\omega^2(t)} \right]^2 \right\rangle +$$

$$+\frac{1}{2}\left\langle \left[\frac{\sqrt{C}}{1+\mathrm{F}} \left(\frac{p(t)}{\sqrt{\omega(t)}} \cos\phi(t) - \sqrt{\mathrm{F}\omega(t)} \sin\phi(t) \right) + \frac{\tilde{q}}{\omega^2(t)} \right]^2 \right\rangle +$$

$$+\frac{\mathrm{F}}{2}\left\langle \left[\frac{\sqrt{C}}{1+\mathrm{F}} \left(\frac{p(t)}{\sqrt{\omega(t)}} \cos\phi(t) + \sqrt{\frac{\omega(t)}{\mathrm{F}}} \sin\phi(t) \right) + \frac{\tilde{q}}{\omega^2(t)} \right]^2 \right\rangle =$$

$$= \frac{1}{2}\left[C\omega(t) + \frac{\tilde{q}^2}{\omega^2(t)} \right] \equiv \tilde{e}^{(\mathrm{w})}(t) + \tilde{e}^{(\mathrm{v})}(t).$$

where $\tilde{e}^{(v)}$, as other vortex parts of (17), is determined by $\tilde{q}$. This equation shows that the wave and vortex component energies are additive at Ro<<1. Besides, if $t_* > 0$, the aperiodic/vortex mode energy $\tilde{e}^{(v)}$ transiently grows for $t < t_*$ achieving a maximum at $t = t_*$ and monotonically decays for $t > t_*$. The oscillating/wave energy $\tilde{e}^{(w)}$ achieves a minimum at $t = t_*$ and then grows linearly at large times. Combining these behaviours

one can easily construct four different scenarios of the total energy time dynamics depending on the values of the parameters *C;* $\tilde{q}$ and t_*.

2.2.2 **Ro ~ 1 regime. Numerical solution**

Here we present the Ro~1 case (Kalashnik et al. 2006). In this regime the adiabatic approximation is no longer valid during the whole evolution. Far from the point $t_*, (|t| << t_*)$, when $|p(t)| >> 1$ the WKB approximation holds, so one can explicitly construct the $\tilde{u}^{(w)}, \tilde{u}^{(v)}$ solutions of Eq.(12) (Nayfeh 1982). For these times the wave mode rapidly oscillates and the vortex mode varies slowly and there is no coupling (energy exchange) between these two modes; they evolve independently. Perturbation is the sum of energies of these two modes. However, on approaching the point t_* the total energy can no longer be represented as a sum of energies because the timescales of the vortex and wave modes are comparable. As a result a mode transformation/conversion (a transfer of energy from one mode to another may take place. This process can easily be traced by numerically integrating Eqs.(11-15).

First consider a pure wave perturbation ($\tilde{q} = 0$) with $t_* = l/k >> 1$ initially imposed on the basic flow. In Fig.2 we present the evolution of the corresponding perturbed quantities $\tilde{u}, \tilde{v}, \tilde{\Phi}$ and normalized wave energy $\tilde{e}^{(w)}$ at *F* = 25 and Ro = 0.9 < 1. In the beginning the energy of the wave perturbation decreases. Then in the vicinity of t_* some algebraic growth of the energy take place that is followed by a linear growth. For large values of *F* (for example, *F*= 100) and at Ro > 1 this algebraic growth acquires exponential nature and is more pronounced and substantial as it is shown in Fig.3. Such a behaviour represents mixed explosive-linear type of instability specific to shear flows. Qualitative analysis of the explosive behaviour of the wave mode is given later in this subsection. Another novelty at Ro ~ 1 is the emergence of oscillations from aperiodic perturbations, or physically, *the generation of the wave mode by the vortex mode* that is a consequence of the above mentioned mode coupling and ultimately of shear.

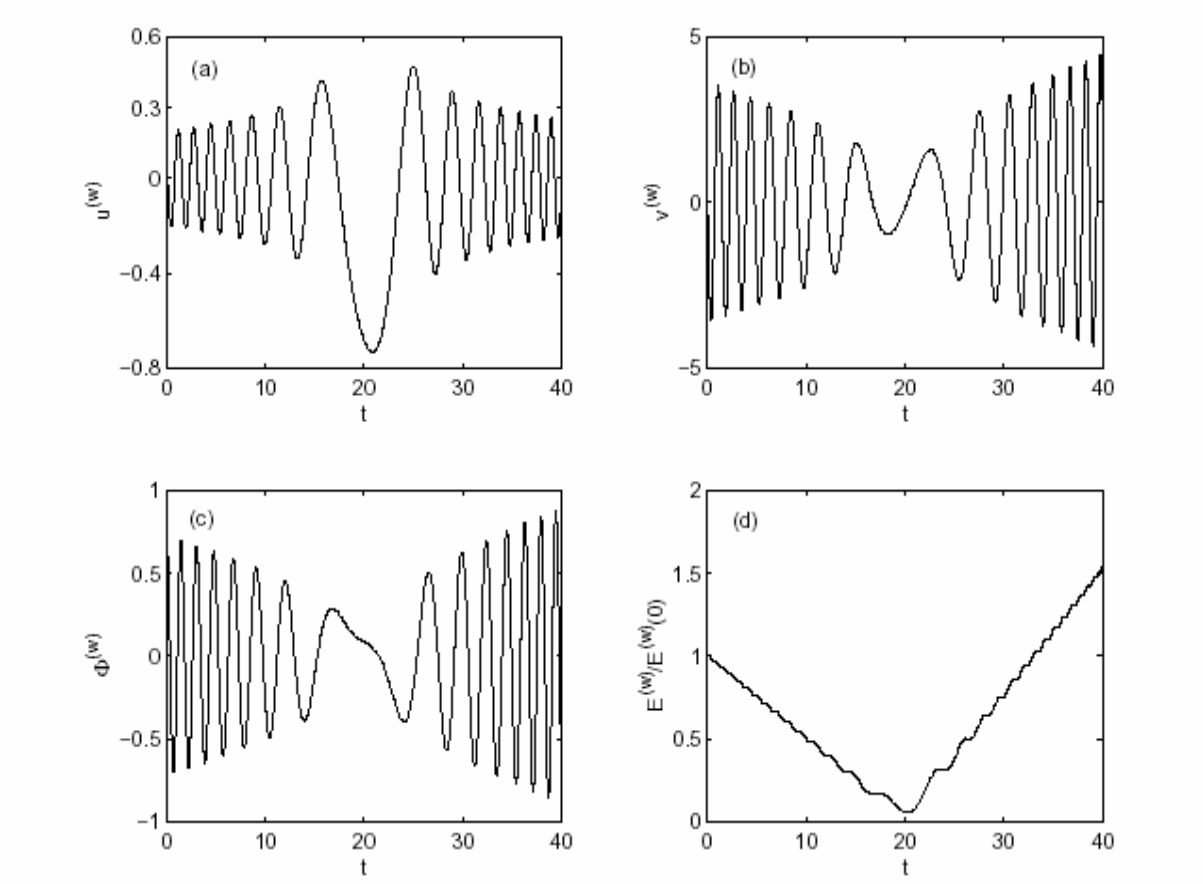

Figure 2. Evolution of the perturbed quantities $\tilde{u}^{(\mathrm{w})}, \tilde{v}^{(\mathrm{w})}, \tilde{\Phi}^{(\mathrm{w})}$ and the normalized energy $\tilde{E}^{(\mathrm{w})}/\tilde{E}^{(\mathrm{w})}(0)$ for a wave mode perturbation $(\bar{q}=0)$ with the initial values $\tilde{u}^{(\mathrm{w})}(0)=0.1, \tilde{v}^{(\mathrm{w})}(0)=0.2, \tilde{\Phi}^{(\mathrm{w})}(0)=0.72$ at $\mathrm{Ro}=0.9, \mathrm{F}=25$ and $t_*=20$ are presented in panels (a)–(d) respectively. In this case the perturbed quantities $\tilde{u}^{(\mathrm{w})}, \tilde{v}^{(\mathrm{w})}, \tilde{\Phi}^{(\mathrm{w})}$ and the wave energy $\tilde{E}^{(\mathrm{w})}$ exhibit transient algebraic amplification in the vicinity of $t=t_*$ and the energy itself increases linearly at $t \gg t_*$. Therefore, the flow is unstable with respect to wave mode perturbations.

the generation becomes noticeable at Ro = 0.4, but in this case (and also for smaller values) large ($O(100)$) transient growth of vortex energy dominates the dynamics (see Fig.4). This transient growth phenomenon is a direct consequence of the non-orthogonality of shear flow operators and resembles that found in Reddy & Henningson (1993) or Farrell & Ioannou (2000) for bounded flows. It is in apparent conflict with the result of modal theory according to which flow of the type considered here (Couette flow) is stable for all Reynolds numbers and at all wavelength. But, as was discussed in the Introduction, there is actually no conflict; the result of modal theory applies for asymptotically large times, while transient growth is essentially a finite time interval phenomenon. Despite asymptotic stability there may be self-sustained turbulence

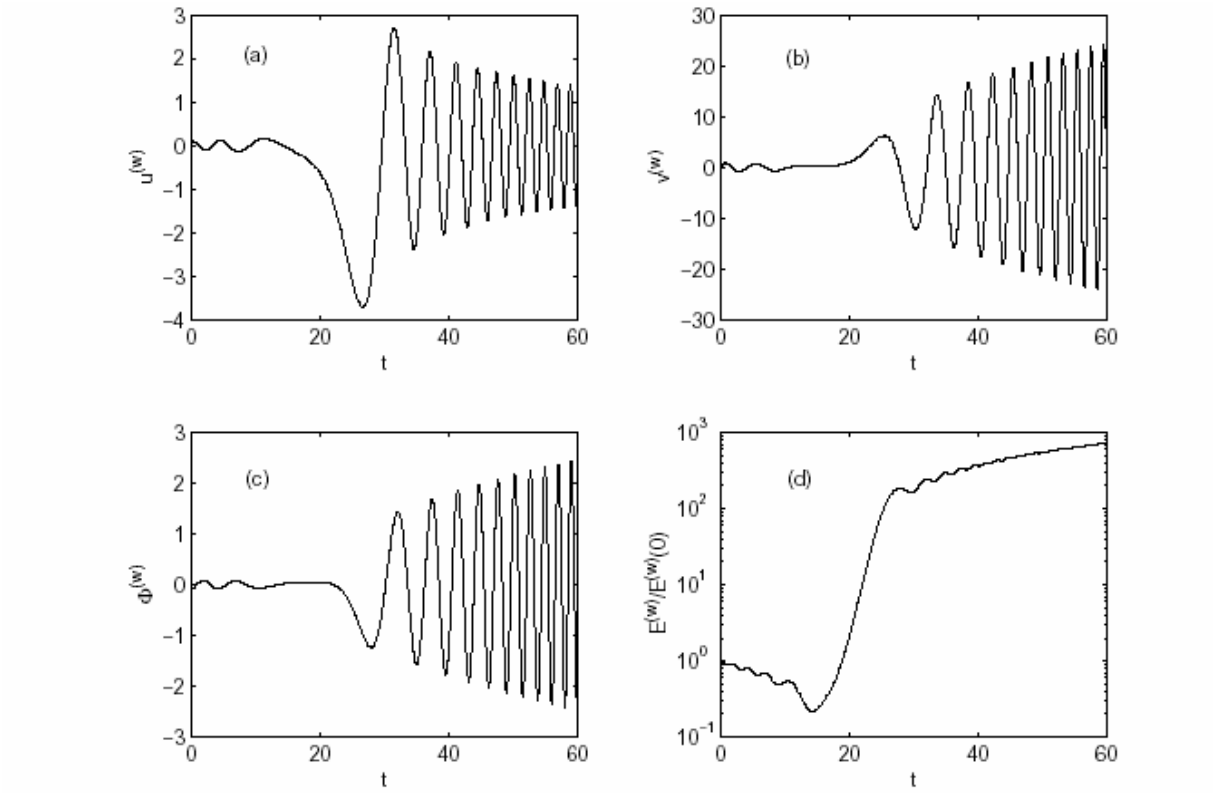

Figure 3. Evolution of the perturbed quantities $\tilde{u}^{(w)}, \tilde{v}^{(w)}, \tilde{\Phi}^{(w)}$ and the normalized energy $\tilde{E}^{(w)}/\tilde{E}^{(w)}(0)$ for a wave mode perturbation ($\tilde{q}=0$) with the initial values $\tilde{u}^{(w)}(0)=0.1, \tilde{v}^{(w)}(0)=0.2, \tilde{\Phi}^{(w)}(0)=-0.09$ at $\mathrm{Ro}=1.2, \mathrm{F}=100$ and $t_*=20$ are presented in panels (a)–(d) respectively. The transient explosive growth is more pronounced. As it is seen, the energy decreases in the interval $0<t<t_*$, goes through the period of rapid and large transient explosive growth in the vicinity of $t=t_*$ and then continues to increase relatively slowly (in the ordinary scale this last stage of evolution corresponds to linear growth).

provoked and fed just by this transient growth (*bypass* scenario) (Reshotko 2002, Chapman 2002, Bagget et al. 1995, Gebhardt & Grossman 1994, Grossman 2000, Chagelishvili et al. 1996a, Rempfer 2003). At Ro > 0.8 wave generation becomes a main feature in the shear flow dynamics (see Fig.5). Below we describe this new phenomenon.

Consider now the case when a pure vortex perturbation ($\tilde{q}\neq 0$) is imposed initially on the mean flow. This perturbation is cleared from wave admixes at $t=0$ using a numerical iterative method (Moiseev 1987, Nayfeh 1982, Bodo et al. 2005 or subsection 3.2.3). The evolution of the perturbed quantities $\tilde{u},\tilde{v},\tilde{\Phi}$ and its normalized energy $\tilde{E}/\tilde{E}(0)$ are shown in Fig.5. Evolving in the shear flow the imposed vortex mode gains energy from the mean flow and grows, but retains its aperiodic nature till $t<t_*$. In the vicinity of t_* oscillations arise, i.e., we observe the appearance of waves. Thus, it turns out that the

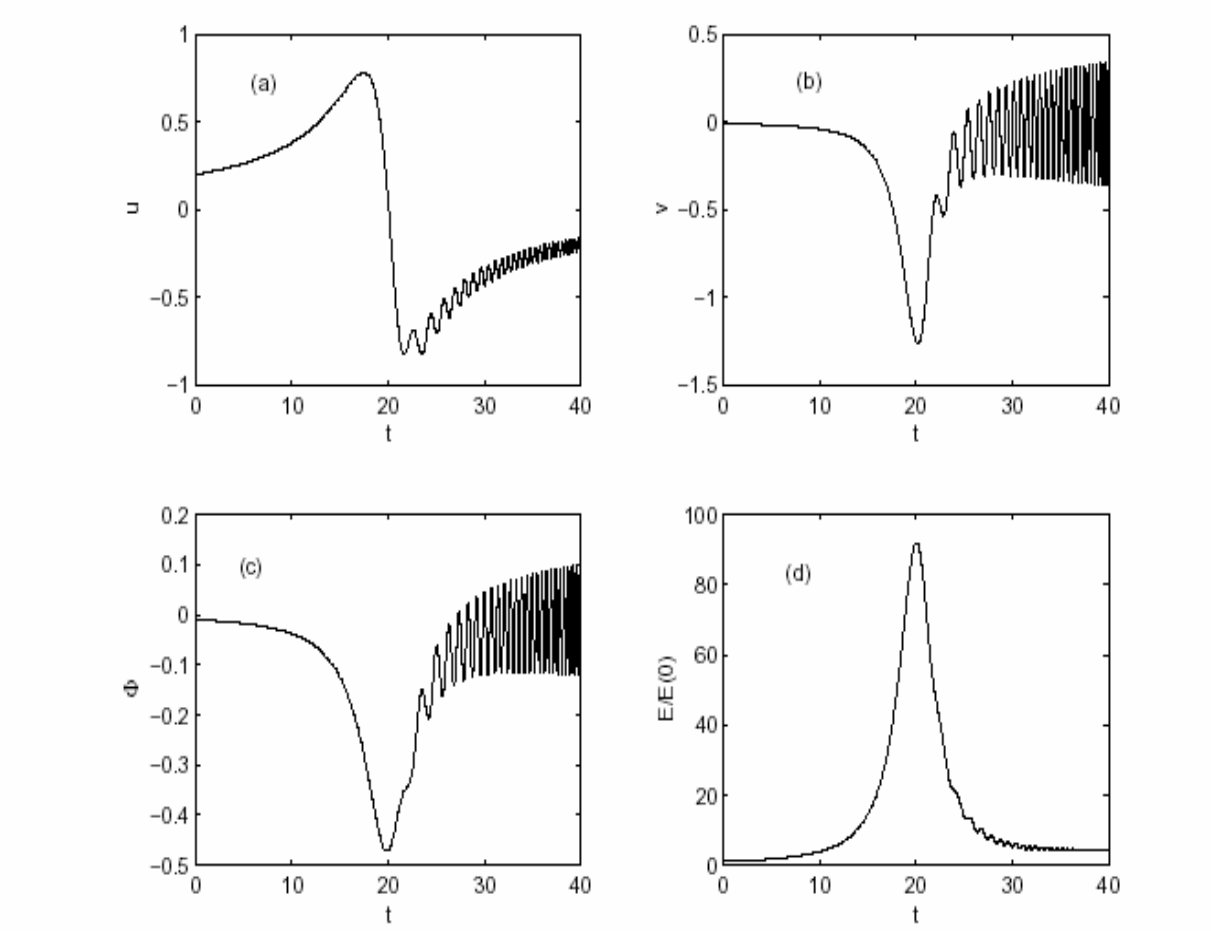

Figure 4. Evolution of the perturbed quantities $\tilde{u}, \tilde{v}, \tilde{\Phi}$ and the normalized energy $\tilde{E}/\tilde{E}(0)$ for an initially imposed pure vortex perturbation $(\tilde{q} \neq 0)$ at $\mathrm{Ro} = 0.4, \mathrm{F} = 10$ and $t_* = 20$ are presented in panels (a) - (d), respectively. Corresponding to this vortex mode initial values are $\tilde{u}(0) = 0.2, \tilde{v}(0) = -0.01, \tilde{\Phi}(0) = -0.01$. In the dynamics of these quantities transient growth is dominant, but the wave generation starts to be noticeable.

linear dynamics of the vortex mode perturbation is followed by the wave generation. In the vicinity of t_* timescales of the vortex and wave modes are comparable and the perturbations are not separable/distinguishable, we have some mix of aperiodic and oscillatory modes. At later times ($t >> t_*$) the characteristic timescale of the wave mode becomes much shorter than that of the vortex mode and the modes are well distinguishable. The nature of the wave generation phenomenon (also called conversion of vortices into waves) is described in detail for the simplest shear flow in Chagelishvili et al. (1997a). Thus, vortex mode perturbations are important in that they are able to generate waves which effectively extract energy from the mean flow and grow asymptotically linearly and may render flow linearly unstable. However, their nonlinear

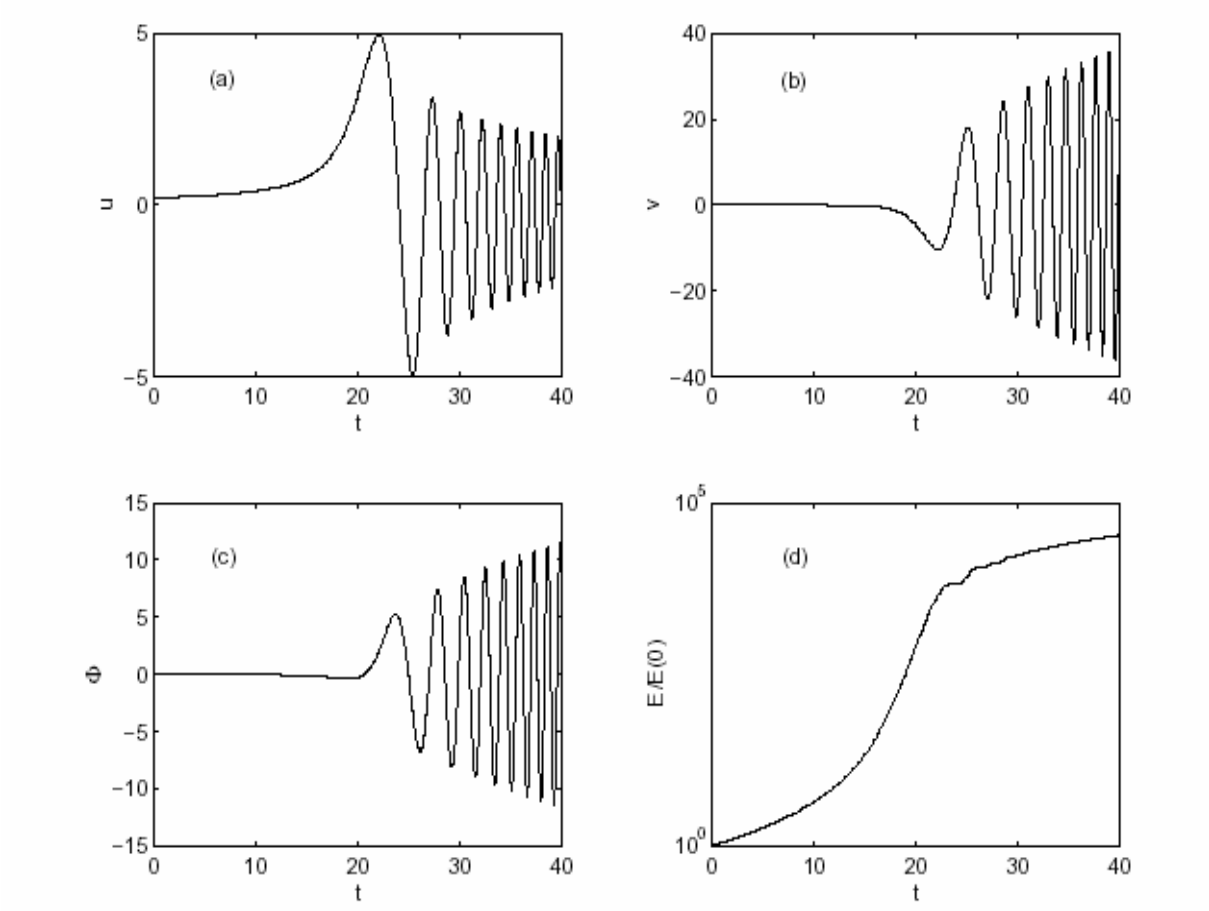

Figure 5. Evolution of the perturbed quantities $\tilde{u}, \tilde{v}, \tilde{\Phi}$ and the normalized energy $\tilde{E}/\tilde{E}(0)$ for an initially imposed pure vortex perturbation ($\tilde{q} \neq 0$) at $\mathrm{Ro} = 1.2, \mathrm{F} = 10$ and $t_* = 20$ are presented in panels (a) - (d) respectively. Evolving in the shear flow the vortex mode perturbation with the initial values $\tilde{u}(0) = 0.2, \tilde{v}(0) = -0.01, \tilde{\Phi}(0) = -0.01$ gaining energy from the mean flow and amplifying, retains its aperiodic nature till $t < t_*$. After time $t = t_*$ (at which $p(t_*) = 0$) the appearance of the wave mode and subsequent amplification of the wave energy is observed.

development should be rigorously analyzed in order to find out whether turbulence eventually sets in or not. This can be done through complex numerical simulations.

Before proceeding to the qualitative analysis we would like to remind the reader of symmetric instability, since it helps to gain a better insight into the explosive behaviour of the wave mode. As it is well known, this type of instability may occur when perturbations do not depend on the streamwise coordinate x. For them $\partial / \partial x = 0$, $D / Dt = \partial / \partial t$ and system (7) is reduced to a single equation for v_n

$$\frac{\partial^2 v_n}{\partial t^2} - f^2(\mathrm{Ro} - 1)v_n - c_n^2 \frac{\partial^2 v_n}{\partial y^2} = 0.$$

Looking for a solution of this equation in the form $v_n = \exp(\gamma t)\cos(ly)$, for the growth rate one gets

$$\gamma^2 = f^2(\mathrm{Ro}-1) - c_n^2 l^2.$$

From this expression we deduce that the flow is symmetrically stable at Ro < 1 and unstable at Ro > 1 for wavenumbers in the range

$$l^2 < (\mathrm{Ro}-1)\frac{f^2}{c_n^2}.$$

One can rewrite the latter condition in the form $L > 2\pi L_R/\sqrt{Ro-1}$, where is $L = 2\pi/l$ the wavelength and $L_R = c_n/f$ the baroclinic radius of the Rossby deformation for *n*-th mode. According to the above expression symmetric instability carries a long wavelength character with the largest growth rate at $l = 0$. One should draw attention that the condition Ro > 1 may be fulfilled for positive (anticyclonic) values of the shear parameter A (for such flows vorticity rot**v**=-A**z** is antiparallel to the planetary vorticity 2f**z**). Thus, cyclonic shear flows ($A < 0$) are always symmetrically stable.

We now turn to the qualitative analysis of the explosive growth. Note that when Ro >1, $\omega^2(t)$ may change its sign (if Ro < 1, $\omega^2(t)$ is always positive and we have not any explosive growth, Fig.2). From Eq. (13) it follows that change of sign occurs at Ro >1+1/F, Taking into account $F = (f/c_n k)^2$, this inequality becomes k^2<(Ro-1)f^2/c_n^2 The last condition formally coincides with the condition of symmetric instability and is satisfied for long waves in the zonal (streamwise) direction. For the further analysis rewrite Eq. (13) as

$$\omega^2(t) = (t-t_1)(t-t_2),$$

where formally $t_{1,2} = t_* \mp \sqrt{F(Ro-1)-1}$. However, in the considered case of Ro > 1 + 1/F and F>>1 it reduces to $t_{1,2} = t_* \mp \sqrt{F(Ro-1)}$. The homogeneous part of Eq. (12) has the form

$$\mathrm{FRo}^2\frac{d^2\tilde{u}^{(\mathrm{w})}}{dt^2} + (t-t_1)(t-t_2)\tilde{u}^{(\mathrm{w})} = 0.$$

The last equation is a classic example of equation with turning points, i.e., points at which coefficient of the second term changes sign. This change of sign is reflected in the alternation of solution types (from oscillatory to exponential or vice versa). If $0 < t_1 < t_2$ there are two turning points. In the interval $(0,\ t_1)$ the solution is oscillatory, in the interval $(t_1,\ t_2)$ has an exponential (explosive) behaviour and at $t > t_2$ is oscillatory again. If $t_1 < 0 < t_2$ in the integration interval there is only one turning point t_2 crossing which the exponential behaviour (at $0 < t < t_2$) changes into oscillatory (at $t > t_2$).

The existence of the turning points in the non-symmetric problem may readily be explained in terms of the symmetric instability. Note that the condition of symmetric instability can be rewritten in the form: $-l_{cr} < l < l_{cr};\ l_{cr} = f\sqrt{Ro-1}/c_n$. As it was stressed earlier, in the physical variables (x,y) solution (9) corresponds to perturbations with a time-dependent meridional wavenumber: $l(t) = l - kt$: If $l(0) = l > {}_{lcr}$, then, as it is clearly seen, the wavenumber $l(t)$ "enters" the symmetric instability interval $(-l_{cr},\ l_{cr})$ at the moment t_1 and leaves it at t_2. The values of t_1 and t_2 are found from the relation $l(t) = l_{cr}$ and have the form $t_{2,1} = (l \pm l_{cr})/k$. These moments are just the turning points $t_1,\ t_2$. If $0 < l(0) < l_{cr}$ then at the initial moment of time the wavenumber $l(t)$ is already within the interval $(-l_{cr},\ l_{cr})$ and leaves it in the course of time; here we have only one turning point t_2. An example of $\tilde{u}^{(w)}, \tilde{v}^{(w)}, \tilde{\Phi}^{(w)}$ time development in the case of two turning points is presented in Fig.3 (turning points in this figure are $t_1 \approx 15.5$ and $t_2 \approx 24.5$). Stress that the energy increases linearly for later times $t > t_2$. The above described behaviour represents mixed exponential-algebraic type of hydrodynamic instability. This kind of instability may be associated with the rather complicated dynamics: t_1 and t_2 are defined by a wavenumber l. I.e., the time interval $(t_1,\ t_2)$ of explosive behaviour is different for different l. Therefore, for waves with different l, the explosive stage sets in at different moments of time. Consequently, the dynamics of some packet of internal waves should represent an alternation of explosion processes.

2.3 Influence of viscosity

Viscosity can be easily incorporated in the main dynamical equations. This is accomplished by adding the terms $\mu\Delta u_n, \mu\Delta v_n, \mu\Delta\Phi_n$ to the rhs of Eqs. (7). Here μ is the coefficient of horizontal viscosity and Δ is the two dimensional Laplas operator. Carrying out the operations (8, 9), for the nondimensional amplitudes instead of (10) we get the system

$$\mathrm{Ro}\frac{d\tilde{u}}{dt} = -(\mathrm{Ro}-1)\tilde{v} - \tilde{\Phi} - \mathrm{E}\left[1+p^2(t)\right]\tilde{u},$$
$$\mathrm{Ro}\frac{d\tilde{v}}{dt} = -\tilde{u} - p(t)\tilde{\Phi} - \mathrm{E}\left[1+p^2(t)\right]\tilde{v},$$
$$\mathrm{FRo}\frac{d\tilde{\Phi}}{dt} = \tilde{u} + p(t)\tilde{v} - \mathrm{FE}\left[1+p^2(t)\right]\tilde{\Phi},$$

where E = $\mu k^2 / f$ is the Eckman number. Making a change of variables

$$(\tilde{u}, \tilde{v}, \tilde{\Phi}) = (\hat{u}, \hat{v}, \hat{\Phi}) \exp\left[-\frac{\mathrm{E}}{\mathrm{Ro}}\int_0^t \left(1+p^2(t')\right)dt'\right],$$

we get the previous system (10). Thus, the influence of the horizontal viscosity is reduced to the multiplication of the physical quantities by the corresponding decaying exponent. It follows that, the viscosity diminishing the amplitudes, does not affect the instant frequency of time oscillations (the latter tends to infinity at large times).

It is interesting to follow how the viscosity damps the wave energy at Ro << 1. In this case the wave energy density takes the form

$$\tilde{\epsilon}^{(\mathrm{w})} = \frac{1}{2}C\omega(t)\exp\left[-\frac{2\mathrm{E}}{\mathrm{Ro}}\int_0^t \left(1+p^2(t')\right)dt'\right].$$

Consider the limit E/Ro =δ << 1*:* From this expression it is easy to show, that the energy decreases till a moment $t^{(1)} = t_* + (1 + F)\delta/2$ and then increases till $t^{(2)} = t_* + (2\delta)^{-1/3}$=3. After that it begins to diminish fully under the action of viscosity. As $t^{(2)} \to \infty$ at $\delta \to 0$, the interval of the algebraic growth is too large at small viscosity.

2.3 Bounded flows

In this section we consider a theorem (Kalashnik 2004, private communication), a sufficient criterion, for the stability of a geostrophic zonal flow when we can not ignore channel walls bounding the flow. This is the case when the azimuthal scale of perturbations is comparable to the channel width. For perturbations with characteristic scales much smaller than the channel dimensions (for example, some localized packet of waves) we can use results obtained in the preceding subsections, however, as perturbation scale increases channel walls come into play and begin to influence the perturbation dynamics. The theorem is valid only for wave mode perturbations although this fact in no way detracts from its importance since, as we have seen, the main part in the asymptotic instability are played by wave-type perturbations. It should also be noted that just such perturbations are usually considered in the modal treatment (Narayan et al. 1987). As for large scale vortex mode perturbations their dynamics/evolution should be analyzed via numerical calculations.

Let us consider a channel bounding the flow in the azimuthal y direction with two rigid walls (Fig. 6).

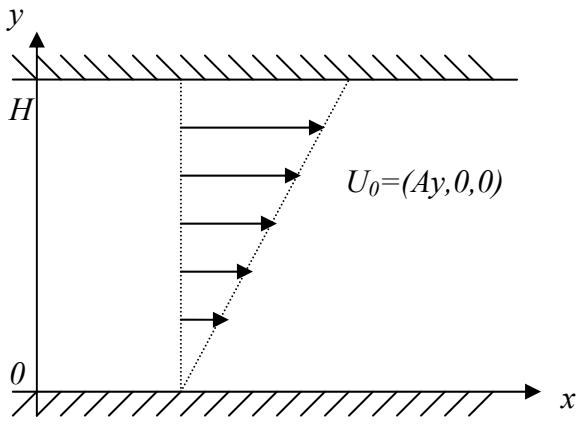

Fig.6

Recall the main equations (7) describing the linear evolution of wave mode perturbations (index n of the vertical mode is omitted)

$$\frac{Du}{Dt} + (A - f)v = -\frac{\partial \Phi}{\partial x}, \qquad \frac{Dv}{Dt} + fu = -\frac{\partial \Phi}{\partial y},$$

$$\frac{D\Phi}{Dt}+c^2\left(\frac{\partial u}{\partial x}+\frac{\partial v}{\partial y}\right)=0,\quad q=\left(\frac{\partial v}{\partial x}-\frac{\partial u}{\partial y}\right)+\frac{A-f}{c^2}\Phi=0, \tag{18}$$

where the last equation is the condition of zero potential vorticity. The channel width is H. The azimuthal component of the velocity v satisfies the boundary conditions: v=0 at y=0, H. This condition is analogous to the condition along the z-axis and states that there is no flow through the rigid walls.

Let us now derive a Lagrangian density that will give us first three equations of (18) (Narayan et al. 1987). First introduce the displacement vector $\vec{\xi}(\xi_x(\vec{r},t),\xi_y(\vec{r},t))$ for fluid elements. This vector characterizes the perturbed motion of each fluid element and is a function of time and element's Lagrangian position vector $\vec{r}$, i.e., the place to which a given fluid element would have been carried at a given time by the unperturbed flow. It is easy to show that the velocity components and pressure are expressed via the displacement vector in the following way

$$u(\vec{r},t)=\frac{D\xi_x}{Dt}-A\xi_y,\qquad v(\vec{r},t)=\frac{D\xi_y}{Dt},\qquad \Phi(\vec{r},t)=-c^2 div\vec{\xi}, \tag{19}$$

where as before $D/Dt=\partial/\partial t+Ay\partial/\partial x$. The third equation is the solution of the corresponding third equation of (18). As it is clear, the introduction of the displacement vector has simplified matters; all perturbed quantities are expressed through this vector.

As it is well known the Lagrangian of a system is the difference between its kinetic and potential energies. If in addition Coriolis force is present then we will have corresponding terms in the Lagrangian. The situation is similar when making up the Lagrangian for continuous medium. Take kinetic, potential energy densities and terms corresponding to Coriolis force and write the following Lagrangian

$$L=\iint \Im dxdy=\frac{\rho_*}{2}\iint\left[\left(\frac{D\vec{\xi}}{Dt}\right)^2-c^2(div\vec{\xi})^2-2f\xi_y\frac{D\xi_x}{Dt}+fA\xi_y^2\right]dxdy$$

where the integration interval for x is $(-\infty,+\infty)$ and for y is $(0,H)$. It is quite straightforward to verify that this Lagrangian after variation with respect to $\vec{\xi}(\vec{r},t)$ gives

indeed the first two equations of (18). As for the third equation, it is already implied in the third equation of (19). Actually we have obtained a set of two equations for two independent variables ξ_x, ξ_y. Since the background flow is independent of zonal x coordinate we can assume that the perturbed quantities are periodic in x coordinate with the period $2\pi/k$, where k is, as before, the zonal wavenumber.

As we can see, our Lagrangian does not depend explicitly on time t and on zonal coordinate x. Consequently, we have two conserved quantities corresponding to translations along these two coordinates (Noether's theorem). The first one is the conservation of wave action that we do not use in our problem and the second one represents the conservation of wave energy. To see this more clearly let us first write the energy conservation in terms of the Lagrangian density

$$\frac{\partial}{\partial t}\left(\frac{\partial \xi_i}{\partial t}\cdot\frac{\partial \Im}{\partial(\partial\xi_i/\partial t)}-\Im\right)+\frac{\partial}{\partial x}\left(\frac{\partial \xi_i}{\partial t}\cdot\frac{\partial \Im}{\partial(\partial\xi_i/\partial x)}\right)+\frac{\partial}{\partial y}\left(\frac{\partial \xi_i}{\partial t}\cdot\frac{\partial \Im}{\partial(\partial\xi_i/\partial y)}\right)=0,$$

where time derivative involved in this equation is a total not partial derivative (the latter is zero). This equation follows from translation invariance with respect to time. The summation convention for repeated indices $i=x,y$ has been used. On averaging this expression over the period $2\pi/k$ along the x-axis, integrating along the y-axis from $y=0$ to $y=H$, using the boundary condition for v and taking into account the condition of zero potential vorticity, we arrive after some algebra at the following expression for the conservation of energy

$$\frac{dL}{dt}=0, \qquad \text{where} \quad L=\tfrac{1}{2}\int_0^H\left\langle v^2+\left(u+Ay\frac{\Phi}{c^2}\right)^2+\left(1-\frac{A^2y^2}{c^2}\right)\cdot\frac{\Phi^2}{c^2}\right\rangle dy \ ,$$

here $\langle\ \rangle$ brackets indicate averaging over x-coordinate. It follows that if $AH<c$ then L is always positive definite and all quantities must remain bounded at all times. This implies that in this case the flow is stable to wave-type perturbations.

Summary

In the present chapter we have investigated the linear dynamics of non-symmetric perturbations imposed on geostrophic flows with a constant horizontal shear by means of the non-modal approach combining numerical and qualitative study. It has been shown that the important feature of non-symmetric perturbations is the conservation of potential vorticity. Depending on the value of the potential vorticity the perturbations are classified as wave/oscillatory perturbations ($\tilde{q} = 0$) and vortex/aperiodic perturbations ($\tilde{q} \neq 0$).

The energy of non-symmetric wave perturbations at large times increases linearly (algebraic instability). If Ro < 1 there takes place only an algebraic growth of non-symmetric shear internal waves. At Ro > 1 a time interval of the linear growth is preceded by an interval of exponential (explosive) growth if $t_* > 0$ (i.e., if initially the angle between the constant phase lines of the perturbation and the streamwise direction is obtuse). This explosive-linear instability is specific to zonal geostrophic shear flows and essential for self-sustained turbulence.

As for vortex perturbations, if $t_* > 0$ and Ro ~ 1, they initially gain the basic flow energy and then are converted into shear internal waves. We can say that in shear flows waves can be excited at the expense of vortex perturbation energy, which is impossible in the shearless limit. By contrast, For Ro<<1 wave and vortex modes evolve independently; there is no coupling. This kind of wave generation by vortices is also distinctive for smooth shear flows (Chagelishvili et al. 1997a)

We have also analyzed viscosity effects on the perturbation dynamics. It has turned out that viscosity diminishes only perturbation amplitudes for large times.

We have also proved the theorem concerning the stability of shear bounded flows. In particular, we have obtained that when $AH < c$ the flow is stable to wave type perturbations. This criterion facilitates study in that saves us from making spectral expansion in time and finding unstable eigenvalues.

One of the main conclusions of this chapter is that in both cases the shear flow instability is related to the growth of fast wave perturbations filtered and, so ignored, in traditional quasigeostrophic models of geophysical hydrodynamics, while the later plays an important role in flow instability

Chapter 3

Linear dynamics of perturbations in astrophysical discs

The importance of spiral density waves in the study of the spiral structure of galaxies has long been recognized. There has been a great deal of research on the subject that advanced considerably the understanding of galaxies spiral nature. The principal tools of investigation are modal approach (spectral expansion in time) and numerical analysis for finding eigenvalues and eigenfunctions. These two methods complement each other to produce a consistent dynamical picture of the processes underling the spiral structure. The same tools are widely employed in the stability study of many astrophysical systems as well. By means of modal approach in the 1970s the basic mechanism of amplification for tightly wound density waves-so called WASER mechanism-was formulated (Mark 1976, 1977, see also Bertin et al. 1989, Bertin & Lin 1996), according to which a mode is amplified by the transfer of angular momentum outwards by trailing waves. The results were tested in many numerical calculations and proved to be in a good agreement with the approximate phase integral relation derived by Mark (1977) and Lau et al. (1976) (see e.g. Berin & Lau 1978, Bertin et al. 1989 and references therein). Generally, there are two basic forms of this WASER process (Bertin et al. 1989, Bertin & Lin 1996), the first one that describes the over-refection at corotation of a radially outward propagating long trailing wave into a radially inward propagating short trailing wave is applicable to normal tightly wound spirals, and the second one, often referred to as

"swing amplification", is for bar type (open spirals) modes and occurs when a leading open wave is converted into a higher amplitude trailing open wave (Toomre 1981, see also Binney & Tremaine 1987). The swing mechanism is known to give considerably larger amplification factors for over-reflected waves than those in the first case, which gives only a moderate amplification (typically 1.4 in its most basic form). The basic reason for large growth factors is the conspiracy between three agents: differential rotation, epicyclic motion and self-gravity (Toomre 1981, Balbus 1988). Apart from bar instabilities Swing amplification is also invoked in the explanation for the formation of self-gravitating cloud complexes (Elmegreen 1996 and references therein) and flocculent spirals (Elmegreen 2003b)

Swing amplification is usually discussed in the shearing sheet model (Goldreich & Lynden-Bell 1965), though different authors treat it differently. Some of them stay in the modal formalism (cf. Drury 1980, Pellat et al. 1990, Tagger et al. 1989, Fuchs 2001) and study the properties of steady waves in co-moving frame, while others (Julian & Toomre 1966, Goldreich & Tremaine 1978, Nakagawa & Sekiya 1992 (NS)) introduce co-moving coordinates and examine the temporal evolution of spatial Fourier harmonics (SFH) of perturbations without any spectral expansion in time, or use so-called *non-modal* approach advantages of which was discussed in the Introduction We note once more that modal approach focuses on the stability of individual normal modes and does not address the question of time evolution of an arbitrary perturbation imposed initially on the unperturbed flow. Just this question is most interesting from the dynamical point of view and can be analyzed with the help of non-modal approach.

In this chapter we apply the non-modal analysis combined with numerical calculations to the study of the dynamics of spiral density waves in gaseous discs in the shearing sheet approximation. Although, the mass fraction of gas in spiral galaxies is small the approach of gaseous disc is often fruitful because the hydrodynamic behavior and stellar dynamic behaviuor of galaxies are very similar. Besides, such gasodynamical treatment allows us to examine more closely the properties of instabilities that dominate

the gas discs and their influence on the stellar component in creating spiral patterns (Jog 1992).

Many investigators studying the development of perturbations numerically take white noise (flat power spectrum) initial distribution for perturbed quantities (cf. Gammie 2001, Wada et al. 2002). Instead here we concentrate on the dynamical properties of localized density wave packets, but first we investigate the properties of individual sheared waves, namely their amplification and reflection, because these are essential for understanding the specific behaviour of localized packets. This issue was first addressed by Toomre (1969). He showed that any localized packet of tightly wound waves winds up in approximately 10^9 years. However, he used modal approach and WKB analysis based on the work by Lin & Shu (1966). Goldreich and Tremaine (1978) used non-modal approach but packets they considered are not localized and are obtained by adding different waves with equal weights/amplitudes. That is why their final result is independent of time and describes steady wave trains. In addition their analysis is based on certain approximations. Here we use non-modal approach that allows us to follow all stages of packet evolution both in real and in wavenumber planes and to proceed without invoking Lindblad and corotation resonances and making approximations of Goldreich and Tremaine. Because the packet is localized it exhibits many interesting properties and the shearing sheet model is the best opportunity to demonstrate clearly the regimes of amplification and the properties of packet propagation in real plane by transforming to Fourier plane. Though our study is carried out in the shearing sheet, the properties of the localized packets obtained here help to grasp the specific features of the packet evolution in global disc simulations of Toomre and Zang (see Toomre (1981) or Binney & Tremaine (1987), Ch.6) (namely, the splitting of a leading wave packet into two trailing ones). These simulations were performed with the aim of examining the swing amplification of density wave packets. Results appeared approximately similar to those given by the shearing sheet mode. This encourages us to consider wave packets in the shearing sheet. Analogous investigation, but in a different context, was carried out by Bodo et al. (2001). They considered the spatial aspect of MHD wave transformations in

astrophysical flows, in particular, flows with uniform velocity shear contained in an external regular magnetic field parallel to the mean velocity.

Another notable phenomenon considered in this chapter is the generation of spiral density waves by vortical perturbations analogous to that found in atmospheric and oceanic flows, but now self-gravity of medium influence the dynamics. This phenomenon has been investigated recently by Bodo et al. (2005) and Tevzadze (2006) in the non-self-gravity limit. In general vortical perturbations play an important role in disc dynamics. First of all, they can be considered as main sources and sustainers of turbulence in accretion discs, because of their transient amplification (Chagelishvili et al. 2003, Yecko 2004, Umurhan 2004, Afshordi et al. 2005). Secondly, they serve as generators of waves in general and spiral density waves in particular in shear flows. In previous works, the role of this vortex mode has been often underestimated (cf. Ryu & Goodman 1992, Goodman & Balbus 2001), or it has been confused with fictitious displacements that arise in Lagragian formalism (Friedman & Schutz 1978).

3.1 Physical model and equations

We study the linear dynamics of 2D small scale perturbations (i.e. with characteristic length scales in radial and azimuthal directions much less than the radial characteristic scale of the background/disk flow) to a differentially rotating axisymmetric razor-thin gaseous disc (Mamatsashvili 2006) in the shearing sheet approximation (e.g., Goldreich & Lynden-Bell 1965; Goldreich & Tremaine 1978; Nakagawa & Sekiya 1992). In this case the dynamical equations are written in the local co-moving Cartesian frame (*x, y*):

$$x \equiv r - r_0; \qquad y \equiv r_0(\phi - \Omega_0 t); \qquad \frac{x}{r_0}, \frac{y}{r_0} \ll 1,$$

where (r,ϕ) are standard cylindrical coordinates and Ω_0 is the local rotation angular velocity of the co-moving coordinate frame at $r = r_0$. Because of the small scale assumption made above, we can consider the expansion

$$\Omega(r) = \Omega_0 + \frac{\partial \Omega}{\partial r}(r - r_0) \equiv \Omega_0 + 2A\frac{x}{r_0}$$

where

$$A \equiv \frac{1}{2}\left[r\frac{\partial \Omega}{\partial r}\right]_{r=r_0}.$$

A parameter characterizes the mean velocity shear in the local frame rotating with angular velocity Ω_0. The standard Oort constant is $B = \Omega_0 + A$. The main assumption of the shearing sheet approximation is the neglect of the basic flow vorticity gradient, the only gradient being considered is differential rotation. The simplifications made above help to clarify the underlying physical processes operating in the disc. Since the forms of continuity and Euler equations in the shearing sheet are well known (Goldreich & Lynden-Bell 1965, Goldreich & Tremaine 1978), we give here only their linearized version

$$\frac{\partial \sigma}{\partial t} + 2Ax\frac{\partial \sigma}{\partial y} + \Sigma_0\left(\frac{\partial u}{\partial x} + \frac{\partial v}{\partial y}\right) = 0, \tag{1}$$

$$\frac{\partial u}{\partial t} + 2Ax\frac{\partial u}{\partial y} - 2\Omega_0 v = -\frac{1}{\Sigma_0}\frac{\partial p}{\partial x} - \frac{\partial \psi}{\partial x}, \tag{2}$$

$$\frac{\partial v}{\partial t} + 2Ax\frac{\partial v}{\partial y} + 2Bu = -\frac{1}{\Sigma_0}\frac{\partial p}{\partial y} - \frac{\partial \psi}{\partial y}, \tag{3}$$

where *u, v, p* and σ are the perturbations of radial and azimuthal velocities, pressure and surface density respectively, ψ is the gravitational potential due to the surface density perturbation. As usual, the unperturbed surface density Σ_0 is assumed to be independent of coordinates over a particular patch of the disc we consider. The set of linear perturbation equations are completed by Poisson's equation

$$\left(\frac{\partial^2}{\partial x^2} + \frac{\partial^2}{\partial y^2} + \frac{\partial^2}{\partial z^2}\right)\psi = 4\pi G\sigma\delta(z) \tag{4}$$

and by the relation between pressure and surface density perturbations

$$p = c_s^2 \sigma,$$

where c_s is the sound speed in the gas.

Following the standard method of nonmodal analysis (cf. Goldreich & Lynden-Bell 1965; Goldreich & Tremaine 1978) we introduce the spatial Fourier harmonics (SFH) of perturbations with time-dependent phases

$$F(\mathbf{r},t) \sim F(k_x,k_y,t)\exp[\mathrm{i}k_x(t)x+\mathrm{i}k_y y], \quad k_x(t) = k_x - 2Ak_y t. \tag{5}$$

where F (u, v, p, σ, ψ). The streamwise/azimuthal wavenumber k_y remains constant and the streamcross/radial wavenumber $k_x(t)$ changes with time at a constant rate, its initial value at $t = 0$ is k_x. In the linear approximation SFH \drifts" in k-plane (wavenumber plane) along the $\boldsymbol{k}_x$-axis. The effect of this change is that the lines of constant phase (wave crests) are rotated by the basic flow.

Substitution of Eqs.(5) into Eqs. (1-4) yields the system of ordinary differential equations that govern the linear dynamics of SFH of perturbations in the described flow:

$$\frac{d\sigma(t)}{dt} + \mathrm{i}\Sigma_0 \left[k_x(t)u(t) + k_y v(t)\right] = 0, \tag{6}$$

$$\frac{du(t)}{dt} - 2\Omega_0 v(t) = -\mathrm{i}k_x(t)\left[c_s^2\frac{\sigma(t)}{\Sigma_0} + \psi(t)\right], \tag{7}$$

$$\frac{dv(t)}{dt} + 2Bu(t) = -\mathrm{i}k_y\left[c_s^2\frac{\sigma(t)}{\Sigma_0} + \psi(t)\right], \tag{8}$$

$$\psi(t) = -\frac{2\pi G}{k(t)}\sigma(t), \tag{9}$$

where $k(t) = (k_x^2(t) + k_y^2)^{1/2}$. The last equation follows from Poisson's equation and is straightforward to obtain (Goldreich & Tremaine 1978, Nakagawa & Sekiya 1990). Introducing $\hat{\sigma}(t) \equiv i\sigma(t)/\Sigma_0$ and $\phi(t) \equiv i\psi(t)$, from Eqs.(6-9) one gets the final set of equations with real coefficient

$$\frac{d\hat{\sigma}(t)}{dt} = k_x(t)u(t) + k_y v(t). \tag{10}$$

$$\frac{du(t)}{dt} - 2\Omega_0 v(t) = -k_x(t)\left[c_s^2\hat{\sigma}(t) + \phi(t)\right], \tag{11}$$

$$\frac{dv(t)}{dt} + 2Bu(t) = -k_y\left[c_s^2\hat{\sigma}(t) + \phi(t)\right], \tag{12}$$

$$\phi(t) = -\frac{2\pi G\Sigma_0}{k(t)}\hat{\sigma}(t). \tag{13}$$

One can readily show that this system possesses an important time invariant

$$k_x(t)v(t) - k_y u(t) + 2B\hat{\sigma}(t) \equiv \mathcal{I} \tag{14}$$

which follows (for SFH of perturbations) from the conservation of potential vorticity. This time invariant *I*, in turn, indicates the existence of the vortex/aperiodic mode in the perturbation spectrum. The properties of the vortex mode are considered later in subsection 3.2.3. So, now we set $I = 0$, which corresponds to the case of spiral density waves.

We define the spectral density of total energy of perturbations in k-plane as

$$E_{\text{tot}}(\mathbf{k},t) = E_{\text{k}}(\mathbf{k},t) + E_{\text{p}}(\mathbf{k},t) + E_{\text{g}}(\mathbf{k},t),$$
$$E_{\text{k}}(\mathbf{k},t) \equiv \Sigma_0\left(|u|^2 + |v|^2\right),$$
$$E_{\text{p}}(\mathbf{k},t) \equiv \frac{1}{2}(\sigma p^* + \sigma^* p) = \Sigma_0 c_s^2|\hat{\sigma}|^2,$$
$$E_{\text{g}}(\mathbf{k},t) \equiv \frac{1}{2}(\sigma\psi^* + \sigma^*\psi) = -\frac{2\pi G\Sigma_0^2}{k(t)}|\hat{\sigma}|^2,$$

where E_k(k,*t*)*;* E_p(k,*t*) and E_g(k,*t*) correspond to the kinetic, potential and gravitational energies of SFH respectively. Note that the total spectral density of the energy would be conserved in the shearless limit, i.e., would not be exchange of energy between perturbations and background flow; its variation is entirely due to shear.

The numerical study of SFH of density wave dynamics is based on Eqs. (10-13). However, for the fundamental comprehension of the linear dynamics of reflection of spiral density waves it is advisable to rewrite them in another form. from Eqs. (10-14) one can derive the following second order differential equation for *φ(t)* (see: Goldreich & Tremaine 1978)

$$\frac{d^2\phi(t)}{dt^2} + \omega^2(k_x(t), k_y, A)\phi(t) = 0, \qquad (19)$$

$$\omega^2(k_x(t), k_y, A) = \kappa^2 - 2\pi G\Sigma_0 k(t) + c_s^2 k^2(t) + \frac{12A^2k_y^4}{k^4(t)} + \frac{8\Omega_0 A k_y^2}{k^2(t)},$$

where κ is the epicyclic frequency, $\kappa^2 = 4B\Omega_0$. This expression in the shearless limit resembles the dispersion relation for tightly wound waves in a fluid model with pressure (Lin & Shu 1968). Describe each term contained in this equation. The first term characterizes the frequency of epicyclic oscillations of fluid particles in the unperturbed gravitational field of the disc, the second term corresponds to self-gravity in the disc (we assume that there is no other external gravitational field), the third term is due to pressure (compressibility) of the gas, the forth and fifth terms, which distinguish this expression from the well known dispersion relation for tightly wound waves, are new and represent the effects of the basic flow shear. Each of these terms dominates in various areas of k-plane: the pressure and self-gravity terms are appreciable at large wavenumbers, the epicyclic term is independent of wavenumber and the shear term operates on small radial wavenumbers $|k_x(t)| \le k_y$. An additional shear effect is also present in the wavenumber $k(t)$; due to this the frequency ω is dime-dependent (through $k_x(t)$) and, as we will show later, interaction between different perturbation modes (vortex and wave) is possible. The epicyclic and pressure terms have a stabilizing influence, while the gravitational term causes instability (Jeans instability). The contribution of the shear to the local stability is discussed below.

We express $u(t)$, $v(t)$ and $\hat{\sigma}(t)$ in terms of $\varphi(t)$ and its time derivative

$$u(t) = \frac{1}{2\pi G\Sigma_0}\left[\left(\frac{2Ak_yk_x^2(t)}{k^3(t)} - \frac{2Bk_y}{k(t)}\right)\phi - \frac{k_x(t)}{k(t)}\frac{d\phi(t)}{dt}\right], \qquad (21)$$

$$v(t) = \frac{1}{2\pi G\Sigma_0}\left[\left(\frac{2Ak_y^2k_x(t)}{k^3(t)} + \frac{2Bk_x(t)}{k(t)}\right)\phi - \frac{k_y}{k(t)}\frac{d\phi(t)}{dt}\right], \qquad (22)$$

$$\hat{\sigma}(t) = -\frac{k(t)}{2\pi G\Sigma_0}\phi(t). \qquad (23)$$

For subsequent analysis it is convenient to introduce dimensionless quantities: $t\kappa \to \tau,\ c_s k_y / \kappa = K_y$, ($c_s / \kappa$ is of the order of disc thickness), $\Omega_0 / \kappa = \hat{\Omega},\quad A/\kappa = \hat{A},$ $B/\kappa = \hat{B},\quad \pi G\Sigma_0 / c_s\kappa = 1/Q$, $u/c_s = \hat{u}, v/c_s = \hat{v}$, $\phi / c_s^2 = \hat{\phi}$, $A/\kappa = \hat{A},\quad E(\mathbf{k},t)/\Sigma_0 c_s^2 = E(\mathbf{K},\tau)$. Here Q is Toomre's parameter. For definiteness in the following we take a Keplerian rotation law. In this case $\hat{\Omega}_0 = 1, \hat{A} = -0.75, \hat{B} = 0.25$, though our analysis can be easily generalized to include flat rotation curves (Sofue et al. 1999) seen over the major portion of discs of most spiral galaxies.

Then Eq.(24) is rewritten as

$$\frac{d^2\hat{\phi}(\tau)}{d\tau^2} + \hat{\omega}^2(K_x(\tau), K_y, A)\hat{\phi}(\tau) = 0, \qquad (24)$$

$$\hat{\omega}^2(K_x(\tau), K_y, \hat{A}) \equiv \frac{\omega_{SD}^2(k_x(\tau), k_y, A)}{\kappa^2} =$$

$$= K^2(\tau) - \frac{2}{Q}K(\tau) + 1 + 12\hat{A}^2\frac{K_y^4}{K^4(\tau)} + 8\hat{\Omega}_0\hat{A}\frac{K_y^2}{K^2(\tau)},$$

when $\omega^2 > 0$ the solution of this equation is oscillatory and we have stability, while for $\omega^2 < 0$ the solution is exponentially growing and we have instability (swing amplification). In the shearless limit the stability or instability of the solution does not change with time, the flow is either stable or unstable for given values of parameters, but in the presence of shear stable regions in K-plane alternate with unstable regions due to the wavenumber drift. To see this more clearly and understand the role of shear in the flow stability we plot in fig.1[1] stable and unstable regions in K-plane for $A = 0$ and $A \neq 0$ for various values of Q. In the case $Q < 1$ instability in the shearless flow occurs only for wavenumbers with components K_x, K_y located between two circles with radii $K_{1,2} = 1/Q \pm \sqrt{1/Q^2 - 1}$ centered at the origin K = 0 in K-plane. This torus widens with decreasing Q, i.e., the influence of self-gravity increases. The same situation with shear is more interesting; shear deforms the inner and outer circles. As a result this torus is transformed into

[1] all figures in this chapter are numbered as in Ch.2

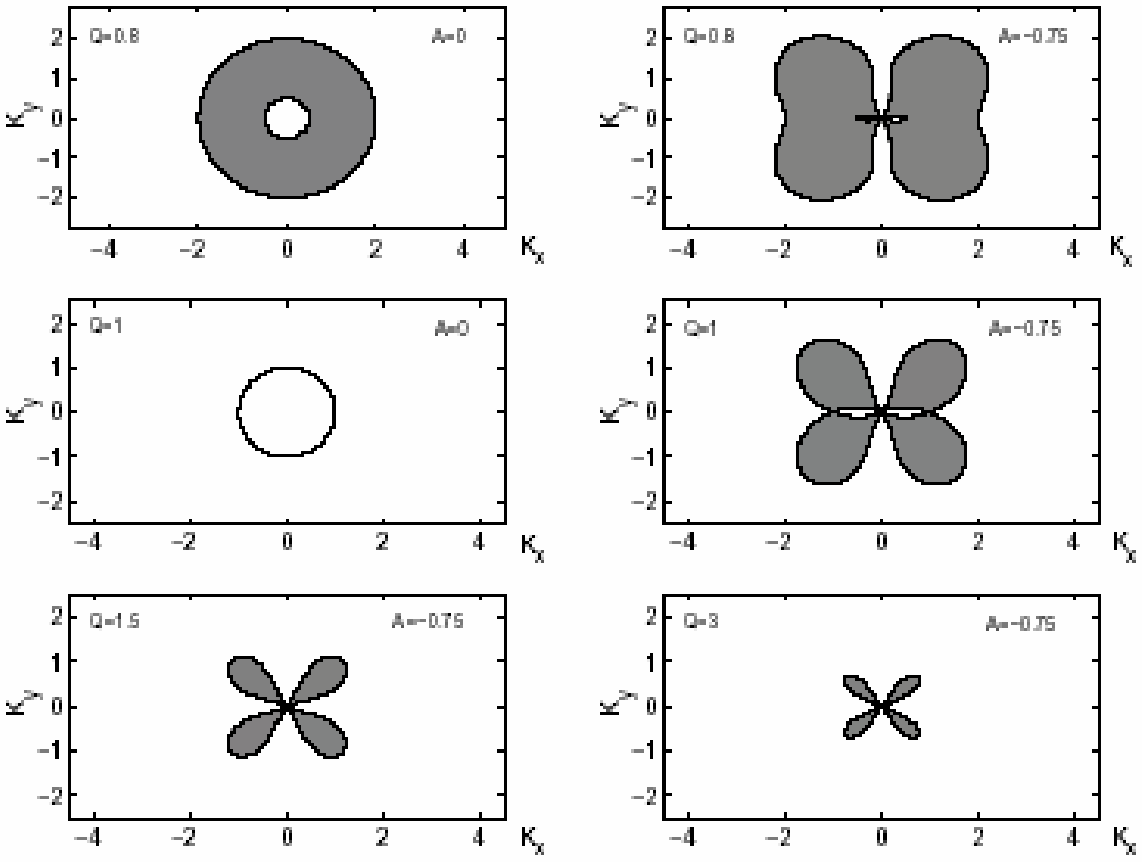

Figure 1. Stable ($\hat{\omega}^2 > 0$) and unstable ($\hat{\omega}^2 < 0$)(hatched) regions in **K**-plane for various values of Q. For $Q \geq 1$ compared with $A = 0$ case shear leads to the emergence of unstable regions. The last two figures are given only for $A \neq 0$, since there are no unstable regions for $Q > 1$ and $A = 0$.

butterfly-like figure. In the case of $Q \geq 1$ there is no unstable region in the shearless flow. The flow is locally stable for all wavenumbers (ω^2 everywhere in K-plane). Contrary to this situation shear leads to the broad unstable regions. Compared with the Q<1 case, now the role of shear is important, it makes the flow locally unstable. Therefore, discs locally stable with respect to axisymmetric perturbations can be locally unstable to nonaxisymmetric perturbations owing to shear. This is a simple derivation of an old and general result confirmed in many numerical simulations of star or fluid discs (cf. Toomre 1981, Sellwood & Carlberg 1984) and is omitted in the Lin-Shu dispersion relation where for $Q \geq 1$ there is always stability to all kinds of perturbations, either axisymmetric

or nonaxisymmetric. Thus in sheared flows together with Jeans instability there exists also shear induced instability. The interesting fact is that though instability for $Q \geq 1$ is caused by shear it diminishes when Q increases ($\omega^2 < 0$ region shrinks). We would like to note that this instability is of transient nature in contrast to modal one, which takes place for $t \rightarrow \infty$.

3.2 SFH dynamics

3.2.1 Numerical integration

Equations (10)-(13) together with appropriate initial values of the perturbed quantities preserving zero potential vorticity pose an initial value problem describing the dynamics of SFH of density waves. We solve them numerically for different values of Q and K_y. A somewhat similar integration was carried out also by Goldreich and Lynden-Bell (1965), but they did not consider different regimes. We wish to perform these calculations in the context of our identification of stable and unstable regions in **K**-plane (Fig.1). This picture allows us to see clearly in what regions we have either exponential/transient growth (swing amplification) or oscillations of a solution. The numerical results are summarized in Fig.2 where we plot the evolution of the normalized energy $E(t)/E(0)$; $E(t) = E_k(k, t) + E_p(k, t)$.

Let us begin with the case $Q = 1$. Consider three different values of the azimuthal wavenumber $K_y = 0.03$, $K_y = 0.3$, $K_y = 3$ (in all cases below $Kx < 0$, i.e. initially wave crests have a leading orientation). First of all, we note once more that all large growths in this case are due to shear and not to self-gravity. For $K_y = 0.03$ drifting wavenumber $K_x(\tau)$, starting from the initial value K_x, crosses two unstable regions and one relatively large intermediate stable region. The corresponding time development of $E/E(0)$ is

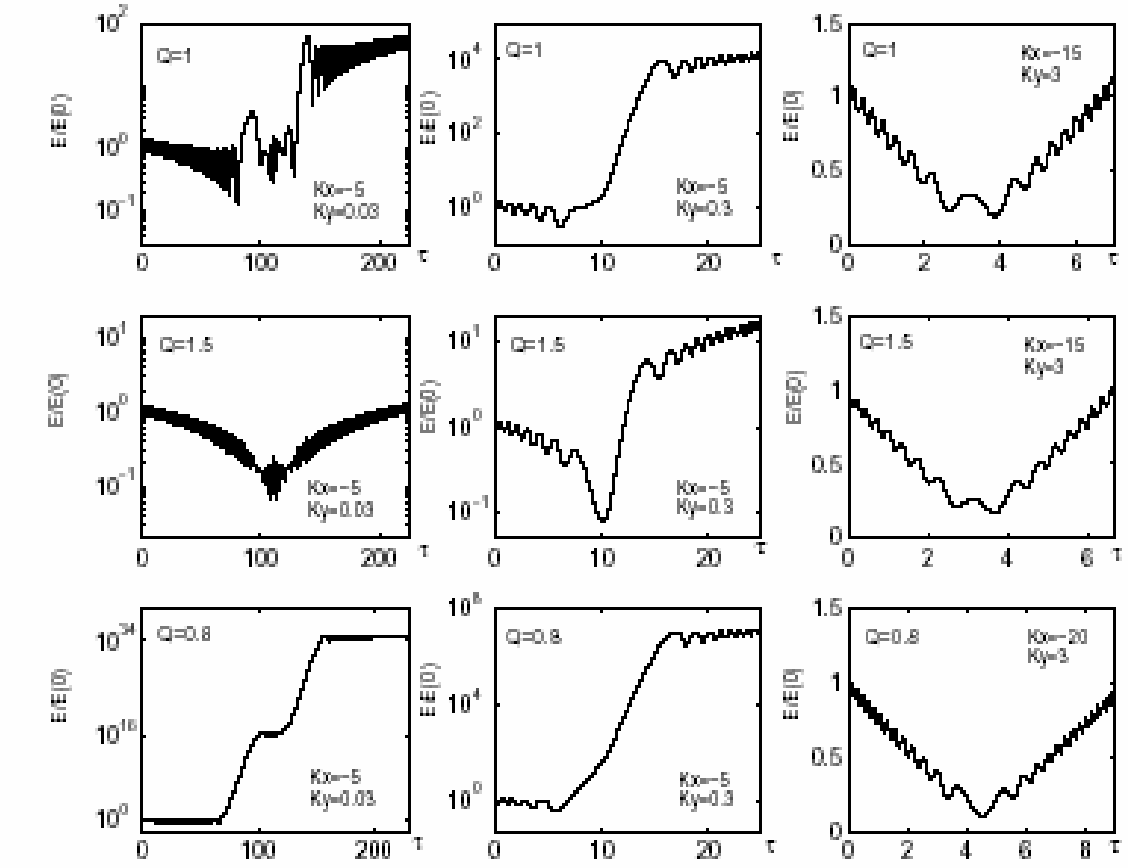

Figure 2. Evolution of E/E(0) of SFH for various values of Q and K_y. For $K_y = 0.3$ the energy experiences strong ($Q \leq 1$) or moderate ($Q > 1$) exponential growth (swing amplification) as a result of non-normality of the shearing sheet. For $K_y = 0.03$ the oscillations of the energy between two amplifications ($Q = 1, 1.5$) and the plateau in the energy curve ($Q = 0.8$) correspond to the intermediate stable regions. For $K_y = 3$ (or greater) energy grows smoothly with small oscillations. No exponential growth is observed in this case, there takes place only asymptotically linear amplification of the wave energy (algebraic instability).

shown in Fig.2. Until $K_x(\tau)$ reaches the first unstable region energy oscillates without increasing its mean value (over the period of oscillations). When it enters the first unstable region the solution turns from an oscillatory into exponential type and energy increases monotonically. This exponential/transient growth (swing amplification) lasts while $K_x(\tau)$ crosses this unstable region. Then it moves to the intermediate stable region and the solution reverts to an oscillatory type, consequently the energy oscillates again;

its mean value grows little. After that there follows again the second unstable region where energy as well as other quantities undergo exponential growth. However, because of the narrowness of both unstable regions this exponential growth does not achieve considerable value as it does for $K_y = 0.3$. In the end $K_x(\tau)$ gets back in the stable region and never leaves it. Here the solution is oscillatory again and energy grows asymptotically linearly (algebraic instability). Of course, this linear growth as well as the exponential growth is at the expense of the basic flow. Differential rotation helps perturbations to extract energy from the mean flow. Thus, exponential growth is followed by asymptotically linear growth of the perturbation energy. This fact is overlooked in the modal treatment of density waves.

The case $K_y = 0.3$ is qualitatively similar to the previous one. Now the unstable regions crossed by the time dependent radial wavenumber are broader and the minimum value of ω^2 is smaller than that for $K_y = 0.03$ and, in addition, the intermediate stable region is narrower (Fig.1). Due to this the time needed for the wavenumber to traverse the intermediate stable region is comparable to the oscillation period and as a consequence intermediate oscillations in the solution and, therefore, the oscillations of the energy between two exponential amplifications as it has been in the previous case, are not noticeable, but growth magnitudes for both energy and other quantities are substantially larger. For this order $O(0.1)$ of azimuthal wavenumbers the unstable regions are largest (Fig.1) and waves are amplified most effectively. As before, the energy grows asymptotically linearly for $\tau \to \infty$. We will further show that the reflection and transmission of waves are largest for such values of K_y.

In the case of $K_y = 3$ the wavenumber drifts above the unstable regions. The solution is oscillatory at all times and the energy varies smoothly with small oscillations. In the beginning it decreases and then increases approximately linearly without undergoing exponential amplification.

For $Q < 1$ (in Fig.2 we show the evolution for $Q = 0.8$) we have qualitatively a similar situation, but growth factors in the two unstable regions are significantly larger than that for $Q = 1$ (in the Fig.2 for $K_y = 0.03$ and $K_y = 0.3$). There are several aspects

that favor such growth: smaller minimum values of ω^2 than that for $Q \geq 1$ (for the same values of Ky) in the unstable regions and the relatively large breadth of the two unstable regions caused by the combined action of shear and self-gravity and, as a result, the large amount of the time required for $K_x(\tau)$ to traverse these two unstable regions due to small K_y. The case $K_y = 3$ is entirely similar to the corresponding one for $Q = 1$, now there is no unstable region and the energy evolves without exponential growth.

The situation with $Q > 1$ (in Fig.2 we show the evolution for $Q = 1.5$) differs from the above considered cases. The two unstable regions traversed by the time-dependent radial wavenumber are small compared with the above cases and become smaller and smaller with increasing Q. For $K_y = 0.03$ the two unstable regions are very narrow; they shrink to the point (K_x=0,K_y=0) with decreasing K_y, consequently the energy evolves without amplification. For $K_y = 0.3$ the drifting radial wavenumber crosses two unstable regions which are narrower than for $Q = 1$, and as a result exponential amplification is not strong, only of order 10. The case $K_y = 3$, as before, is identical to the one for $Q = 1$.

We would like to note that the very large growth factors for $Q < 1$ obtained in our numerical calculations are, of course, unrealistic in a real system because nonlinear effects will eventually take over. These were examined in detail by Kim & Ostriker (2001) (see their purely hydrodynamical case). Besides, such values of Q are not often realized. For example, in the solar neighborhood Q lies probably between 1 and 2 (Jog & Solomon 1984). So below we deal only with the case Q=1. Nevertheless, they emphasize the importance of transient amplification of perturbations that is a direct result of the non-normality of the operators governing perturbation dynamics in shear flows as mentioned in the Introduction. Transient amplification of waves occurs also for $Q > 1$, but is not as powerful; however in this case vortical perturbations may display larger transient growth factors. Studies in laboratory shear flows showed that transient amplification may sometimes achieve values as large as $O(10^{10})$ (Reddy, Shmidt and Henningson 1992). The modal treatment can predict the stability only in asymptotic for large times, but unable to account for transient phenomena that are common to shear flows.

3.2.2 Reflection and transmission

Now we go on to examine the reflection and transmission of spiral waves. For this purpose it is convenient to take the azimuthal wavenumber K_y to be positive without loss of generality (we can do that freely because our basic equation (24) is invariant under transformation $K_y \rightarrow -K_y$ and therefore the reflection coefficient is independent of the sign of K_y and to redefine the origin of time as (henceforth hats will be omitted) $\tau \rightarrow \tau - K_x / 2AK_y$ (in this subsection only). Now $K_x(\tau) = -2AK_y\tau$ and, since $A < 0$, the sign of $K_x(\tau)$ is the same as that of τ. For $|\tau| \rightarrow \infty$, i.e. when the wavenumber $K_x(\tau)$ is far from the vicinity of $K_x = 0$, the adiabatic condition $|d\omega / d\tau| << \omega^2(\tau)$ is met, which means that for large τ we can use the WKB approximation to construct the solutions of Eq.(24) (NS). Generally, solution at $\tau \rightarrow -\infty$ is a superposition of waves with the different signs of frequency that propagate in opposite directions. We choose the positive-frequency solution as the incident wave. For simplicity we set the amplitude to unity:

$$\phi^{in}(\tau) = \frac{1}{\sqrt{\omega(\tau)}} e^{-i\int^{\tau} \omega(\tau')d\tau'}, \qquad \tau \rightarrow -\infty, \qquad (25)$$

where ω is the positive root of the expression in Eq.(24). To avoid confusion we note that the wave is "incident" in time not in space as it is in quantum mechanical problems or in the modal theory of density waves where an incident wave is over-reflected at corotation resonance (Mark 1976, Bertin et al. 1989). In this case all three waves incident wave itself and the over-reflected and (over)-transmitted waves are present simultaneously. In our case instead the "incident" wave is initiated in the distant past and evolves with time. In space it is spread out to infinity. The phase velocity $\omega(\tau) / K_x(\tau)$ is negative for $\tau<0$. Then the radial wavenumber $K_x(\tau)$ approaches the region in K-plane where the WKB approximation breaks down. So now we can no longer separate two

wave branches with positive and negative frequencies; we have some mix of waves which interact and exchange energy with each other and with the basic flow. The dependence on the spatial coordinates of this mixture is a simple harmonic $exp(ik_x(t)x + ik_y y)$, but the amplitude is some function of time which does not fall into the sum of exponents of the type (25). This situation is somewhat analogous to the over-reflection at corotation discussed by Mark (1976) except that the role of spatial coordinates is played by time and "corotation point" is at $\tau = 0$ that corresponds to $K_x = 0$. After crossing this nonadiabatic region which together with the intermediate stable region may include the two unstable regions, the drifting radial wavenumber gets again into the adiabatic region with a positive sign. At time $\tau \to \infty$ for the solution we have

$$\phi(\tau) = \phi^{tr}(\tau) + \phi^{refl}(\tau) = \\ = \frac{T}{\sqrt{\omega(\tau)}} e^{-i\int^{\tau}\omega(\tau')d\tau'} + \frac{R}{\sqrt{\omega(\tau)}} e^{i\int^{\tau}\omega(\tau')d\tau'} \qquad (26)$$

where T and R are the transmission and reflection coefficients, respectively, and the corresponding waves are called the transmitted and reflected waves. The transmitted wave has the same sign of frequency as the incident wave, however its phase velocity is directed opposite to the phase velocity of the incident wave, i.e., it travels outwards, and the reflected wave, with the opposite sign of frequency, propagates inwards in the radial direction. At first sight it might seem that the transmitted wave is a reflected wave because of the opposite phase velocity (NS), but this is not the case, because actually the change in the direction of the phase velocity is merely due to the wavenumber drift and the question of which wave is transmitted and which reflected is resolved in terms of the time variable τ (and not in spatial coordinates) according to the form of Eq. (26). If we formally replace τ by x in Eqs. (25, 26) we obtain correspondence to the analogous definition of incident and transmitted waves accepted in quantum mechanics (Landau & Lifshitz 1974). Thus, behaviour of the waves in real space is entirely described by the characteristics in K-plane. The splitting of the incident wave into transmitted and

reflected parts in real space occurs around the "corotation point" $K_x = 0$, and the moment of splitting is found by the initial wavenumber, $\tau_{sp} = K_x / 2AK_y$ (in former notations).

From the wave action conservation law (NS) or directly from Eq.(24) we obtain a general relation between the transmission and reflection coefficients $|T|^2 = 1 + |R|^2$ (as mentioned above our definition of the transmitted and reflected waves differs from that of Nakagawa and Sekiya and the conservation of wave action looks differently). This relation simply means that the amplitude of the transmitted wave is always larger or at least equal to the amplitude of the incident wave (over-transmission). This is because the non-axisymmetric waves are able to extract energy efficiently from the basic flow and amplify as we have seen in the preceding subsection. This process is possible only in the presence of differential rotation. If $|R|$ exceeds unity then over-reflection occurs in addition to over-transmission.

Like Nakagawa and Sekiya (1992), we numerically calculated the reflection coefficient (its absolute value $|R|$) as a function of K_y for various Q (Fig.3) (a detailed procedure of the calculation is given in NS. For the calculation they used the equation for the azimuthal velocity v, their Eq. (2.24). Our curves for $|R|$ coincide with their $|T|$ curves). We explain the peculiarities of this dependence on the basis of the obtained stable and unstable regions for ω^2. We start with the case Q = 1. Consider first the interval $0.01<K_y<0.1$. For such values we have two narrow unstable regions and one larger intermediate stable region (Fig.1) where the adiabatic condition is satisfied only far from and between these unstable regions and, therefore, the solution here is given as a superposition of two waves. The T and R coefficients in the solution depend on the value (phase) of φ with which it enters the second unstable region. But this value is roughly given as a periodic function of K_y (owing to the WKBJ approximation there) which oscillates more and more rapidly with decreasing K_y, and following from it the necessary conditions for the total ($|R| = 0$) or with reflection transmission alternate quickly. As a result, the reflection coefficient behaves in the same fast oscillatory way (see also Appendix A). Note that the period of $|R|$ oscillations increases with growing K_y. Because

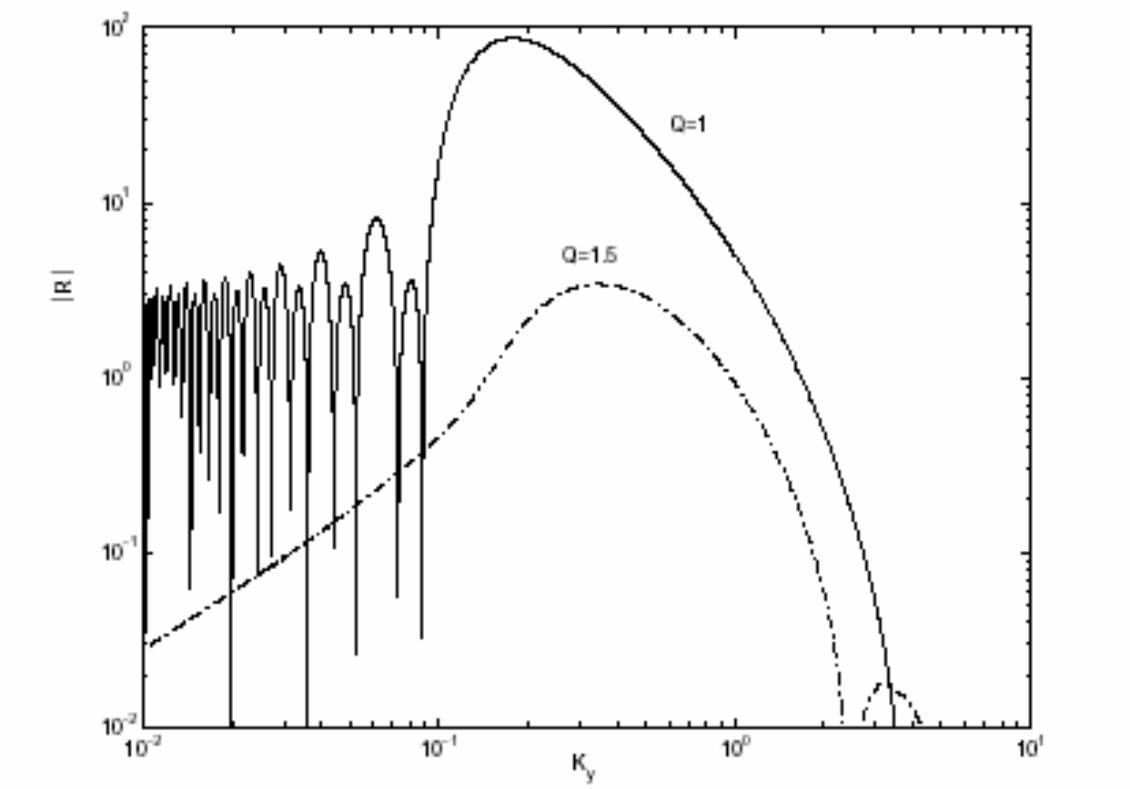

Figure 3. The reflection coefficient $\mid R \mid$ as a function of the azimuthal wavenumber K_y for $Q = 1$ and $Q = 1.5$. The large values of the reflection coefficient for $Q = 1$ are associated with the unstable regions in fig.1.

of the narrowness of the unstable regions the reflection and transmission coefficients are not large in this case. As the azimuthal wavenumber increases ($0.1<K_y$) the adiabatic condition becomes invalid and the oscillations of the solution in the intermediate stable region are not pronounced, accordingly $|R|$ varies smoothly with K_y. At first it increases with the broadening of the unstable regions reaching a maximum and then decreases. The coefficients $|R|$ and $|T|$ are now considerably larger compared with those for small wavenumbers. To make certain that only shear is responsible for the growth (NS associated it with self-gravity), we run calculations when the terms proportional to A was dropped in Eq.(24) (Fig.4). As expected, the reflection coefficient is not large for $0.1<K_y$.

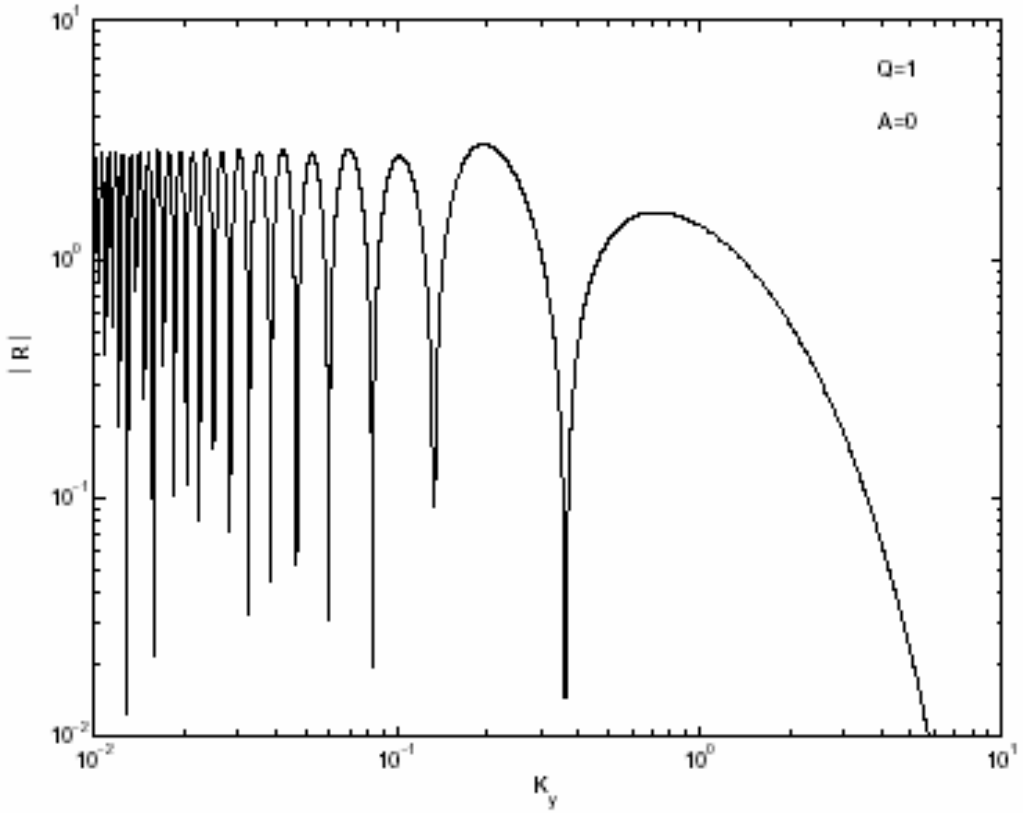

Figure 4. The reflection coefficient obtained from Eq.(24) with shear proportional terms omitted. As clearly seen $|R|$ is significantly smaller than that in fig.3 for $0.1 \leq K_y$.

When K_y>>1 the reflection coefficient is very small. Here the compressibility term begins to dominate over all other terms in ω^2 and the evolution is adiabatic at all times. So an initially incident wave propagates without splitting and turns gradually into a transmitted one for $\tau \to +\infty$.

The case when $Q > 1$ is distinct from the previous case. Now we have two leaf-like unstable regions (Fig.1). These leaves shrink towards the origin and, consequently, there is little reflection for small K_y. The breadth of these leaves increases and then decreases to zero and the behaviour of the transmission coefficient follows it. The absence of fast oscillations for small K_y~O(0.01) is explained by the fact that the intermediate stable region, unlike the above situation with Q=1, is very narrow for the validity of the adiabatic approximation there, while it is fairly well satisfied in the stable region. So

there are no intermediate oscillations in the solution. The above argument applies also for $K_y \sim O(0.1)$. However, there follows another peak produced by the resonance between compressibility and epicyclic terms. The latter peak becomes higher, whereas the former lower with increasing Q (NS).

3.2.3 Generation of spiral density waves by vortices

The dynamics of vortices in astrophysical disks has recently attract much interest both because vortices in protoplanetary discs can represent aggregation regions of solid particles for the eventual formation of planets (Barge & Sommeria 1995) and more generally for understanding accretion disc dynamics and the basic problem of angular momentum transport (Lovelace et al. 1999, Li et al. 2000). Several works have been devoted to the analysis of the possibility of forming and maintaining coherent vortex structures in the strongly sheared flow pertaining to Keplerian disc both in barotropic configurations, where the initial potential vorticity perturbation is conserved (Bracco et al. 1999, Godon & Livio 1999, 2000, Davis et al. 2000, Davis 2002) and in baroclinic situations where one can have vorticity generation (Klahr & Bodenheimer 2003, Klahr 2004). In the incompressible case it has been shown that coherent vortex structures can indeed form (under conservation of potential vorticity) and anticyclonic vortices can survive longer than cyclonic ones (Bracco et al. 1999) and give rise to the appearance of Rossby waves in the system (Davis et al. 2000). The effects of compressibility have not yet been fully analyzed and require rigorous study. Godon and Livio (1999) performed two dimensional time-dependent simulations of vortices in viscous compressible Keplerian discs. Vorticity waves are considered as one of the constituents of (anticyclonic) vortex dynamics, but without specification of the wave properties and analysis of their genesis and dynamics (the subject of the study was the stability and lifetime of vortices). Davis (2002) performed fully compressible numerical simulations of the dynamics of a single vortical structure in a Keplerian disc flow and has reported the generation of outward-moving compressible waves by the coherent vortex (the

generation was attributed to nonlinear processes. By contrast, in this subsection we show that such a generation is present already in the linear approximation) pointing out the potential importance of this phenomenon for vortex dynamics. Johansen, Andersen & Branderburg (2004) considered the dynamics of nonlinear vortices by numerical 3D simulations in the local shearing sheet approximation, also observing indications of wave generation. Klahr & Bodenheimer (2003) performing 2D and 3D hydrodynamical simulations of protoplanetary discs, found that a radial entropy gradient can generate Rossby waves which eventually break into vortices. Klahr (2004), by a linear stability analysis in fact showed that a radial entropy gradient leads to continuous generation of potential vorticity and to a transient swing-like amplification of the vortical/aperiodic mode, without the subsequent decay observed in the linear barotropic configurations.

In this subsection we study the linear dynamics of initially imposed vortex mode perturbations in Keplerian discs having in view understanding the linear phenomenon of generation of spiral density waves by vortical perturbations. It is analogous to that found in Chapter 2, however, now the self-gravity of medium comes into play. As before, our comprehension of wave generation phenomenon is based on paper Chagelishvili et al. (1997a). This phenomenon was studied in the non-self-gravity limit by Bodo et al. (2005) in global disc simulations and by Tevzadze (2006) in the shearing sheet approximation taking into account vertical stratification of the disc. The properties of wave generation in global disc simulations of Bodo et al. (2005) are well characterized in the shearing sheet model. Vortical motions were also observed in several spiral galaxies (Fridman & Khoruzhii 1999a,b) and the present study can be applied to this case as well.

To study the vortex dynamics we first need a relevant procedure for picking out vortex mode perturbations at the beginning of evolution. To do this, recall that in 3.1 we set the potential vorticity to zero. In the present case I is nonzero and the equation (24) for the gravitational potential perturbation is modified as

$$\frac{d\phi}{dt}+\omega^2(\tau)\phi=-\frac{2I}{QK(\tau)}\left(2\Omega+\frac{4AK_y^2}{K^2(\tau)}\right) \qquad (27)$$

(here I is appropriately nondimensionalized $I \to I/\kappa$. Hats are omitted). For other perturbed quantities we obtain

$$u(\tau) = \frac{Q}{2}\left(\left(\frac{2AK_y K_x^2(\tau)}{K^3(\tau)} - \frac{2BK_y}{K(\tau)}\right)\phi - \frac{K_x(\tau)}{K(\tau)}\frac{d\phi}{d\tau}\right) - \frac{K_y I}{K^2(\tau)} \qquad (28a)$$

$$v(\tau) = \frac{Q}{2}\left(\left(\frac{2AK_y^2 K_x(\tau)}{K^3(\tau)} + \frac{2BK_x(\tau)}{K(\tau)}\right)\phi - \frac{K_y}{K(\tau)}\frac{d\phi}{d\tau}\right) + \frac{K_x(\tau) I}{K^2(\tau)} \qquad (28b)$$

$$\sigma(\tau) = -\frac{QK(\tau)}{2}\phi(\tau). \qquad (28c)$$

Equation (27) is of the type considered in atmospheric and oceanic flows (Eq.(12) in 2.1) and the described in 2.1 separation of perturbation modes applies here too. So in this case we again keep to the physical standpoint of separation of perturbation modes and write each quantity as

$$u = u^{(w)} + u^{(v)}, \quad v = v^{(w)} + v^{(v)}, \quad \sigma = \sigma^{(w)} + \sigma^{(v)}, \quad \phi = \phi^{(w)} + \phi^{(v)}$$

where the wave parts (w) in these quantities correspond to spiral density waves (I=0, solutions of homogenious equation (24)) and the vortex parts (v) are related to the potential vorticity I. We below obtain the exact form of this relation (see also Appendix in Bodo et al. 2005).

$I, \phi(0), \phi'(0)$ form the full set of initial conditions for Eq.(27). We seek the vortex mode solution in the following analytic form:

$$\phi^v(0) = \phi_0^v(0) + \phi_1^v(0) + ... + \phi_n^v(0) + ..., \qquad (29)$$

where the zero order term is deduced from the stationary form of the solution (Eq. 27 with A=0) and subsequent terms are derived using the iterative method

$$\phi_0^v(0) = -\frac{2I}{QK(\tau)\omega^2(\tau)}\left(2\Omega + \frac{4AK_y}{K^2(\tau)}\right)_{\tau=0}$$

$$\phi_n^v(0) = -\left[\frac{1}{\omega^2(\tau)}\frac{d^2\phi_{n-1}^v(\tau)}{d\tau^2}\right]_{\tau=0}.$$

The principal concern with such a solution is its convergence. For instance, this solution diverges at $\tau = \tau_*$, $K_x(\tau_*) = 0$ or more generally over the whole of the nonadiabatic region, which depends on the azimuthal wavenumber K_y. However, the first two terms of this series can be considered to be an excellent approximation to the exact numerical solution for large times, sufficiently far from the nonadiabatic region. Therefore, we can use this analytic solution to compose initially at $\tau = 0$ the vortex mode perturbation. From these formulae we see that the initial value $\phi(0)$ is expressed via *I* and the corresponding solution (29) is called the vortex/aperiodic mode. As stressed, such a separation of modes is valid only in the adiabatic region. In the nonadiabatic region the above series diverges and the mode separation does not have any meaning. Here the timescales of vortex and wave modes are comparable; we have some mix of both modes in the solution. However, with going away from the nonadiabatic region modes get clearly separated and we can calculate the amplitudes of generated waves. As for the vortex mode it gradually dies out after going through the nonadiabatic region. Newly created waves extract energy from the mean flow; the vortex energetics is not changed by waves. In other words, we can say that vortex acts as a mediator between the background flow and the wave and then gradually returns its energy to the flow.

In Figs.5-8 we present the evolution of perturbed quantities and the normalized energy pertaining to the initially imposed vortex $E/E(0)$, $E = (u^2 + v^2 + \sigma^2)/2$ for various values of K_y (we take Q=1 and I=0.3 in calculations). A qualitative picture of evolution is similar to that in meteorological flows. Initially, when we are in the adiabatic region, imposed vortex mode gains energy from the mean flow and amplifies, but retains its aperiodic nature. On approaching the nonadiabatic region an oscillating part in the solution begins to appear. Thus, the linear vortex mode is followed by the generation of spiral density waves. In this region, as mentioned, the timescales of the vortex and the waves are comparable and the perturbations are not separable/distinguishable, we have a mix of aperiodic and oscillating modes. There follows again the adiabatic region and the timescale of the waves becomes much shorter than that of the vortex and the modes are

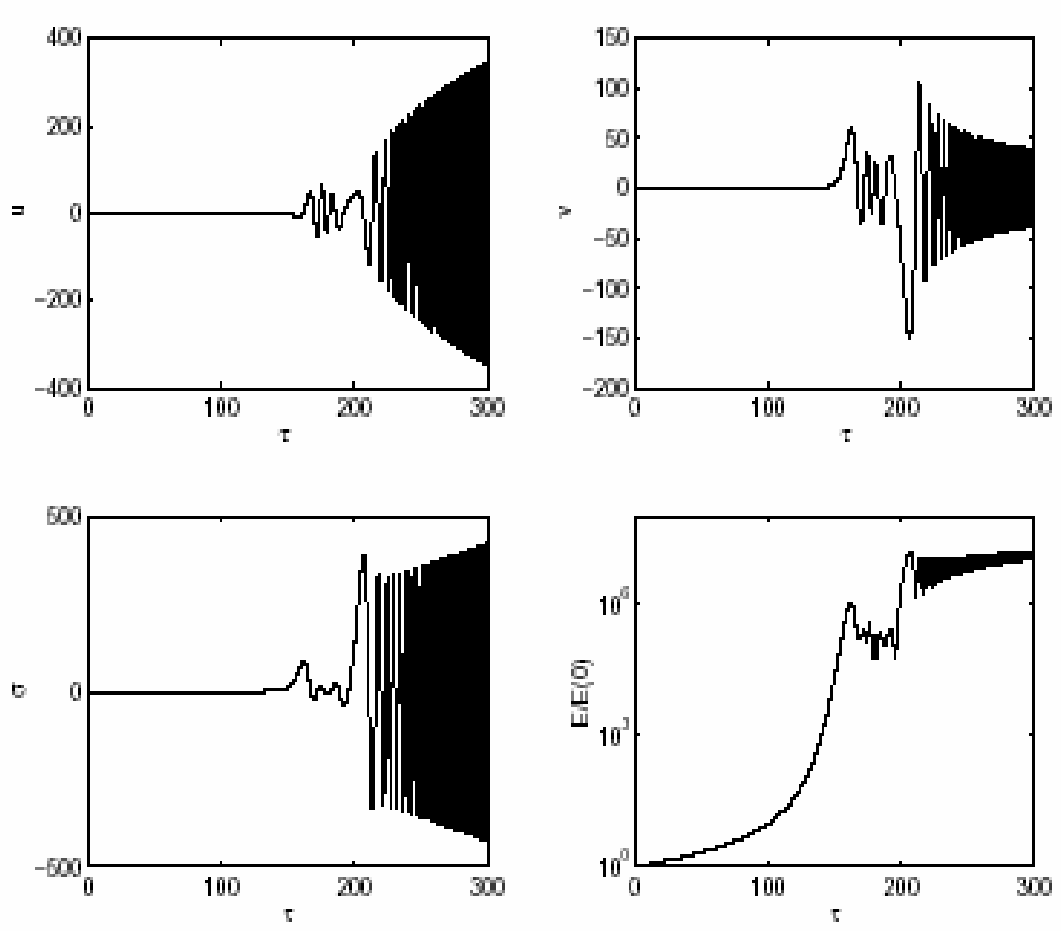

Figure 5. Evolution of an initially imposed vortex mode for $Q = 1$ and $K_y = 0.03$. Befor reaching the first unstable region in **K**-plane the vortex mode gains energy from the mean flow and amplifies, but retains its aperiodic nature. In the unstable region osscillations begin to appear in the perturbed quantities. The energy of the perturbation initially increases monotonically (transient growth) because of the vortex mode and, after going through the unstable region, asymptotically linearly corresponding to the generated waves (the energy curve is in logaritmic scale, so the flat region is actually linear growth). The contribution of the vortex mode energy to the total perturbation energy is negligible at this asymptotic stage. The vortex mode simply dies out giving way to waves.

well distinguishable. From these figures we see that the energy increases initially monotonically (transient growth) and then linearly. The first stage corresponds to a

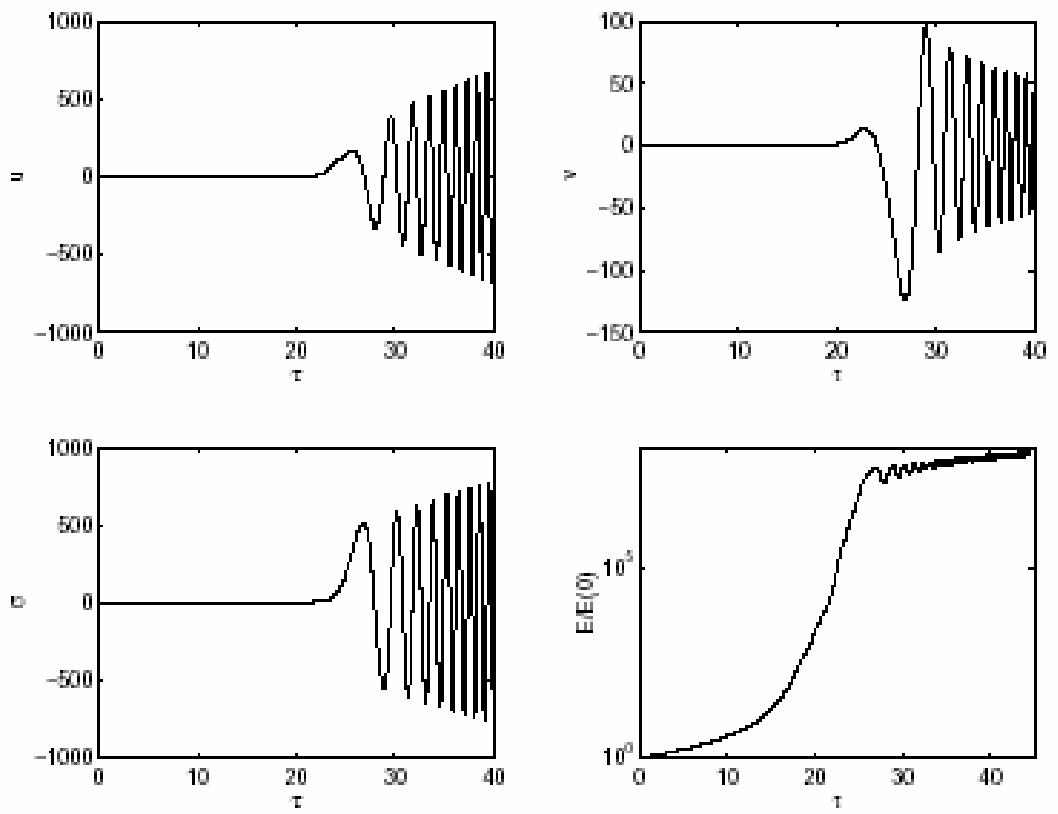

Figure 6. Same as in Fig.5, but with $K_y = 0.3$.

purely vortex mode evolution and the second one is the asymptotically linear amplification of the generated waves' energy. For $K_y < 1$ transient amplification is considerably enhanced by the unstable regions (Fig.5,6,10). Wave generation is strongest in this interval as well (Fig.9). For moderate K_y~1 (Fig.7,8,10) transient amplification is solely due to the non-orthogonality of the shearing sheet and can reach considerably larger values (O(100)) compared with wave amplification factors for the same K_y (see Fig.2). Wave generation is little noticeable for large K_y>10 (Fig.8,9) (due to the fact that the adiabatic condition is satisfied all along the vortex evolution), but now transient amplification of the vortex mode energy plays a central part in the perturbation dynamics. As stressed many times the existence of such transient amplification of the perturbation energy may be important for self-sustenance of turbulence in astrophysical discs.

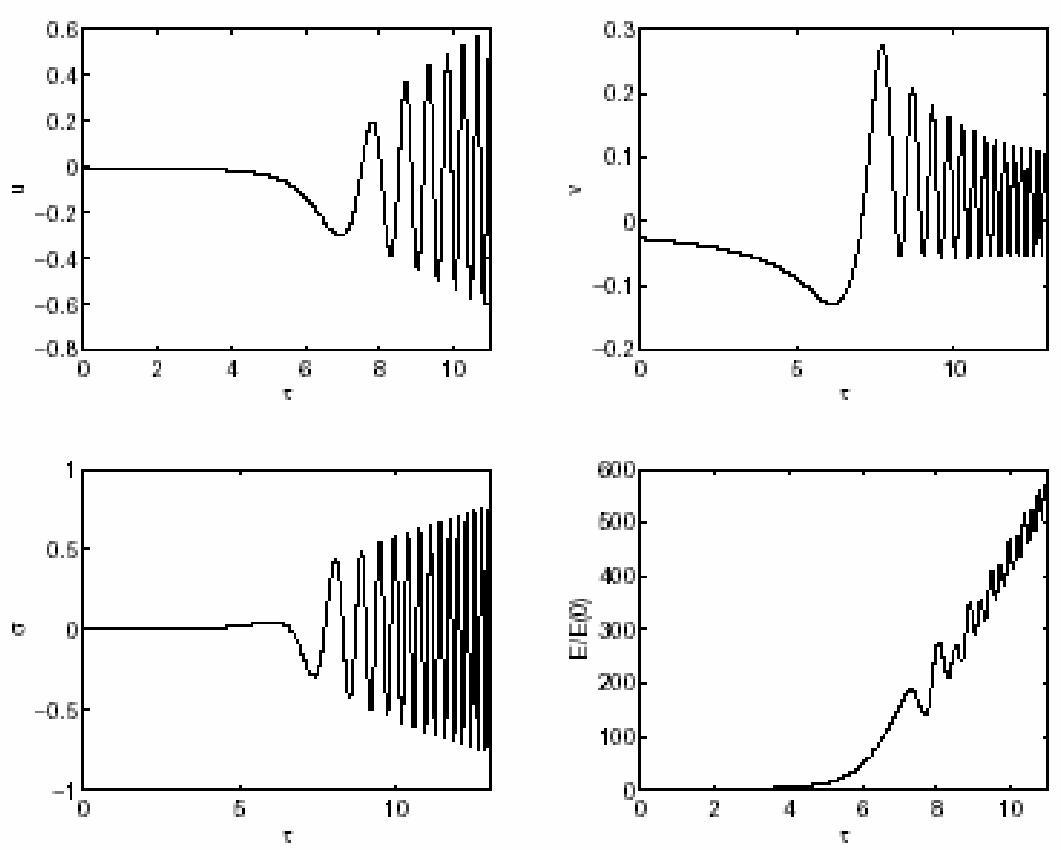

Figure 7. Same as in Fig.5, but with $K_y = 3$. Transient growth is not as powerful as in Fig.6, but larger than the amplification of waves in Fig.2 for the same K_y.

To calculate the amplitudes of generated waves as a function of K_y we note that at $\tau \to -\infty$ the solution contains only vortex mode (for τ we again redefine the origin of time as in 3.2.2)

$$\phi = \phi^{(v)} = -\frac{2I}{QK\omega^2}\left(2\Omega + \frac{4AK_y}{K^2}\right),$$

for simplicity here we have omitted further terms in the asymptotic expression (29). After going through the nonadiabatic region at $\tau \to \infty$ we have both wave and vortex parts

$$\phi = \phi^{(w)} + \phi^{(v)} = \frac{a}{\sqrt{\omega(\tau)}} e^{-i\int_0^\tau \omega(\tau')d\tau'} + \frac{a^*}{\sqrt{\omega(\tau)}} e^{i\int_0^\tau \omega(\tau')d\tau'} - \frac{2I}{QK\omega^2}\left(2\Omega + \frac{4AK_y}{K^2}\right)$$

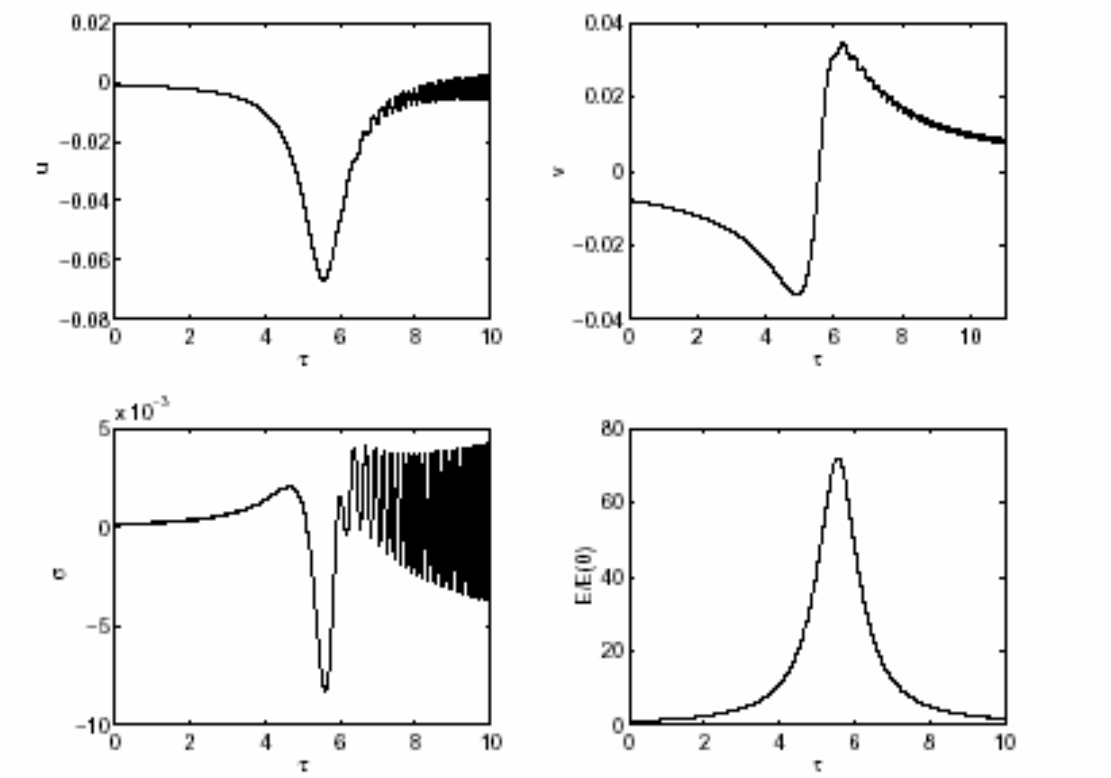

Figure 8. Same as in Fig.5, but with $K_y = 12$. Now wave generation starts to be noticiable, but the transient growth dominates the dynamics. The perturbation is composed almost only of the vortex mode during the whole evolution, which grows transiently and then decays asymptotically to zero.

where the last term is the vortex mode and the first two terms are the excited waves with amplitudes a and a^*. Of course, these amplitudes are proportional to I, since it is the main generator of waves. In Fig.9 we plot $|a|$ as a function of K_y. This curve resembles in appearance the one in Fig.3 for Q=1. The existence of fast oscillations is due to the same reason as in the reflection coefficient. Wave excitation is greatly enhanced for K_y<1 due to the large transient amplification of vortex perturbations producers of waves.

In Fig. 10 we also plot maximum energy during transient amplification when the self-gravity of the gas is ignored. As expected, transient growth is considerably larger in self-gravitating discs.

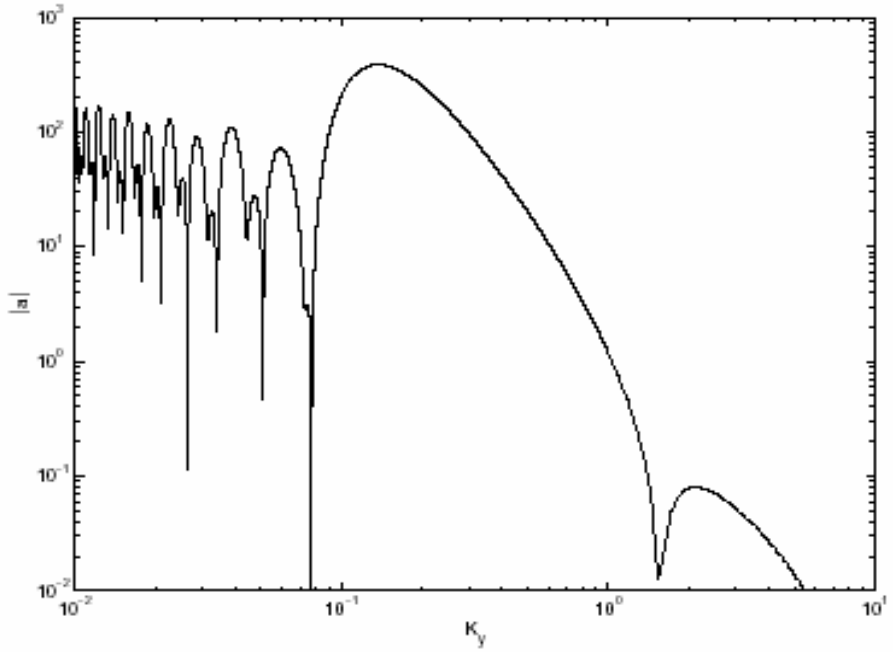

Figure 9. Amplitude $\mid a \mid$ of generated waves as a function of K_y. Wave generation is very effective for $K_y < 1$.

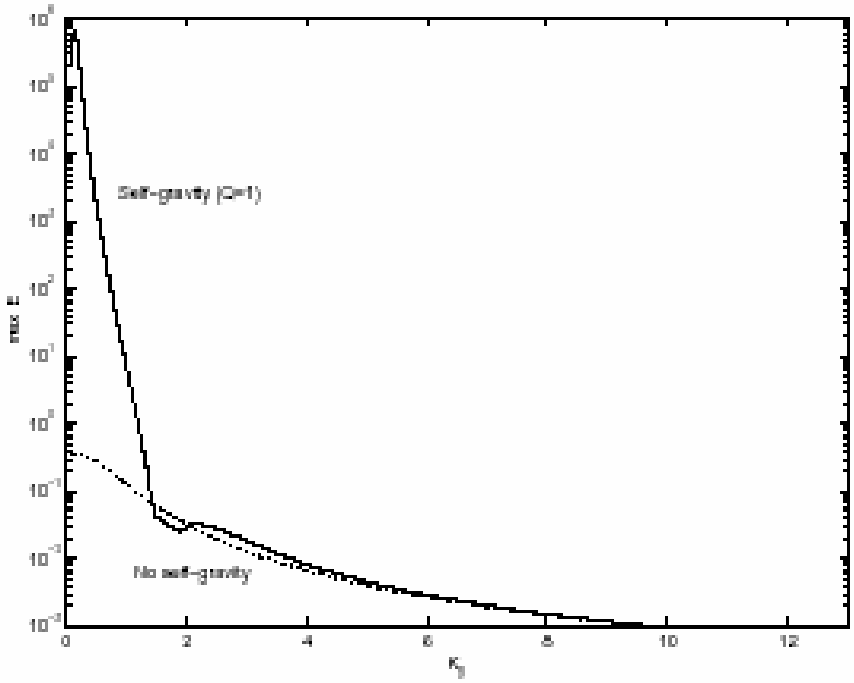

Figure 10. Maximum value of energy during the transient amplification as a function of K_y for $Q = 1$ (solid curve) and $Q = \infty$ (no self gravity)(dotted curve). Transient amplification is largest for $K_y \sim O(0.1)$. As it is obvious, self-gravity greatly enhances transient growth of vortex energy.

We would like to stress that this phenomenon of generation of nonvortical/wave perturbations by vortical perturbations is a fundamental property of shear flows. It was observed in complex numerical simulations of graviturbulence in galactic discs (Wada et al. 2002), where the energy spectrum of vortical (solenoidal) component of turbulent velocity after some time becomes similar to that of wave (compresible) component.

3.3 Dynamics of localized density wave packets

The behaviour of individual SFH of wave perturbations summarized in the preceding section gives us important information on the mechanisms of amplification and over-reflection of density waves. However, a complete and vivid picture of the phenomenon can be obtained by examining the behaviour of the solutions in real space for a wave packet (superposition of different Fourier harmonics) that is localized both in real and wavenumber planes. In this section we undertake this task.

As an initial condition, we superimpose on the basic shear flow a localized wave packet, that we define in **K**-plane centered around a point (K_{x0},K_{y0}) (of course, there is a counterpart centered around (-K_{x0},-K_{y0}) since all perturbed quantities are real). The location and appearance of the perturbations for the different physical variables in real space for all times can then be obtained through the inverse Fourier transform and expressed in the following form:

$$u(x,y,\tau) = \int\int dK_x dK_y u(K_x,K_y,\tau) exp(iK_x x + iK_y y)$$

$$v(x,y,\tau) = \int\int dK_x dK_y v(K_x,K_y,\tau) exp(iK_x x + iK_y y)$$

$$\sigma(x,y,\tau) = \int\int dK_x dK_y \sigma(K_x,K_y,\tau) exp(iK_x x + iK_y y)$$

$$\phi(x,y,\tau) = \int\int dK_x dK_y \phi(K_x,K_y,\tau) exp(iK_x x + iK_y y)$$

where $(u,v,\sigma,\varphi)(K,\tau)$ characterize the shapes (packets) for the distributions of the radial and azimuthal velocities, surface density and gravitational potential in **K**-plane (we remind that, as made above, hats over these dimensionless quantities are omitted. (x, y) coordinates are nondimensionalized by c_s/κ). In general, any initial packet in K-plane far from nonadiabatic regions contains contributions from two waves with oppositely directed phase velocities (negative and positive frequency waves of Eq.(24)). Below we describe how to excite a packet which initially has a group velocity directed in a certain direction. Initially for the shape of the surface density perturbation in the packet we choose the form

$$\sigma(K_x, K_y, 0) = i\epsilon_p exp(-iK_x x_0 - iK_y y_0)(H_- + H_+),$$

where

$$H_\mp(K_x, K_y) = exp\left(-\frac{(K_x \mp K_{x0})^2}{\Delta K_x^2} - \frac{(K_y \mp K_{y0})^2}{\Delta K_y^2}\right)$$

An analogous expression for the packet initial shape was adopted by Bodo et al. (2001) in their numerical simulations of localized packets of MHD waves in shear flows. It consists of two oval shaped localization areas in K-plane with sizes defined by ΔK_x, ΔK_y and centres situated at (K_{x0},K_{y0}) and $(-K_{x0},-K_{y0})$, as has been mentioned above. The quantities x_0 and y_0 specify the initial position of the packet centre in real space (that is easy to see if we make inverse Fourier transform of this expression. It is also clear that the resultant packet in real space is localized as well). The amplitude of the perturbation is defined by the scaling factor $\varepsilon_p = 0.01$, which is taken to be sufficiently small in order for the linear approximation, in which we work, to be valid. In our calculations we make the parameters K_{x0},K_{y0} take on various values because we are interested in the packet dynamics when its center is situated at the beginning of evolution in different positions (provided the adiabatic condition is fulfilled there) in **K**-plane relative to the unstable regions (Fig.1). If (K_{x0},K_{y0}) is located in the second quadrant of **K**-plane we have a packet of leading waves, if in the first quadrant then we have a packet of trailing waves.

(The cases where (K_{x0},K_{y0}) is located in the lower half plane reduce to the previous cases, so below in all calculations (K_{x0},K_{y0}) lies in the upper half plane $K_y > 0$.)

As we have mentioned, any packet in the adiabatic region contains positive and negative frequency waves and as a result it divides at the beginning of the evolution due to the oppositely directed group velocities corresponding to these waves (for the definition of group velocity in the context of non-modal approach see Appendix B). To avoid such initial splitting, which does not represent a novelty, we should consider from the outset a packet composed of one sort of waves either with negative or positive frequency and follow its subsequent evolution. Here we choose positive-frequency waves (Eq.(25)), so the x-component of the group velocity at $\tau = 0$ is directed radially inwards if $K_{x0} < 0$ (packet of leading waves) and outwards if $K_{x0} > 0$ (packet of trailing waves). This choice requires (u,v)(K,0) to be related to σ(K,0) through the expressions

$$u(\mathbf{K},0) = \left(\frac{2BK_y}{K^2} - \frac{2AK_yK_x^2}{K^4} - \frac{iK_x\omega(\mathbf{K})}{K^2} \right) \sigma(\mathbf{K},0)$$

$$v(\mathbf{K},0) = \left(-\frac{2BK_x}{K^2} - \frac{2AK_xK_y^2}{K^4} - \frac{iK_y\omega(\mathbf{K})}{K^2} \right) \sigma(\mathbf{K},0)$$

$$\phi(\mathbf{K},0) = -\frac{2}{QK}\sigma(\mathbf{K},0)$$

which follow from Eq. (21)-(23) and the form of the positive-frequency waves (25). We would like to note that this method of initial preparation of the packet with only positive-frequency waves is approximate in the sense that it is based on the asymptotic expansion of the WKB approximation far from the nonadiabatic regions. It would be exact for oscillatory systems with constant characteristics, while the parameters ($\omega(\tau)$,K(τ)) of our system varies with time. Nevertheless, it is fairly satisfactory in our calculations.

We examine all the peculiarities of packets composed originally of short leading waves ($K_{x0} < 0$, $|K_{x0}| >> K_{y0}$). Specifically, we describe the dynamics for three different

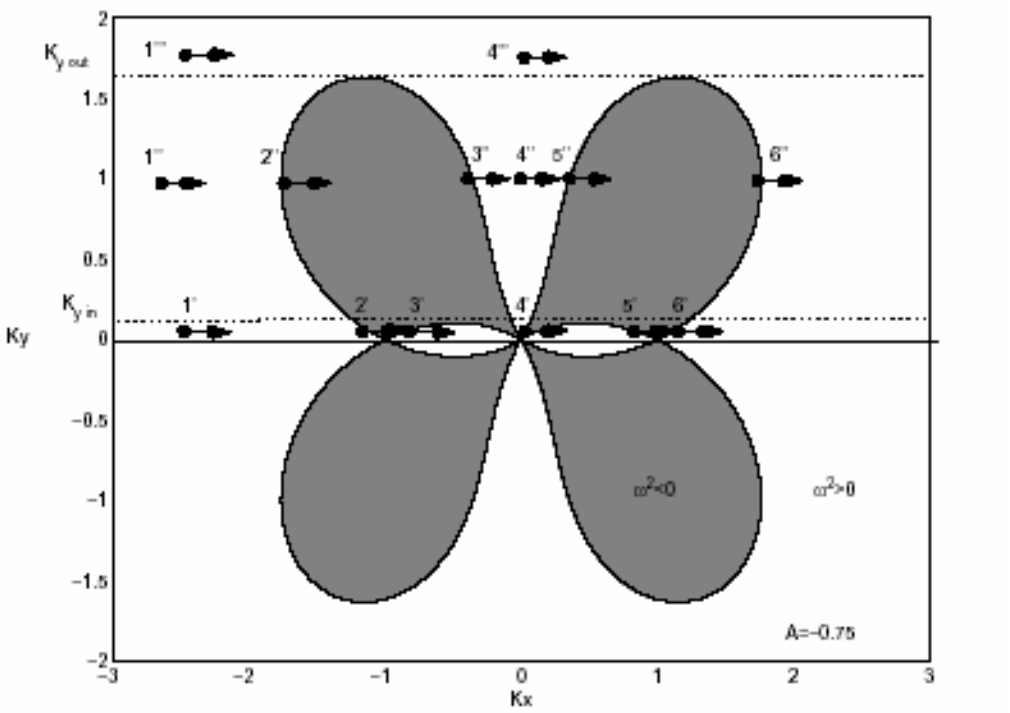

Figure 11. Schematic illustration of the packet drift in **K**-plane. The sequences $1' \to 2' \to 3' \to 4' \to 5' \to 6' \to$, $1'' \to 2'' \to 3'' \to 4'' \to 5'' \to 6'' \to$ and $1''' \to 4''' \to$ correspond to $K_y = 0.04\ (a), K_y = 0.4\ (b)$ and $K_y = 4\ (c)$ respectively.

bands of the packet parameters (see Fig.11, this figure is only schematic, so numerical values of K_{x0} and K_{y0} in this figure do not match their actual values used in calculations):

(a) The initial short leading packet with $0 < K_y \pm \Delta K_y < K_{yin}$ is situated at the point $1'$,

(b) The initial short leading packet with $K_{yin} < K_y \pm \Delta K_y < K_{yout}$ is situated at the point $1''$,

(c) The initial short leading packet with $K_y \pm \Delta K_y > K_{yout}$ is situated at the point $1'''$.

The dynamics of packets of short trailing waves (K_{x0}>>K_{y0}) is less interesting and quite predictable; they propagate without splitting and the group velocity never changes sign. Besides, the final stage of evolution of short leading wave packets are short trailing packets, so we do not consider later as a special case. We take the quantity $e(x,y,\tau) = (u^2(x,y,\tau)+v^2(x,y,\tau)+\sigma^2(x,y,\tau))/2$ as a measure of the packet intensity, which we call the packet energy density. In the following we consider marginally stable disks $Q = 1$. The dynamics for $Q > 1$ does not differ qualitatively from that for $Q = 1$ and can be considered by analogy. Thus, we elaborate on the value $Q = 1$ in more detail.

As stressed earlier, due to differential rotation the radial wavenumber $K_x(\tau)$ of each SFH composing the packet changes/drifts with time. As a result, the packet itself also starts to drift in **K**-plane from its initial position along the K_x-axis in the positive direction (since $A<0$) and crosses the stable and unstable regions discussed in 3.1. Since the drift velocity is different for different K_y the packet alongside the drift undergoes a shearing deformation. The schematic illustration of the packet drift is presented in Fig.11. We will see below that *all the peculiarities of the dynamical picture in physical* **r**-*plane stem just from this drift*. The general evolution in **r**-plane can be seen in Fig.12,13,14 where we show images of the packet energy density $e(x,y,\tau)$ at different times for various values of K_{x0} and K_{y0} (although a qualitative picture of evolution is identical for the packets of all perturbed quantities)

We now give an interpretation of this behaviour in terms of the various locations of the packet centre relative to the unstable regions in **K**-plane in the course of its evolution/drift. Begin with the case (a) when the centre of a short leading wave packet during its drift crosses the two narrow unstable regions and one longer intermediate stable region (K_y = 0.04 in Fig.11). From Fig.12 we can see that in the beginning the group velocity of the packet inverse Fourier transform (PIFT) (i.e.,the corresponding localized packet in **r**-plane) is directed towards the origin of (x,y), according to our choice, and propagates as a whole without initial splitting. Along with the propagation it also rotates in the anticlockwise direction. The rotation is associated with the shearing deformation of the packet. However, at the time when the packet begins to enter the first unstable region (point 2' in Fig.11), PIFT gradually stops (τ = 45 in Fig.12), since the group velocity for $\omega^2<0$ is zero (not defined). From this moment the first amplification of the packet $E(\tau)=\frac{1}{2}\iint(u^2+v^2+\sigma^2)dxdy$ energy occurs (Fig. 15). Then the packet leaves this region (point 3') and starts crossing the relatively long intermediate region of $\omega^2>0$ where it can be approximately represented as a superposition of positive (transmitted) and negative (reflected) frequency waves traveling in the opposite directions. The wavenumber of each SFH decreases and constituent waves become long leading. At this

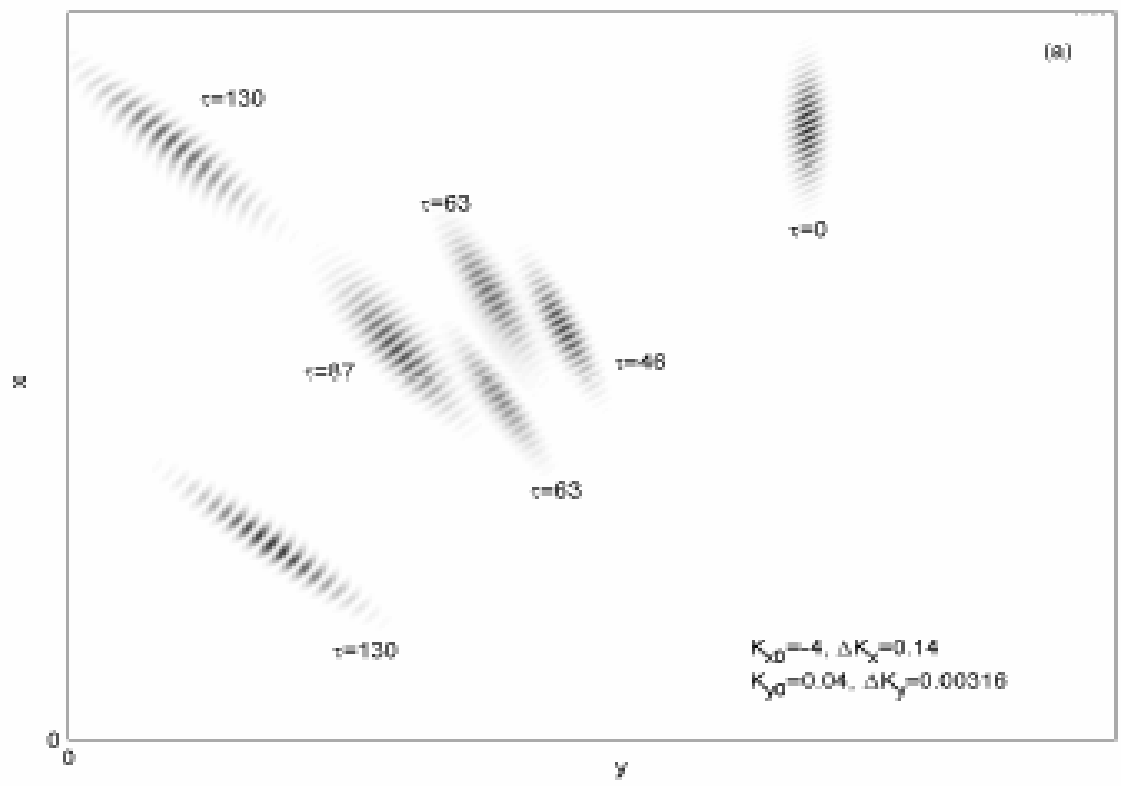

Figure 12. Evolution of the packet energy density $e(x, y, \tau)$ (shaded)in r-plane for $K_{x0} = -4$ and $K_{y0} = 0.04$. In the beginning the packet propagates as a whole, then in r-plane splits into two parts as its FT enters the intermediate stable region and then these two parts join when PFT leaves this region. After that the packet splits again when PFT moves onto another stabile region throughout which ω^2 is positive.

time the PIFT is split into two parts (τ=63), which propagate along different trajectories as each consists of one from these two kinds of waves. However, as the packet crosses the line/corotation point $K_x = 0$ (point 4') the waves in it change from long leading to long trailing. As a consequence, in r-plane the split fragments reverse the sign of the *x*-component of their group velocities and begin to near each other. From the above it follows that these two parts are initially made up of long leading and then of long trailing positive and negative frequency waves. After this intermediate region the packet moves onto the second $\omega^2<0$ region. On entering that (point 5') these split parts merge and the resultant packet in **r**-plane stops for some time (τ=67) until the packet leaves this region (point 6'). There occurs the second amplification of the packet energy (Fig.15).

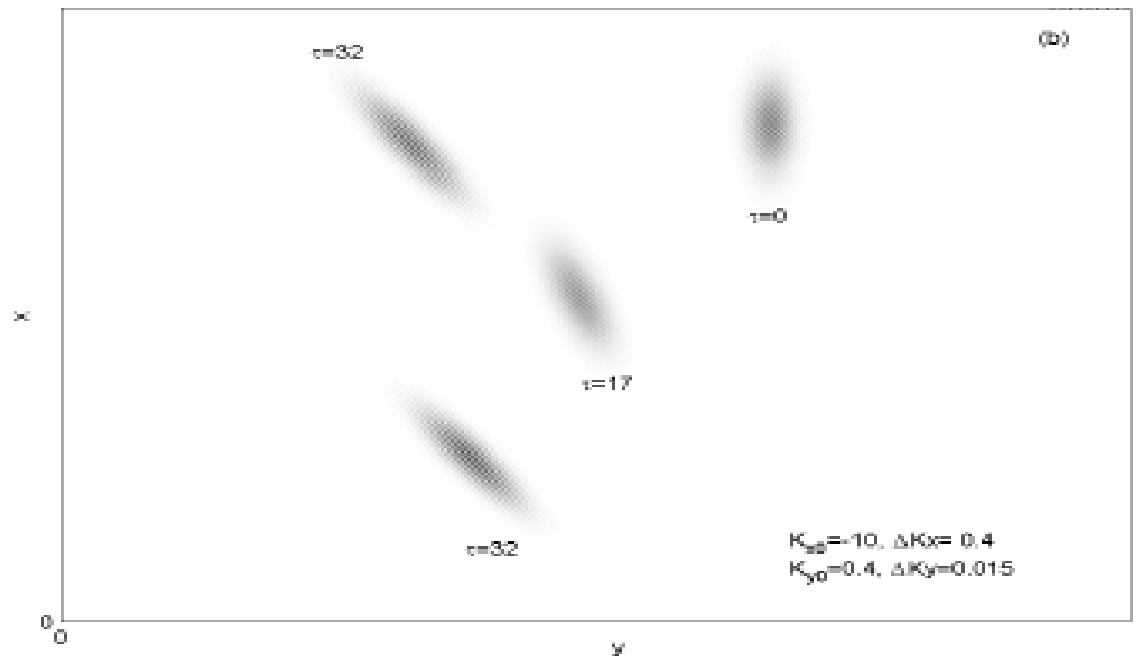

Figure 13. Same as in Fig.12 but with $K_{x0} = -10$ and $K_{y0} = 0.4$. In this case the packet directly splits into transmitted and reflected parts in r-plane when PFT passes through the unstable region.

On leaving this region it gets into the region $\omega^2>0$ and never leaves it. Here, as in the analogous intermediate stable region, the solution is a superposition of oppositely traveling waves. So the composite packet in **r**-plane splits again (τ=130), but now both split parts are composed of short trailing waves and continue to remain so. Corresponding group velocities retain their direction, since wavenumber K_x does not change sign throughout this last $\omega^2>0$ region. In analogy to the above choice of transmitted and reflected waves, we call a transmitted packet the part made up of transmitted (positive frequency) waves and a reflected packet the part that is composed of reflected (negative frequency) waves. The *x*-component of the group velocity of the transmitted packet is directed opposite to that of the incident packet and gives the impression of being the reflected one, but this is not the case, since the change in the

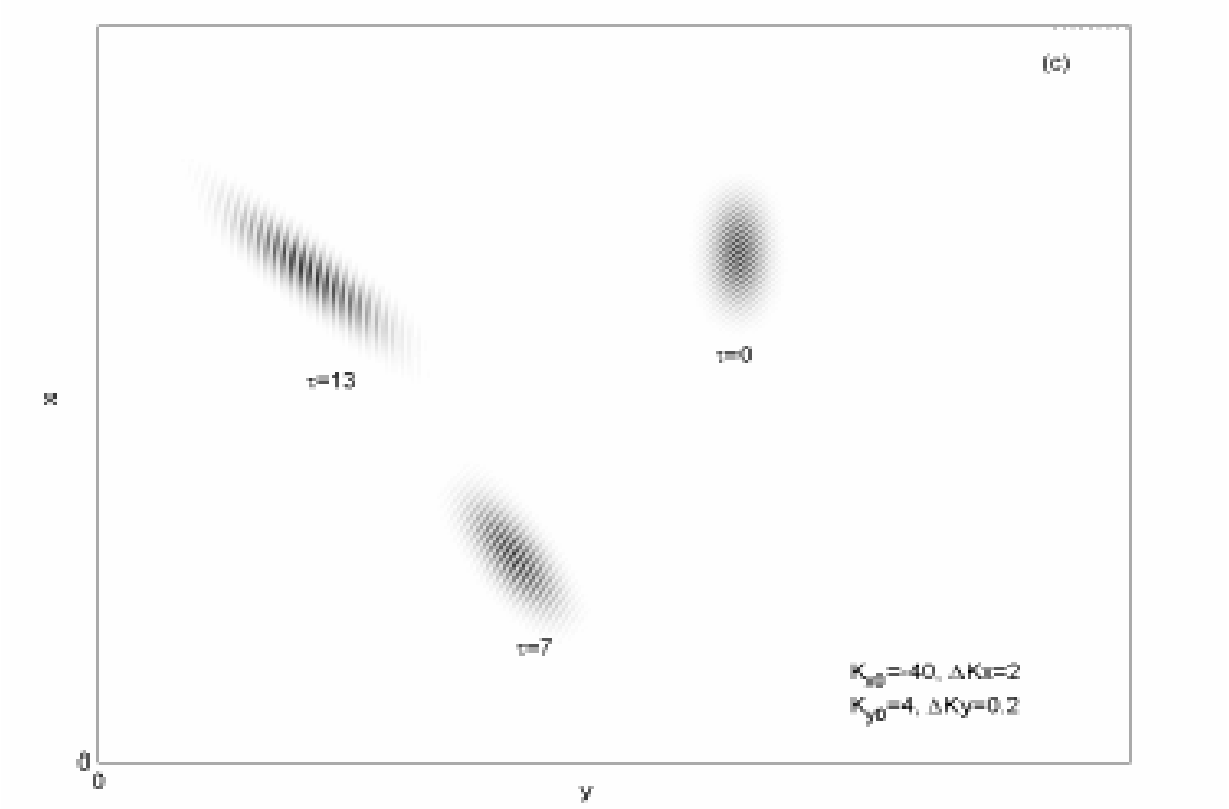

Figure 14. Same as in Fig.12 but with $K_{x0} = -40$ and $K_{y0} = 4$. The packet propagates without splitting, since its FT crosses neither unstable region and fraction of reflected waves is negligible (see Fig.3). It just reverses the direction of propagation at the moment when its FT crosses the line $K_x = 0$ in K-plane.

direction of group velocity of the positive frequency packet is associated with the sign reversal of the drifting central wavenumber $K_{x0}(\tau) = K_{x0}\text{-}2AK_{y0}\tau$. That is seen most clearly in the case (c) considered below, when the fraction of the reflected short trailing waves (packet) is negligible. From now on the energies of these enhanced split fragments increases linearly (Fig.15). Because of the shearing deformation of the packet in K-plane these two split parts gradually become more and more tightly wound.

In the considered case the energies of these two packets are nearly the same, since for $K_{y0} = 0.04$ the transmitted and reflected coefficients of waves are comparable (Fig.3), but if we took K_{y0} corresponding to small values $|R|$ (for example, $K_{y0} = 0.03625$ in Fig.3) and the size ΔK_y of the initial packet was small enough as well, much of the initial packet energy would be concentrated in the transmitted packet. It should be noted that such

properties of the packet behaviour are connected with the differential rotation (the shear A parameter) that leads to the modified Lin-Shu dispersion relation (24) (Fig.1). Indeed, the moments when the packet splits and the two parts then join are determined by the shape of the $\omega^2 = 0$ curve in **K**-plane and the initial position (K_{x0},K_{y0}) of the packet centre relative to this curve. Knowing these moments it is also possible to determine an approximate location of splitting and merging points of a packet in **r**-plane by integrating the group velocity over time. Thus, all the peculiarities of the packet behaviour in **r**-plane can be explained by analyzing the dynamics/drift of its Fourier transform in **K**-plane and the behaviour of the group velocity, which is given as a function of the central wavenumber of the packet and system parameters. It would be rather difficult to analyze/interpret packet propagation properties described above based on the normal modes of the shearing sheet alone.

Consider now the case (b) (Fig. 13) when the centre of the packet during its drift crosses larger unstable regions. This case is qualitatively similar to the previous case, but there are some quantitative distinctions. Before reaching the first unstable region (point 2") the packet proceeds in much the same way as in the case (a) in both planes. Then follows the amplification of the packet energy (Fig. 16) corresponding to its location in the large unstable region between points 2" and 3". However, intermediate splitting of the packet in r-plane is no longer observed, because the adiabatic approximation between points 3" and 5" is not met (the time interval during which the packet crosses this intermediate stable region is comparable to the period of oscillations) and therefore in this region the packet does not divide into waves with certain frequencies (of course, the spatial dependence of these waves is, as before, plane harmonic. in this region they change from long leading to long trailing). Accordingly, during this stage PIFT does not move. It is not possible to define the group velocity for such a non-WKB solution. Then the packet moves onto the second unstable region (point 5") where its energy increases further. The growth of the energy in both unstable regions is considerably higher than that for the preceding case. The reason is the same as that for individual SFH in 3.2.1.

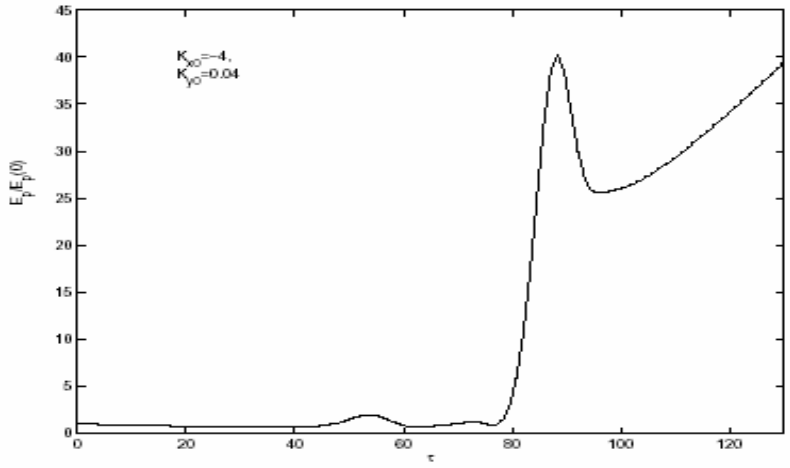

Figure 15. Time-development of the packet(s) total energy for $K_{x0} = -4, K_{y0} = 0.04$

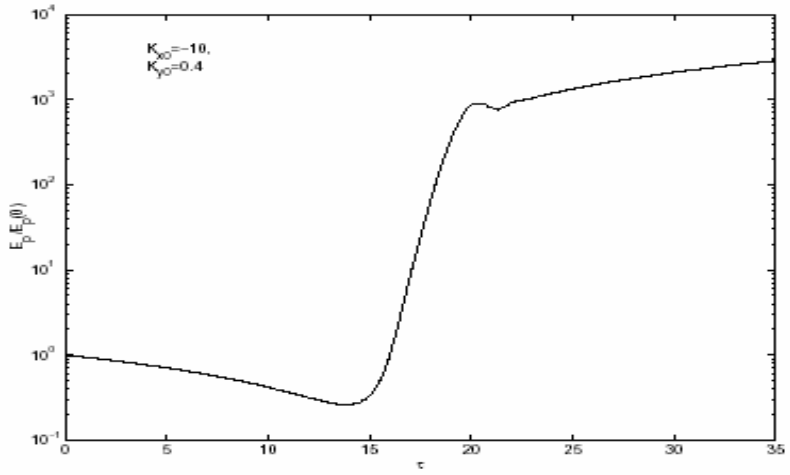

Figure 16. Same as in Fig.15, but with $K_{x0} = -10, K_{y0} = 0.4$

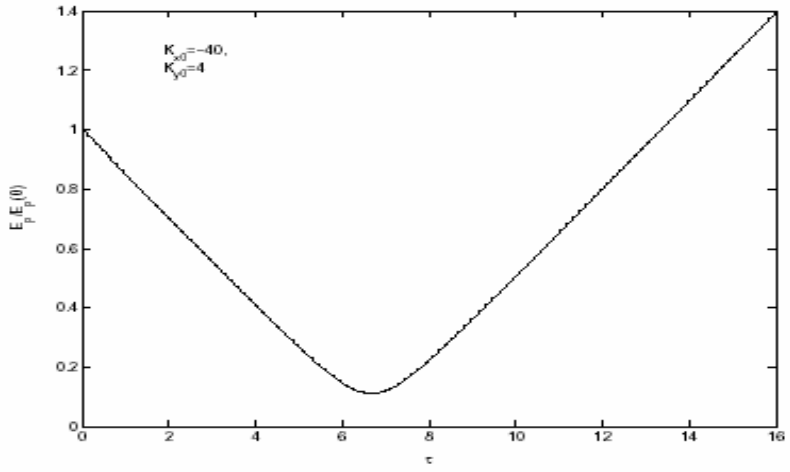

Figure 17. Same as in Fig.15, but with $K_{x0} = -40, K_{y0} = 4$

After leaving (point 6") it again gets into the adiabatic region and becomes, as before, composed of positive and negative frequency short trailing waves. As a result, we again see the splitting of the incident packet into transmitted and reflected ones. The transmitted packet propagates opposite to the incident one (x-component of the group velocity is reversed).

In the case (c) (Fig.14) the packet centre crosses neither unstable region. The PIFT in **r**-plane starts from being a packet of positive frequency short leading waves and propagates towards the origin of (x,y), then gradually becomes a packet of long leading waves, of long trailing waves, when the packet in K-plane crosses the line $Kx = 0$, and at the same time changes the sign of the x-component of the group velocity due to the sign reversal of $K_{x0}(\tau)$ and propagates outwards from the origin. Finally, composing long trailing waves are gradually converted into short trailing ones and the packet in **r**-plane winds tighter and tighter with time due to the shearing deformation. There is no splitting in this case, since the adiabatic condition is met all along the evolution and, therefore, the portion of reflected waves is negligible. The packet energy initially decreases until the corotation $K_x = 0$ point and then increases linearly (Fig. 17).

The case of an initial trailing wave packet ($K_{x0} > 0$) is not as interesting as other considered cases. There is no conversion between waves and the packet remains composed of trailing waves with the same sign of frequency at all times. Following from it the group velocity never changes sign. During the drift it does not cross any dynamically interesting regions in **K**-plane. If an initial packet consists of positive frequency waves its PIFT propagates along the x-axis, otherwise the propagation is opposite. It does not split during the whole evolution and winds tighter and tighter.

Summary

In this chapter we have analyzed the dynamics of individual SFH and localized packets of spiral density waves in the shearing sheet approximation using non-modal approach combined with numerical calculations. We have shown that density waves (packets) experience strong swing amplification as they swing from a leading to a trailing orientation. The growth for $Q \sim 1$ is most effective when the inverse of the azimuthal wavenumber is comparable to the disc thickness (see also NS) and is due to flow shear. For large times swing amplification is followed by asymptotically linear growth of wave energy. Large swing amplification of both waves and vortices can expedite fragmentation of medium (Kim & Ostriker 2002, Gammie 2001) or turbulization of flow (Wada et al. 2002) (depending on the value of Q) and serve as a main extractor of energy from the mean flow in case of turbulence. We have also analyzed the reflection and transmission of waves. It has been shown that the reflection coefficient behaves in an oscillatory manner for small azimuthal wavenumbers and is greatly enhanced due to flow shear for $K_y \sim O(0.1)$ (K_y nondimensionalized azimuthal wavenumber)

We have also examined the properties of vortical perturbations. It has been shown that vortical perturbations undergo transient amplification, which increases with decreasing K_y For $K_y>1$ wave generation by vortices is noticeable, but the dynamics is dominated by transient growth which may be larger than wave amplification for the same K_y. For $K_y<1$ vortices can effectively excite spiral density waves after transient amplification stage. This effect is possible only in sheared flows and tends to zero in the shearless limit.

We have also studied the peculiarities of propagation of localized packets of density waves. Non-modal approach allows considerably simpler and clearer for comprehension treatment of this problem compared with modal approach. From the above analysis it is obvious that we can judge the packet dynamics knowing how its Fourier transform evolves in **K**-plane. So we no longer need to introduce corotation and Lindblad resonances in the shearing sheet model, as was done in Goldreich & Tremaine (1978)

and also in Binney & Tremaine (1987). The positions where a packet splits and split parts merge are defined entirely by its Fourier transform characteristics. Although the shearing sheet model does not allow us to analyze the packet evolution all over the disc but it is particularly helpful in examining the situation near a particular area in the disc, and the splitting of packets observed in global disc simulations by Toomre and Zang (Toomre 1981) can be readily explained in terms of our analysis. There is other valuable asset of the shearing sheet; it admits the treatment of initial value problems by means of non-modal approach saving us from summing many interfering eigenfunctions. It is hardly possible to explain the properties of localized density wave packets described here based on the modal approach alone.

Chapter 4

Summary and Discussions

In this thesis we have investigated the phenomena taking place due to non-orthogonality of shear flows, which are quite common in meteorology or astrophysics. In principle, these phenomena can be analyzed in the framework of modal approach, but having done that we encounter rather serious difficulties associated with the non-normality and interference of eigenfunctions, whereas non-modal approach permits simple and elegant description of phenomena.

In Chapter 2 we have considered dynamics of two kinds of perturbations, vortices and waves in zonal geostrophic shear flows. The classification of perturbation modes has been made based on the value of potential vorticity. Traditionally, in quasigeostrophic models of geophysical hydrodynamics wave perturbations are filtered and the main subject of study is the dynamics of vortical perturbations. Our investigation instead has shown that waves are equally important. We have considered two regimes $Ro \ll 1$ and $Ro \sim 1$, which are typical of most atmospheric and oceanic flows (atmospheric and oceanic synoptic vortices, jet streams associated with atmospheric fronts, oceanic jet streams). In the first regime wave and vortex modes evolve separately; there is no transformation between modes. Because of the fact that the frequency of oscillations is time-dependent, energy of wave perturbations increases asymptotically linearly. Vortical perturbations die out after transient amplification. It can be said that the flow is

algebraically unstable to waves but stable to vortical perturbations. Transient and linear amplification of perturbations in this case may be important for the instability of synoptic cyclones. Thus, traditional quasigeostrophic approach is valid for small Rossby numbers. Accordingly, in this case the role of shear is less effective. In the second case the flow shear plays a central role in perturbation dynamics. First we have examined the properties of pure wave perturbations initially imposed on the flow. It has been shown that for Ro<1 waves grow asymptotically linearly for large times (algebraic instability), as in the first case, however for Ro>1 linear amplification is preceded by exponential amplification of wave energy. The existence of exponential amplification may prompt transition to turbulence by *bypass* scenario. Note that according to modal analysis the flow of the type considered (Couette flow) here is stable and there seems to be no linear mechanism capable of extracting energy from shear.

As regards vortical perturbations, they generate internal waves which amplify further. Vortical perturbations themselves after transient amplification return energy to the mean flow and die out. They act as a mediator between the background flow and waves. This phenomenon of wave generation by vortiacal/aperiodic perturbations cast doubt on the validity of quasigeostrophic approach, which underestimates the role of wave perturbations, while they play a decisive role in the instability of shear flows.

We have also briefly discussed the effects of viscosity. Viscosity merely diminishes the wave amplitudes without affecting the frequency. For bounded flows by means of variational approach we have derived the sufficient criterion for stability $AH < c$, where A is the shear parameter, H is the distance between bounding walls and c is the sound speed. If this condition is satisfied then a flow is linearly stable to wave perturbations. This criterion facilitates study in that saves us from making spectral expansion in time and finding unstable normal modes.

As was estimated in the text the value Ro~1 is related to atmospheric and oceanic jet streams associated with fronts. Our analysis sheds new light on the properties of these flows and shows that they are much richer than that predicted by modal analysis. Particularly, wave generation, explosive-algebraic type of instability and transient

growth of vortex mode perturbations may be important in the stability study of jet streams and, consequently, of fronts. The problem of the stability of frontal interfaces is of high importance for geophysical hydrodynamics. In the first approximation this is a problem of the stability of inclined surface separating rotating mediums with different characteristics. Solution of this problem is important in meteorology, primarily in connection with a so called wave hypothesis of cyclogenesis, offered by Norwegian meteorology. According to this hypothesis non-tropical cyclones and anticyclones are generated as a result of instability of a wave on inclined surface that separates air masses with different properties (frontal interface).

First attempts to analyze the stability of frontal interfaces can be found in Kochin (1949). In the framework of an oversimplified model, he has formulated analytical criterion for the stability of frontal surface and discovered that length scales of unstable waves closely match the size of frontal cyclones on moderate latitudes. These results were further developed by Blinova, Kibel and others and were generalized to the case of compressible medium. Numerical investigation of the stability of frontal interfaces can be found in Orlanski (1968), Abramov et al. (1972), Tang (1972), Joly & Thorpe (1990), Sinton & Heise (1993). Notwithstanding a more realistic consideration, the physical interpretation of these results is highly complicated due to various models and parameters employed and absence of reliable experimental data. Besides, linear stability analysis does not allows the description of finite amplitude perturbations that lead to the development of frontal cyclones. Nevertheless, it shows by the use of non-modal approach that instabilities do exist in spectrally stable flows that potentially can result in the emergence of frontal cyclones. Thus, the problem of stability of frontal interfaces is far from the deep understanding and require further investigation and the main tool should be non-modal approach combined with numerical simulations to analyze nonlinear evolution if we want to describe the phenomena adequately.

In Chapter 3 we have studied the dynamics of spiral density waves and vortices in differentially rotating astrophysical thin discs with self-gravity in the shearing sheet approximation by means of non-modal approach and numerical calculations. First we

have introduced the shearing sheet equations and made spatial Fourier transform of perturbed quantities. Then we have analyzed the evolution of individual spatial Fourier harmonics (SFH) and found that the energies of both vortex and wave SFH experience strong swing amplification (transient growth) when the inverse of the azimuthal wavenumber is comparable to the disc thickness. Due to this multi-arm spiral structure often emerge in many numerical simulations of galactic discs (see e.g. Sellwood & Carlberg 1984). Swing amplification is followed by asymptotically linear amplification of wave energy. Strong swing amplification together with linear amplification is important for forming gravitationally bound complexes (e.g. giant molecular clouds) in the interstellar medium of galaxies or for triggering turbulence in accretion discs by the *bypass* transition scenario that was observed in complex numerical simulations of Wada et al. (2002) or Kim & Ostriker (2001)

We have also analyzed the reflection and transmission of density waves. (Over)-reflection coefficient attains its maximum ($O(100)$) for azimuthal wavenumbers of the order of 0.1, which is brought about by flow shear; for small shear parameters reflection coefficient remains of order unity. The properties of over-reflection of density waves in real plane are characterized by the drift of radial wavenumber in **K**-plane. The specific behaviour of the reflection coefficient with azimuthal wavenumber can be simply explained based on the shape of unstable regions in **K**-plane.

We would like to note that shear enhanced reflection of waves are essential and effective to the instabilities associated with resonances found by Papaloizou and Savonije (1991) in their numerical investigations of non-axisymmetric perturbations in thin self-gravitating discs.

For nondimensionalized azimuthal wavenumber $K_y<1$ vortices can effectively excite spiral density waves after transient amplification stage. This effect is possible only in sheared flows and tends to zero in the shearless limit. This effect is undetectable in the modal treatment of the shearing sheet. This wave generation is seen in global disc simulations of vortices (Bodo et al. 2005) and its characteristics are well explained in the shearing sheet. Thus, from our analysis it is clear that vortices can be considered as a

novel source of spiral density waves in addition to already well-known ones (bar excitation, companion galaxy, instabilities in discs).

We would like to stress that this phenomenon of generation of nonvortical/wave perturbations by vortical perturbations is a fundamental property of shear flows. It was observed in complex numerical simulations of graviturbulence in galactic discs (Wada et al. 2002), where the energy spectrum of vortical (solenoidal) component of turbulent velocity after some time becomes similar to that of wave (compresible) component.

We have also studied the peculiarities of propagation of localized packets of density waves. Non-modal approach allows considerably simpler and clearer for comprehension treatment of this problem compared with modal approach. As individual SFH, localized packets undergo swing amplification when evolving from being leading packet to trailing one. From the above analysis it is obvious that we can judge the packet dynamics knowing how its Fourier transform evolves in **K**-plane. So we no longer need to introduce corotation and Lindblad resonances in the shearing sheet model as was done in Goldreich & Tremaine (1978) or Binney & Tremaine (1987). The positions where a packet splits and reflects in real plane are defined entirely by its Fourier transform characteristics.

Once again below we list the main results of the thesis

- For Ro<<1 (Ro is the Rossby number) wave and vortex modes evolve independently; there is no coupling between modes. The energy of the wave mode increases asymptotically linearly. The vortex mode after transient amplification gradually dies out;

- In atmospheric and oceanic shear flows novel features of wave and vortex modes have been found at moderate ($O(1)$) Rossby numbers. The energy of non-symmetric wave perturbations at large times increases linearly (algebraic instability). If Ro < 1 there takes place only an algebraic growth of non-symmetric shear internal waves. At

Ro > 1 a time interval of the linear growth is preceded by an interval of exponential (explosive) growth. This explosive growth is explained in terms of symmetric instability. At Ro > 0.8 vortex mode perturbations initially gain the basic flow energy and then are converted into shear internal waves, energy of which then grows linearly. For Ro=0.4 wave generation starts to be noticeable, but transient amplification of vortex mode is a dominant feature in the dynamics. Such transient amplification may be important for triggering and maintaining turbulence in shear atmospheric and oceanic flows;

- Viscosity effects on the perturbation dynamics have been analyzed. It has turned out that viscosity diminishes only perturbation amplitudes for large times and does not affect the instant frequency of time oscillations;

- There has been proved a theorem concerning the stability of shear bounded flows. In particular, when $AH < c$, where A is the shear parameter, H is the distance between walls bounding the flow in the azimuthal direction and c is the sound speed, a flow is stable to wave type perturbations. This theorem facilitates study in that saves us from making spectral expansion in time and finding unstable eigenvalues;

- For Q~1 (Q is Toomre's stability parameter) the swing amplification of waves in discs is most effective when the inverse of the azimuthal wavenumber is comparable to the disc thickness and is due to flow shear. For large times swing amplification is followed by asymptotically linear growth of wave energy;

- Reflection and transmission of waves have also been analyzed. It has been shown that the reflection coefficient behaves in an oscillatory manner for small azimuthal wavenumbers and is greatly enhanced (O(100)) due to flow shear for K_y~O(0.1);

- Specific properties of vortical perturbations have been investigated. It has been shown that vertical perturbations undergo transient amplification which increases with decreasing azimuthal wavenumber $K_{y.}$ For $K_y>1$ wave generation by vortices is noticeable, but becomes weaker and weaker with increasing K_y; the dynamics is dominated by transient growth of vortex mode which may be larger than wave amplification factors for the same K_y. For $K_y<1$ vortices can effectively excite spiral density waves after a transient amplification stage. This effect is possible only in sheared flows and tends to zero in the shearless limit;

- The peculiarities of propagation of localized packets of density waves have been studied. From the analysis it has turned out that we can judge the packet evolution knowing how its Fourier transform evolves/drifts in **K**-plane. So we no longer need to introduce corotation and Lindblad resonances in the shearing sheet model as was done in previous works.

Appendix A

Analytical derivation of the oscillatory behaviour of the reflection coefficient for small K_y~O(0.01)

As it is obvious from Fig.3 for Q = 1 and for the considered here azimuthal wavenumbers K_y~O(0.01) shear leads only to a little amplification of the reflection coefficient compared with Fig.4 without affecting the oscillatory behaviour. Therefore for understanding the basic reason for the oscillatory nature for small Ky we can set A = 0. In this case Eq.(24) reduces to (hats are ommitted)

$$\frac{d^2\phi(\tau)}{d\tau^2} + \omega^2(\tau)\phi(\tau) = 0,$$

where

$$\omega^2(\tau) = \left(K_y\sqrt{4A^2\tau^2+1} - 1\right)^2.$$

In this equation, as in subsection 3.2, we have made substitution $\tau \to \tau - K_x/2AK_y$. The function $\omega^2(\tau)$ has two minima at $\tau_\pm = \pm\frac{1}{2|A|}\sqrt{\frac{1}{K_y^2}-1}$ and one maximum at τ = 0 (Fig.A1). It is easy to show that the adiabatic condition is satisfied far from these minima between as well as outside them. So in these regions we can use the WKB solutions $\frac{1}{\sqrt{\omega(\tau)}}\exp\left(\pm i\int_0^\tau \omega(\tau')d\tau'\right)$, $\omega(\tau) = \left|K_y\sqrt{4A^2\tau^2+1}-1\right|$ or after evaluating the elementary integral we have $\frac{1}{\sqrt{\omega(\tau)}}\exp(\pm if(\tau))$,

$$f(\tau) \equiv \frac{\tau K_y}{2}\sqrt{4A^2\tau^2+1} - \frac{K_y}{4A}\ln(\sqrt{4A^2\tau^2+1} - 2A\tau) - \tau.$$

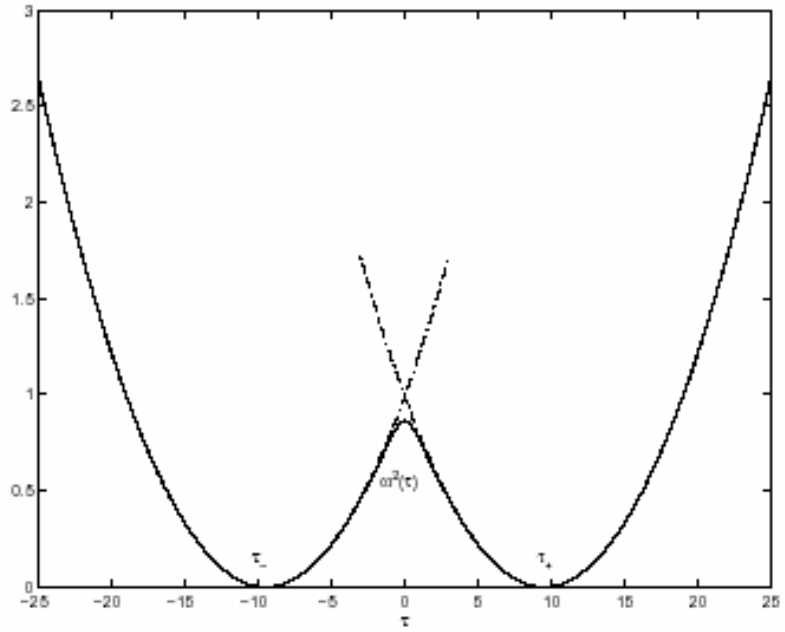

Figure A1. Solid curve is $\omega^2(\tau)$ for $K_y = 0.07$. Dash-dot curves represent second order approximation in the Taylor expansion around $\tau_{+,-} \approx \pm 9.5$.

In the vicinity of each minimum we can expand $\omega^2(\tau)$ in a Taylor series with respect to $\tau - \tau_{\pm}$ and keep only second order terms (it can be shown that for small K_y it is a very good approximation). The coefficients of zero and first order terms in this expansion are zero as it is clear from Fig.A1. After that our basic equation close to the point $\tau_{\pm}$ takes the form of the parabolic cylinder equation

$$\frac{d^2\phi(\tau)}{d\tau^2} + 4A^2K_y^2(1-K_y^2)(\tau-\tau_{+,-})^2\phi(\tau) = 0,$$

whose solutions as well as the connection formulae for waves on either side far from the nonadiabatic region are well known (see also Goldreich & Tremaine 1978 and Nakagawa & Sekiya 1992).

Let us start from $\tau << \tau_-$. Here the solution has the form of the incident positive frequency wave with unity amplitude $\frac{1}{\sqrt{\omega(\tau)}}\exp(-if(\tau))$, , which close to the point τ_- (but still sufficiently far so that the adiabatic condition is satisfied. This requires that $1/\sqrt{2|A|K_y} << |\tau - \tau_-| << 1/2|A|K_y^2$) can be represented

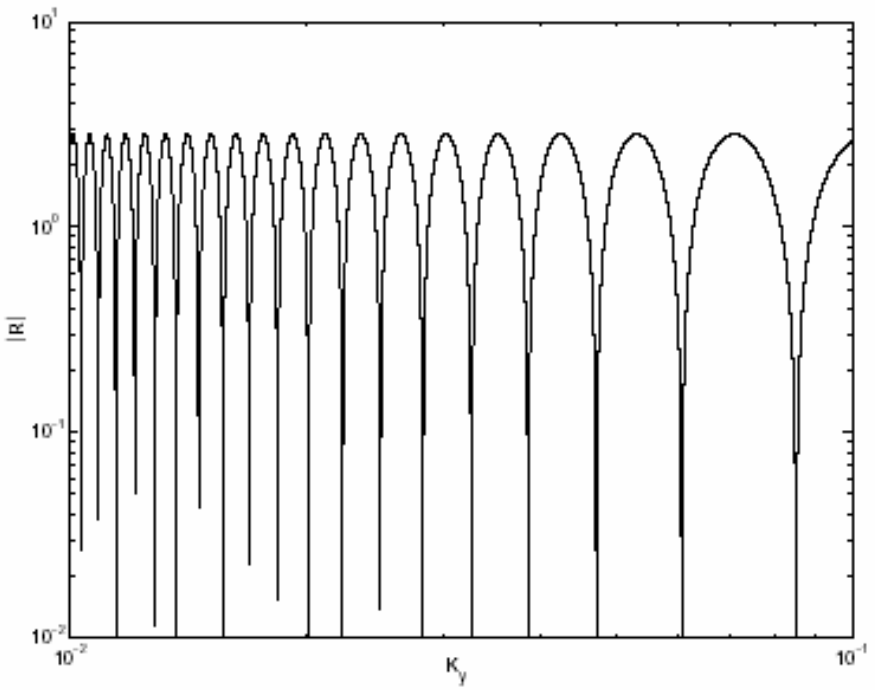

Figure A2. Analytically derived reflection coefficient as a function of K_y.

$$\phi(\tau) = \frac{e^{-if(\tau_-)} e^{i|A|K_y\sqrt{1-K_y^2}(\tau-\tau_-)^2}}{(4A^2K_y^2(1-K_y^2)(\tau-\tau_-)^2)^{1/4}}.$$

We now connect this solution to the WKB solution at $\tau_- < \tau < \tau_+$ with the help of the well-known relation for parabolic cylinder functions and their asymptotic expansion (Goldreich & Tremaine 1978; in our case $b = 0$ corresponding to $Q = 1$)

$$\sqrt{2}E(0,x) - E^*(0,x) = iE^*(0,-x),$$

$$E(0,x) = \left(\frac{2}{x}\right)^{1/2} exp\left[i\left(\frac{x^2}{4} + \frac{\pi}{4}\right)\right], \qquad x \gg 0.$$

As a result we get

$$\phi(\tau) = \frac{1}{\sqrt{\omega(\tau)}}\left(-ie^{-if(\tau)} + \sqrt{2}e^{-2if(\tau_-)}e^{if(\tau)}\right),$$

for $\tau_- < \tau < \tau_+$. The exponents in this expression after analogous connection through the point τ_+ go over to the following sums at $\tau >> \tau_+$

$$-ie^{-if(\tau)} \longrightarrow e^{-if(\tau)} - i\sqrt{2}e^{-2if(\tau_+)}e^{if(\tau)}$$

$$\sqrt{2}e^{-2if(\tau_-)}e^{if(\tau)} \longrightarrow$$

$$\longrightarrow -i\sqrt{2}e^{-2if(\tau_-)}e^{if(\tau)} + 2e^{2i(f(\tau_+)-f(\tau_-))}e^{-if(\tau)}.$$

Hence, for the solution for $\tau >> \tau_+$ we have

$$\phi(\tau) = \frac{1}{\sqrt{\omega(\tau)}}\left(-i\sqrt{2}e^{-2if(\tau_+)} - i\sqrt{2}e^{-2if(\tau_-)}\right)e^{if(\tau)} +$$

$$+ \frac{1}{\sqrt{\omega(\tau)}}\left(1 + 2e^{2i(f(\tau_+)-f(\tau_-))}\right)e^{-if(\tau)}.$$

From this expression we can identify the reflection and transmission coefficients

$$T = \left(1 + 2e^{2i(f(\tau_+)-f(\tau_-))}\right)$$

$$R = \left(-i\sqrt{2}e^{-2if(\tau_+)} - i\sqrt{2}e^{-2if(\tau_-)}\right),$$

Or after evaluating the module we have

$$|R| = 2\sqrt{2}|cos(f(\tau_+) - f(\tau_-))| \approx 2\sqrt{2}\left|cos\left(\frac{1}{2AK_g}\right)\right|.$$

Shown in Fig.A2 is this function.

Appendix B

Derivation of group velocity for a localized wave packet

In this Appendix we derive group velocity at which the energy of the localized packet is transported. To do this we first need an equation for the normalized surface density $\vartheta = \sigma / \Sigma_0$, which can be derived from the shearing sheet equations (1-3), Poisson equation (4) and condition of zero potential vorticity (we consider here only density waves) $\partial u / \partial y - \partial v / \partial x + 2B\vartheta = 0$ and has the form

$$\Delta \frac{D^2\vartheta}{Dt^2} + 4A\frac{\partial^2}{\partial x \partial y}\frac{D\vartheta}{Dt} + 4B\Omega\frac{\partial^2\vartheta}{\partial x^2} + (8AB + 4B\Omega)\frac{\partial^2\vartheta}{\partial y^2} = \Delta^2\chi\,, \qquad \text{(B1)}$$

where $\Delta = \partial^2/\partial x^2 + \partial^2/\partial y^2$, $D/Dt = \partial/\partial t + 2Ax\partial/\partial y$, $\chi = c^2\vartheta + \psi + \psi_{ext}$, ψ is the perturbation of the gravitational potential corresponding to ϑ, ψ_{ext} is an external potential.

To find an expression for the packet energy let us first consider driving of the surface potential perturbation by some external gravitational field ψ_{ext} (our derivation of the energy of perturbation parallels that of Mark (1974) and Landau & Lifshitz (1960)). The total work done by this external potential on surface area of the disc per unit time is given by

$$P = -\iint \Sigma\vec{u}\cdot\nabla\psi_{ext}\,dxdy = -\iint \psi_{ext}\frac{\partial\sigma}{\partial t}\,dxdy\,, \qquad \text{(B2)}$$

where we have used continuity equation and assumed that perturbations are either localized or periodic in spatial coordinates; in the latter case integration is assumed over spatial periods. Suppose that the external potential has the form $\psi_{ext} = \psi_0(t)\exp(-i\int_0^t \omega(t')dt' + ik_x(t)x + ik_y y)$, where $\psi_0(t)$ is a slowly varying function of time and the frequency is given by Eq. (19) of Ch.3. It follows that generated surface density perturbations will be of the same form $\vartheta = \vartheta_0(t)\exp(-i\int_0^t \omega(t')dt' + ik_x(t)x + ik_y y)$. The amplitude $\vartheta_0(t)$ is found from Eq.(B1) and is related to $\psi_0(t)$ in the following way

$$\psi_0(t) = i\left(\frac{\omega}{k^2}\right)' \vartheta_0(t) + \frac{2i\omega}{k^2}\frac{d\vartheta_0}{dt}.$$

For periodic perturbations of the above considered type Eq.(B2) is rewritten as

$$P = -\frac{\Sigma_0}{4} i\omega \iint (\psi_0 \vartheta_0^* - \psi_0^* \vartheta_0) dxdy,$$

which after some algebra reduces to the expression

$$P = \iint \frac{\omega\Sigma_0}{2}\frac{d}{dt}\left(\frac{\omega|\vartheta_0|^2}{k^2}\right) = \frac{d}{dt}\iint \frac{\Sigma_0\omega^2|\vartheta_0|^2}{2k^2} dxdy - \iint \frac{\omega'\omega\Sigma_0|\vartheta_0|^2}{2k^2} dxdy,$$

(WKB small terms are neglected) or, equivalently

$$\frac{d}{dt}\iint \frac{\Sigma_0\omega^2|\vartheta_0|^2}{2k^2} dxdy = P + \iint \frac{\omega'\omega\Sigma_0|\vartheta_0|^2}{2k^2} dxdy.$$

This relation can be viewed as a conservation of energy if we identify the integrand in the left hand side with the energy of perturbations. A change in energy is due to the work done by external forces and to the exchange with the mean flow. In the shearless limit exchange with the mean flow is absent and we have only the work of external forces. Thus the energy density of perturbations is $e = \frac{\Sigma_0\omega^2|\vartheta_0|^2}{2k^2}$.

Assume now that ϑ_0 is in addition a slowly varying function of spatial coordinates *(x,y)*,i.e., $k_x >> \partial/\partial x, k_y >> \partial/\partial y$ and is localized in space. In this case the packet is $\vartheta = \vartheta_0(x,y,t)\exp(-i\int_0^t \omega(t')dt' + ik_x(t)x + ik_y y)$. If we now substitute this solution into Eq.(B1) and retain only first derivatives of $\vartheta_0(x,y,t)$, we finally get

$$\frac{\partial e}{\partial t} + \frac{k_x}{\omega}\left(c^2 - \frac{\pi G\Sigma_0}{k} - \frac{8A\Omega k_y^2}{k^4} - \frac{12A^2k_y^4}{k^6}\right)\cdot\frac{\partial e}{\partial x} +$$

$$+\left(2Ax + \frac{k_y}{\omega}\left(c^2 - \frac{\pi G\Sigma_0}{k} - \frac{8A\Omega k_y^2}{k^4} - \frac{12A^2k_y^4}{k^6} + \frac{4A^2+8AB}{k^2}\right)\right)\cdot\frac{\partial e}{\partial y} = \frac{\omega'}{\omega}e.$$

This is an energy conservation law and shows that the energy of a packet is transported with the group velocity $\vec{U}_g(U_{gx}, U_{gy})$, where U_{gx} and U_{gy} are given by

$$U_{gx} = \frac{k_x}{\omega}\left(c^2 - \frac{\pi G\Sigma_0}{k} - \frac{8A\Omega k_y^2}{k^4} - \frac{12A^2k_y^4}{k^6}\right)$$

$$U_{gy} = 2Ax + \frac{k_y}{\omega}\left(c^2 - \frac{\pi G\Sigma_0}{k} - \frac{8A\Omega k_y^2}{k^4} - \frac{12A^2k_y^4}{k^6} + \frac{4A^2 + 8AB}{k^2}\right)$$

and varies due to the exchange with the mean flow that is reflected in the source term on the right hand side of this equation. As it is obvious U_{gx} is proportional to $k_x(t)$ and changes sign with it. So, an apparent reflection of the packet in fig. 14 is connected with this change of sign.

Acknowledgments

This thesis is a summary of my work that I have done in the Abastumani Astrophysical Observatory during 2 years.

I would like to express special thanks to my supervisor George Chagelishvili for his continuous support and help in the work.

I am also grateful to Drs. M. Kalashnik from SPA *"Typhoon"* (Russia), A. Tevzadze and R. Chanishvili from Center of Plasma Astrophysics of Abastumani Astrophysical Observatory for helpful and illuminating discussions.

I would like to thank Dr. K. Chargeishvili who helped with formalities necessary for defense and Dr. T. Kakhniashvili for being an expert of the thesis and also Drs. E. Khutsishvili and N. Shatashvili for being referees of the thesis and for their valuable comments.

References

1. Abramov A. A., Tareev B. A., Ulianov V. I., *Barotrophic instability of two layered Kochin model on beta-plane,* Izvestya AN, **8**, 131, (1972)

2. Afshordi N., Mukhopadhyay B., Narayan R., *Turbulence in hydrodynamical accretion: lagrangian analysis of energy growth,* ApJ., **629**, 373, (2005)

3. Baggett J. S., Driscoll T. A. and Trefethen L. N., *A mostly linear model of transition to turbulence*, Phys. Fluids*,* **9,** 1043, (1995)

4. Bakas N. A., Ioannou P. J., Kefalikos J. E., *The emergence of coherent structures in stratified shear flow.* J. Atmos. Sci*.,* **58**, 2790-2806, (2001)

5. Balbus S., *Local interstellar gasdynamical stability and substructure in spiral arms*, ApJ*.,* **324**, 60, (1988)

6. Balbus S. A., Hawley J. F., *Instability, turbulence and enhanced transport in accretion discs,* Rev. Mod. Phys., **70**, 1, (1998)

7. Balbus S., Goodman J., *Stratified disks are locally stable*. astro.ph.10229, (2001)

8. Balbus S. A., *Accretion disk turbulence,* ASPC, **261**, 356, (2002)

9. Balbus S. A., *Enhanced Angular Momentum Transport in Accretion Disks*, ARA&A, **41**, 555, (2003)

10. Barcilon A., and Bishop C. H., *Nonmodal development of baroclinic waves undergoing horizontal shear deformation,* J. Atmos. Sci*.,* **55**, 3583-3597, (1998)

11. Barge P., Sommeria J., *Did planet formation begin inside persistent gaseous vortices?*, A&A, **295**, 1, (1995)

12. Bartello P. *Geostrophic adjustment and inverse cascades in rotating stratified turbulence*, J. Atmos. Sci*.,* **52,** 4410-4428, (1995)

13. Bayly B. J., *Three-dimensional instability of elliptical flow*, Phys. Rev. Letters, **57**, 2160, (1986)

14. Bayly B. J., Orszag S. A. and Herbert T., *Instability mechanisms in shear flow transitions*, Ann. Rev. Fluid Mech., **20**, 359, (1988)

15. Bennets P. A., Hoskins B. J., *Conditional symmetric instability - a possible explanation for frontal rainbands*. Q. J. R. Meteorol. Soc., 105, 945-962, (1979)

16. Bertin G., Lin C. C., Lowe S. A., Thurstans R. P., *Modal Approach to the Morphology of Spiral Galaxies. II. Dynamical Mechanisms,* ApJ., **338**, 104, (1989)

17. Bertin G., Lin C.C., *Spiral structure in galaxies, a density wave theory*, Cambridge, MA MIT Press, (1996)

18. Binney J., Tremaine S., *Galactic dynamics*, (Princeton: Princeton Univ. Press), (1987)

19. Blumen W., *Geostrophic adjustment*, Geophys. Space Phys*.,* **10**, 485-528, (1972)

20. Bodo G., Poedts S., Rogava A. D., Rossi P., *Spatial aspect of wave transformations in astrophysical flows*, A&A, **374**, 337, (2001)

21. Bodo G., Chagelishvili G., Murante G., Tevzadze A., Rossi P., Ferrari A., *Spiral density wave generation by vortices in Keplerian flows,* A&A, **437**, 9, (2005)

22. Bottin S., Dauchot O., Daviaud F. and Manneville P., *Experimental evidence of streamwise vortices as finite amplitude solutions in transitional plane Couette flow,* Phys. Fluids, **10**, 2597, (1998)

23. Bracco A., Chavanis P. H., Provanzale A., Spergel E. A., Phys. Fluids, **11**, 2280, (1999)

24. Broberg L. and Brosa U., Z. Naturforschung Teil, **43a**, 697, (1988)

25. Butler K. M. and Farrell B. F., *Three dimensional optimal perturbations in viscous channel flows,* Phys. Fluids A, **4**, 1637, (1992)

26. Case, K. M., *Stability of inviscid plane Couette flow*, Phys. Fluids, **3**, 143, (1960)

27. Chagelishvili G. D., Khristov T. S., Chanishvili R. G., Lominadze J. G., Phys. Rev. E, **47**, 366, (1993)

28. Chagelishvili G. D., Rogava A. D., Segal I. N., *Hydrodynamic stability of compressible plane Couette flow*, Phys. Rev. E, **50**, R4283, (1994)

29. Chagelishvili G. D., Chkhetiani O. G., *Linear transformation of Rossby waves in shear flows*, JETP Letters, **62**, 301, (1995)

30. Chagelishvili G. D., Chanishvili R. G., Lominadze J. G., *Physics of the amplification of vortex disturbances in shear flows,* JETP Letters, **63**, 301, (1996a)

31. Chagelishvili G. D., Rogava A. D., Tsiklauri D. G., *Effect of coupling and linear transformation of waves in shear flows,* Phys. Rev. E, **53**, 6028, (1996b)

32. Chagelishvili G. D., Tevzadze A. G., Bodo G. and Moiseev S. S., *Linear mechanism of wave emergence from vortices in smooth shear flows*, Phys. Rev. Letters, **79**, 3178, (1997a)

33. Chagelishvili G. D., Khujadze G. R., Lominadze J. G. and Rogava A. D., *Acoustic waves in unbounded shear flows,* Phys. Fluids, **9**, 1955, (1997b)

34. Chagelishvili G. D., Chanishvili R. G. Lominadze J. G. and Tevzadze A. G., *Magnetohydrodynamic wave linear evolution in parallel shear flows: Amplification and mutual transformations,* Phys. Plasmas, **4**, 259, (1997c)

35. Chagelishvili G. D., Tevzadze A. G., and Goossens M., *Generation of oscillations in solar convection zone: linear mechanism of mode conversion in shear flows,* Proceedings of the conference: 9th European Meeting on solar physics, "Magnetic fields and Solar Processes", Florence, Italy, ESA SP-448, pp. 75-80, (1999)

36. Chagelishvili G. D., Chanishvili R. G., Christov T. S. and Lominadze J. G., *A turbulence model in unbounded smooth shear flows. The weak turbulence approach*, J.E.T.P., **94**, 434, (2002)

37. Chagelishvili G., Zahn J.-P., Tevzadze A., Lominadze J., *On hydrodynamic shear turbulence in Keplerian disks: via transient growth to bypass transition*, A&A, **402**, 401, (2003)

38. Chapman S. J., *Subcritical Transition in Channel Flows*, J. Fluid Mech., **451**, 35, (2002)

39. Coles D., J. Fluid Mech., **21**, 385, (1965)

40. Craik A. D. D., and Criminale W. O., *Evolution of wave like perturbations in shear flows: a class of exact solutions of the Navier-Stokes equation,* Proc. R. Soc. of London, Ser. A **406**,13, (1986)

41. Criminale W. O. and Drazin P. G. *The evolution of linearized perturbations of parallel flows*, Studies Appl. Math., **83**, 133, (1990)

42. Dauchot O., Daviaud F., *Streamwise vortices in plane Couette flow*, Phys. Fluids, **7**, 901, (1995)

43. Davis S. S., Sheehan D. P., Cuzzi J. N., *On the Persistence of Small Regions of Vorticity in the Protoplanetary Nebula*, ApJ., **545**, 494, (2000)

44. Davis S. S., *Vorticity-induced Wave Motion in a Compressible Protoplanetary Disk,* ApJ., **576**, 450, (2002)

45. Dimnikov V. P., Filatov A. N., *Stability of large-scale atmospheric processes.* Gidrometeoizdat, Leningrad, (1990)

46. Doljanski F. V., Krimov V. A., Manin D. U., *Stability and vortex structures of quasi-two-dimensional shear flows*. Usp. Fiz. Nauk [Sov. Phys-Usp], **160**, 1-47. (1990)

47. Drazin P. G., Reid W. H., *hydrodynamic stability*, Cambridge University Press, (1981)

48. Drury L. O. C., *On normal modes of gas sheets and discs*, MNRAS, **193**, 337, (1980)

49. Dykii, L. A. Dokl. Akad. Nauk S.S.S.R., **135**, 1068, (1960)

50. Elmegreen B. G., *What do we really know about Cloud Formation?,* IAUS, **169**, 551, (1996)

51. Elmegreen B. G., Leitner S. N., Elmegreen D. M., Cuillandre J.-C., *A Turbulent Origin for Flocculent Spiral Structure in Galaxies. II. Observations and Models of M33*, ApJ., **593**, 333, (2003a)

52. Elmegreen B. G., Elmegreen D. M., Leitner, S. N., *A Turbulent Origin for Flocculent Spiral Structure in Galaxies,* ApJ., **590**, 271, (2003b)

53. Emanuel K. A., *The lagrangian parcel dynamics of moist symmetric stability,* J. Atmos. Sci*.,* **40**, 2368-2376, (1983)

54. Farrell B. F., *Optimal excitation of perturbations in viscous channel flows*, Phys. Fluids, **31**, 2093-2102, (1988)

55. Farrell B. F., Ioannou P. J. *Transient development of perturbations in stratified shear flow*. J. Atmos. Sci*.,* **50**, 2201-2214, (1993a)

56. Farrell B. F., Ioannou P. J. *Perturbation growth in shear flow exhibit universality*, Phys. Fluids, **9**, 883, (1993b)

57. Farrell B. F., Ioannou P. J., *Generalized stability theory. Part I: Autonomous operators*, J. Atmos. Sci., **53**, 2025, (1996)

58. Farrell B. F., Ioannou P. J., *Transient and asymptotic growth of two-dimensional perturbations in viscous compressible shear flow*, Phys. Fluids, **12**, 3021, (2000)

59. Farrell, B. F. and Ioannou, P. J. *Perturbation growth and structure in uncertain flows. part1*, J. Atmos. Sci*.,* **59**, 2629-2664, (2002)

60. Fjørtøft R., Geofis. Publ., **17**, 52, (1950)

61. Friedman J. L., Schutz B. F., *Lagrangian perturbation theory of nonrelativistic fluids,* ApJ., **221**, 937, (1978)

62. Fridman A. M., Khoruzhii O. V., *Vortices in Astrophysical Discs*, ASPC, **160**, 341, (1999a)

63. Fridman A. M., Khoruzhii O. V., *Velocity Fields in Spiral Galaxies,* IAUS, **194**, 269, (1999b)

64. Fuchs B., *Density waves in the shearing sheet. I. Swing amplification*, A&A, **368**, 107, (2001)

65. Gammie C. F. *Nonlinear Outcome of Gravitational Instability in Cooling, Gaseous Disks*, ApJ, **553**, 174, (2001)

66. Gebhardt T. and Grossmann S., *Chaos transition despite linear stability*, Phys. Rev. E*,* **50**, 3705, (1994)

67. Gill, A. E., *Atmosphere-Ocean Dynamics.* Academic Press, New York, (1982)

68. Godon P., Livio M., *Vortices in Protoplanetary Disks,* ApJ., **523**, 350, (1999)

69. Godon P., Livio M., *The Formation and Role of Vortices in Protoplanetary Disks,* ApJ., **537**, 396, (2000)

70. Goldreich P., Lynden-Bell D., *Spiral arms as sheared gravitational instabilities*, MNRAS., **130**, 125, (1965)

71. Goldreich P., Tremaine S., *The excitation and evolution of density waves*, ApJ., **222**, 850, (1978)

72. Grossmann S., *The onset of shear flow turbulence*, Rev. Mod. Phys*,* **72**, 603, (2000)

73. Gustavsson L. H., Hultgren L. S., *A resonant mechanism in plane Couette flow*, J. Fluid Mech., 98, 149, (1980)

74. Gustavsson L. H., *Energy growth of three-dimensional perturbations in plane Poiseuille flow,* J. Fluid Mech., **224**, 241, (1991)

75. Hakim G. J., *Role of nonmodal growths and nonlinearity in cyclogenesis initial value problem*, J. Atmos. Sci, **57**, 2951-2967, (2000)

76. Herbert T., *Secondary instability of boundary layers*, Ann. Rev. Fluid Mech., **20**, 487-526, (1988)

77. Hodyss D. and Grotjahn R., *Nonmodal and unstable normal mode baroclinic growths as a function of horizontal scale*, Dyn. Atmos. Oceans*,* **37**, 1-24, (2003)

78. Hoskins, B. J., *The role of potential vorticity in symmetric stability and instability of flows*. Q. J. R. Meteorol. Soc.*,* **100**, 480-482, (1974)

79. Jog C. J., Solomon P. M., *Two-fluid gravitational instabilities in a galactic disk,* ApJ, **276**, 114, (1984)

80. Jog C., *Swing amplification of nonaxisymmetric perturbations in stars and gas in a sheared galactic disk*, ApJ., **390**, 378-386, (1992)

81. Johansen A., Andersen A. C., Brandenburg A., *Simulations of dust-trapping vortices in protoplanetary discs,* A&A, **417**, 361, (2004)

82. Joly A., Thorpe A., *Frontal instability generated by tropospheric potential vorticity anomalies*, QJRMS., **116**, 525, (1990)

83. Julian W. H., Toomre A., *Non-Axisymmetric Responses of Differentially Rotating Disks of Stars,* ApJ., **146**, 810, (1966)

84. Kalashnik M. V., *Criteria of symmetric and non-symmetric stability of geostrophical and gradient flows of stratified rotating fuids*. Trans. (Doklady) Russian Acad. Sci.*,* **371**, 383-386, (2000)

85. Kalashnik M. V., *On the theory of symmetric and non-symmetric stability of zonal geostrophic flows*. Izv. Acad. Sci., Russia, Atmos. Oceanic Phys.*,* **37**, 418-421, (2001)

86. Kalashnik, M.V., Mamatsashvili G. R., Chagelishvili G. D., Lominadze J. G.*, Dynamics of non-symmetric perturbations in geostrophic flows with a constant horizontal shear*, Dokl. Ross. Akad. Nauk (Trans.(Doklady) Russian Acad. Sci.), **399**, 1-6, (2004) (in Russian)

87. Kalashnik, M.V., Mamatsashvili G. R., Chagelishvili G. D., Lominadze J. G.*, Linear dynamics of non-symmetric perturbations in geostrophic horizontal shear flows,* Q.J.R. Meteorol. Soc., **132**, 505-518, (2006)

88. Kim W., Ostriker E., *Amplification, saturation, and Q thresholds for runaway: growth of self-gravitating structures in models of magnetized galactic gas disks,* ApJ, **559**, 70-95, (2001)

89. Klahr H. H., Bodenheimer P., *Turbulence in Accretion Disks: Vorticity Generation and Angular Momentum Transport via the Global Baroclinic Instability*, ApJ., **582,** 869, (2003)

90. Klahr H., *The Global Baroclinic Instability in Accretion Disks. II. Local Linear Analysis*, ApJ, **606**, 1070, (2004)

91. Kochin N. E., *On the stability of Margeules interfaces*, Sobranie AN, **1**, 149, (1949) (in Russian)

92. Landahl M. T., *A note of an algebraic instability of inviscid parallel shear flows,* J. Fluid Mech., **98**, 243, (1980)

93. Landau L., Lifshitz E., *Eloctrodynamics of continuous media*, Pergamon Press, New York, (1960)

94. Landau L., Lifshitz E., *Quantum Mechanics*, Nauka, Moscow, (1974) (in Russian)

95. Lau Y. Y., Lin C. C., Mark J. W.-K., *Unstable Spiral Modes in Disk-Shaped Galaxies*, PNAS, **73**,1379, (1976)

96. Lau Y. Y., Bertin, G., *Discrete spiral modes, spiral waves, and the local dispersion relationship*, ApJ., **226**, 508, (1978)

97. LeBlond P. H., Mysak L. A., *Waves in the Ocean*, Elsevier Scientific Publishing Company, Amsterdam-Oxford-New York, (1978)

98. Li H., Finn J. M., Lovelace R. V. E., Colgate S. A., *Rossby Wave Instability of Thin Accretion Disks. II. Detailed Linear Theory*, ApJ., **533**, 1023, (2000)

99. Lin C. C., Shu F. H., *On the Spiral Structure of Disk Galaxies,* ApJ., **140**, 646, (1964)

100. Lin C. C., Shu F. H., *On the Spiral Structure of Disk Galaxies, II. Outline of a Theory of Density Waves,* PNAS, **55**, 229, (1966)

101. Lin C. C., Shu F. H., in Astrophysics and General relativity, ed. M. Chretien et al. (New York: Gordon & Breach), (1968)

102. Lord Kelvin (W. Thomson), Phil. Mag. **24**, Ser. 5, 188, (1887)

103. Lovelace R. V. E., Li H., Colgate S. A., Nelson A. F., *Rossby Wave Instability of Keplerian Accretion Disks*, ApJ., **513**, 805, (1999)

104. Mamatsashvili G., *Dynamics of localized packets of spiral density waves in gaseous disks,* Bull. Georg. Natl. Acad. Sci., **173**, N 3, 490-493, (2006)

105. Marcuss S., Press W. H., *The evolution of nonaxisymmetric shear perturbations in accretion disks,* J. Fluid Mech., **79**, 525, (1997)

106. Mark J.W.K., *On density waves in galaxies I. Source terms and action conservation*, ApJ., **193**, 539, (1974)

107. Mark J.W.K., *On Density Waves in Galaxies. III-Wave Amplification by Stimulated Emission,* ApJ, **205**, 363, (1976)

108. Mark J.W.K., *On density waves in galaxies. V-Maintenance of spiral structure and discrete spiral modes,* ApJ., **212**, 645, (1977)

109. Moiseev M. V., *Asymptotic methods of nonlinear mechanics,* Nauka, Moscow, (1987) (in Russian)

110. Mu, M., Vladimirov, V. and Wu, Y. H. *Energy-Casimir and energy-Lagrange methods in the study of nonlinear symmetric stability problems*, J. Atmos. Sci*.,* **56**, 400-411, (1999)

111. Nakagawa Y., Sekiya M., *Wave action conservation, over-reflection and over-transmission of non-axisymmetric waves in differentially rotating thin discs with self-gravity,* MNRAS, **256**, 685, (1992)

112. Narayan R., Goldreich P., Goodman J., *Physics of modes in a differentially rotating system - Analysis of the shearing sheet*, MNRAS, **228**, 1, (1987)

113. Nayfeh A. E., *Perturbation Methods.* Wiley-Interscience, New York, (1982)

114. Nolan, D. S. and Farrell, B. F. *The structure and dynamics of Tornado-like vortices*, J. Atmos. Sci*.,* **56**, 2908-2939, (1999a)

115. Nolan D. S. and Farrell B. F., *The intensification of two-dimensional swirling flows by stochastic asymmetric forcing,* J. Atmos. Sci., **56**, 3937-3962, (1999b)

116. Nolan D. S. and Montgomery M. T., *The algebraic growth of wavenumber one disturbances in Hurricane-like vortices*, J. Atmos. Sci*.,* **57**, 3514-3538, (2000)

117. Obukhov A. M., *On the question of geostrophic wind*, Izv. Acad. Nauk. S.S.S.R., Ser. Geograph.-Geophys, **13**, 281-306, (1949)

118. Orlanski I., *Instability of frontal waves*, J. Atmos. Sci., **25**, 168, (1968)

119. Orszag S. A., *Galerkin approximations to flows within slabs, spheres and cylinders,* Phys. Rev. Letters, **26**, 1100, (1971)

120. Orszag S. A., Kells L. C., *Transition to turbulence in plane Couette and plane Poiseuille flows* J. Fluid Mech., **96**, 161, (1980)

121. Orszag S. A., Patera A. T., *Subcritical transition to turbulence in plane channel flows*, Phys. Rev. Letters, **45**, 989, (1980)

122. Papaloizou J. C., Savonije G. J., *Instabilities in self-gravitating gaseous discs*, MNRAS, **248**, 353, (1991)

123. Pazy A*., Semigroups of linear operators and applications to partial differential equations*, Springer, (1983)

124. Pedlosky, J., *Geophysical fluid dynamics.* 2nd ed. Springer Verlag, (1987)

125. Pellat R., Tagger M., Sygnet J. F., *Swing amplification of spiral waves in low-mass discs,* A&A, **231**, 347, (1990)

126. Pierrehumbert, R., Swanson, K. *Baroclinic instability*, Ann. Rev. Fluid Mech*.,* **27**, 419-467, (1995)

127. Poedts S., Rogava A. D., Mahajan S., *Shear flow induced wave couplings in the solar wind*, ApJ., **505**, 369, (1998)

128. Poedts S., Rogava A. D., *Does spiral galaxy IC 342 exhibit shear induced wave transformations?*, A&A, **385**, 22, (2002)

129. Reddy S.C., Shmidt P.J., and Henningson D.S., *Pseudospectra of the Orr-Sommerfeld operator*, SIAM J. Appl. Math. **53**, 15, (1993)

130. Reddy S.C., and Henningson D.S., *Energy growth in viscous channel flows*, J. Fluid Mech. **252**, 209, (1993)

131. Rempfer D., *Low-dimensional modeling and numerical simulation of transition in simple shear flows,* Ann. Rev. Fluid Mech., **35**, 229, (2003)

132. Reshotko E., *Transient growth: a factor in bypass transition*, Phys. Fluid*,* **13**, 1067, (2001)

133. Reynolds O., *An experimental investigation of the circumstances which determine whether the motion of water shall be direct or sinuous, and of the law of resistence in parallel channels,* Phil. Trans. Roy, Soc. **174**, 935-82, (1883). Also Scientific papers (1901), vol. II, pp. 51-105, Cambridge University Press.

134. Rogava A. D., Mahajan S., *Coupling of sound and internal waves in shear flows,* Phys. Rev. E, **55**, 1185, (1997)

135. Rogava A. D., Poedts P. and Heirman S., *Are galactic magnetohydrodynamic waves coupled?*, MNRAS, **307**, L31, (1999)

136. Ryu D., Goodman J., *Convective instability in differentially rotating disks*, ApJ., **388**, 438, (1992)

137. Sellwood J. A., Carlberg R. G. *Spiral instabilities provoked by accretion and star formation*, ApJ., **282**, 61, (1984)

138. Shakina, N. P. *Hydrodynamical instability in the atmosphere.* Gidrometeoizdat, Leningrad, (1990)

139. Sinton D., Heise W., *Frontal instability in a sheared basic state*, J. Atmos. Sci., **50**, 1691, (1993)

140. Sofue Y., Tutui Y., Honma M., Tomita A., Takamiya T., Koda J., Takeda Y., *Central Rotation Curves of Spiral Galaxies,* ApJ., **523**, 136, (1999)

141. Straub D. N., *Instability of 2D flows to hydrostatic 3D perturbations*, J. Atmos. Sci., **60**, 79-102, (2003)

142. Tagger M., Sygnet J. F., Pellat R., *Bars and barred spirals - Linear theory revisited,* ApJ., **337**L, 9, (1989)

143. Tang C. H., *On the instability of a free layer atmosphere with an isentrohic stratosphere*, Tellus, **24**, 293, (1972)

144. Tevzadze A. G., *Emission of magnetosonic waves by vortices in high shear flows,* Phys. Plasmas, **5**, 1557, (1998)

145. Tevzadze A., Chagelishvili G. D., Chanishvili R. G., Lominadze J. G., Zahn J.-P. *On hydrodynamic shear turbulence in stratified Keplerian disks: Transient growth of small-scale 3D vortex mode perturbations,* A&A, **407**, 779, (2003)

146. Tevzadze A., Ph.D. thesis, Katholieke Universiteit Leuven, (2006)

147. Toomre A., *Group Velocity of Spiral Waves in Galactic Disks*, ApJ., **158**, 899, (1969)

148. Toomre A., *What amplifies spirals*, in Structure and Evolution of Normal Galaxies, ed. S. M. Fall & D. Lynden-Bell (Cambridge: Cambridge Univ. Press), 111, (1981)

149. Trefethen L. N., Trefethen A. E., Reddy S. C. and Driscoll T. A., *Hydrodynamic stability without eigenvalues*, Science, **261**, 578, (1993)

150. Trefethen L. N. *Pseudospectra of linear operators*, SIAM Review, **39**, 383, (1997)

151. Umurhan O. M., Regev O., *Hydrodynamic stability of rotationally supported flows: linear and nonlinear 2D shearing box results*, A&A, **427**, 855, (2004)

152. Van Kampen, N. G., *On the theory of stationary waves in plasma*., Physica, **51**, 949, (1957)

153. Wada K., Meurer G., Norman C. A.. *Gravity-driven Turbulence in Galactic Disks*, ApJ., **577,** 197, (2002)

154. Waleffe F., *On a self-sustaining process in shear flows*, Phys. Fluids, **9**, 883, (1997)

155. Weber J. E., *Symmetric instability of stratified geostrophic flow,* Tellus, **32**, 176-185, (1980)

156. Xu Qin, *Generalized energetics for linear and nonlinear symmetric instability*. J. Atmos. Sci., **43**, 972-984, (1986)

157. Yecko P. A., *Accretion disk instability revisited. Transient dynamics of rotating shear flow*, A&A, **425**, 385, (2002)

158. Zeitlin V., Reznik G. M. and Ben Jelloul M., *Nonlinear theory of geostrophic adjustment. Part 2. Two-layer and continuously stratified primitive equations*, J.Fluid Mech., **491**, 207-228, (2003)